N° Ordre……../Institut/UMBB/2024

People's Democratic Republic of Algeria
Ministry of Higher Education and Scientific Research
University M'Hamed BOUGARA – Boumerdes

Institute of Electrical and Electronic Engineering

PHD DISSERTATION

Presented by:

Merabet Oussama

In partial fulfillment of the requirement for the degree of doctorate

Field: ELECTROTECHNIQUE

Option: ELECTROTECHNIQUE

TITLE:
Coordination of Protection Systems Applied to the Electrical Network Using Modern Techniques

JURY MEMBERS:

• Mr.	BENTARZI	Hamid	Prof	UMBB	Jury president
• Mr.	BOUCHAHDANE	Mohamed	Prof	UMBB	Supervisor
• Mr.	ELTOM	Ahmed	Prof	University of Tennessee/Chattanooga	Co-supervisor
• Mr.	BENDJEGHABA	OMAR	Prof	UMBB	Examiner
• Mr.	KHODJA	DJALAL EDDINE	Prof	University of M'sila	Examiner
• Mr.	AMMAR	Abdelkarim	MCA	UMBB	Examiner
• Mr.	KHELDOUN	AISSA	Prof	UMBB	Invited

Academic year: 2023/2024

Abstract

The improvement of technology in the previous several decades has enabled a significant presence of renewable power sources in the distribution network (DN). The integrating of such resources has a significant influence on DN by reducing power loss and enhancing network dependability. Aside from that, the current protection system has met coordination issues as a result of bidirectional power flow, varied types and capacities of generating sources, and variations in fault levels as a result of network operating modes (grid-connected or islanded). Moreover, there is a lack of expertise in the creation of adaptive microgrid protection schemes for relay coordination that takes into account all N-1 scenarios through the nonstandard relay characteristics. Therefore, an effective and optimum coordination strategies are required to deal with relays coordination problem. The coordination problem of the directional overcurrent relays (DOCRs) is a restricted and nonlinear optimization issue that involves determining appropriate settings to reduce relays operating time while maintaining the sensitivity and the selectivity characteristics. The protection coordination scheme takes into account relay curve settings (A and B), time dial setting (TDS) and plug setting (PS) to achieve the shortest running time and attain optimal settings. Currently, a various nontraditional optimization strategies have been presented to overcome this challenge. In this work, the coordination optimization problem (COP) of directional overcurrent relays is tackled. The optimization is carried out using a modified versions of an optimization algorithms. The performance of the proposed method is assessed using an IEEE standard test power systems and a distribution system while considering all the N-1 contingencies. The results are compared to the traditional approaches as well as those obtained by other current optimization methods provided in the literature in order to demonstrate the effectiveness and superiority of the proposed modified techniques in lowering relay operation time for optimum DOCRs coordination.

Keywords: Power systems; microgrid; optimal coordination; DOCRs; protection system; optimization algorithm; metaheuristics.

Résumé

L'amélioration de la technologie au cours des dernières décennies a permis une présence significative de sources d'énergie renouvelable dans le réseau de distribution (RD). L'intégration de ces ressources a eu une influence importante sur le RD en réduisant les pertes d'énergie et en améliorant la fiabilité du réseau. Outre cela, le système de protection actuel rencontre des problèmes de coordination en raison du flux bidirectionnel d'énergie, des types et capacités variés de sources de génération, et des variations des niveaux de défaut en raison des modes d'exploitation du réseau (connecté au réseau ou isolé). De plus, il existe un manque d'expertise dans la création de schémas adaptatifs de protection de micro-réseaux pour la coordination des relais, prenant en compte tous les scénarios N-1 à travers les caractéristiques non standard des relais. Par conséquent, des stratégies de coordination efficaces et optimales sont nécessaires pour résoudre le problème de coordination des relais. Le problème de coordination des relais de surintensité directionnels (DOCRs) est un problème d'optimisation restreint et non linéaire qui implique de déterminer des réglages appropriés pour réduire le temps de fonctionnement des relais tout en maintenant les caractéristiques de sensibilité et de sélectivité. Le schéma de coordination de protection prend en compte les réglages des courbes de relais (A et B), le réglage du cadran temporel (TDS) et le réglage de la fiche (PS) pour obtenir le temps de fonctionnement le plus court et atteindre des réglages optimaux. Actuellement, diverses stratégies d'optimisation non traditionnelles ont été présentées pour surmonter ce défi. Dans ce travail, le problème d'optimisation de la coordination (COP) des relais de surintensité directionnels est abordé. L'optimisation est réalisée à l'aide de versions modifiées d'algorithmes d'optimisation. Les performances de la méthode proposée sont évaluées en utilisant des systèmes d'alimentation d'essai standard de l'IEEE et un système de distribution tout en tenant compte de toutes les contingences N-1. Les résultats sont comparés aux approches traditionnelles ainsi qu'aux résultats obtenus par d'autres méthodes d'optimisation actuelles présentes dans la littérature afin de démontrer l'efficacité et la supériorité des techniques modifiées proposées dans la réduction du temps de fonctionnement des relais pour une coordination optimale des DOCRs.

Mots-clés : Systèmes d'alimentation ; micro-réseau ; coordination optimale ; DOCRs (relais de surintensité directionnels) ; système de protection ; algorithme d'optimisation ; métaheuristiques.

ملخص

لقد أتاح التحسن التكنولوجي في العقود القليلة الماضية وجودًا كبيرًا لمصادر الطاقة المتجددة في شبكة التوزيع (DN). كان لتكامل هذه الموارد تأثير كبير على DN من خلال تقليل فقدان الطاقة وتعزيز اعتمادية الشبكة. وبصرف النظر عن ذلك، فقد واجه نظام الحماية الحالي مشكلات التنسيق نتيجة لتدفق الطاقة ثنائي الاتجاه، وأنواع وقدرات مصادر التوليد المتنوعة، والاختلافات في مستويات الأعطال نتيجة لأنماط تشغيل الشبكة (متصلة بالشبكة أو منعزلة). علاوة على ذلك، هناك نقص في الخبرة في إنشاء خطط حماية للشبكات الصغيرة التكيفية لتنسيق الترحيل والتي تأخذ في الاعتبار جميع سيناريوهات N-1 من خلال خصائص الترحيل غير القياسية. لذلك، هناك حاجة إلى استراتيجيات تنسيق فعالة ومثالية للتعامل مع مشكلة تنسيق المرحلات. مشكلة التنسيق لمرحلات التيار الزائد الاتجاهي (DOCRs) هي مشكلة تحسين مقيدة وغير خطية تتضمن تحديد الإعدادات المناسبة لتقليل وقت تشغيل المرحلات مع الحفاظ على الحساسية وخصائص الانتقائية. يأخذ نظام تنسيق الحماية في الاعتبار إعدادات منحنى التتابع (A وB)، وإعداد قرص الوقت (TDS) وإعداد القابس (PS) لتحقيق أقصر وقت تشغيل وتحقيق الإعدادات المثالية. حاليًا، تم تقديم العديد من استراتيجيات التحسين غير التقليدية للتغلب على هذا التحدي. في هذا العمل، تمت معالجة مشكلة تحسين التنسيق (COP) لمرحلات التيار الزائد الاتجاهية. يتم إجراء التحسين باستخدام إصدارات معدلة من خوارزميات التحسين. يتم تقييم أداء الطريقة المقترحة باستخدام أنظمة طاقة اختبار IEEE القياسية ونظام التوزيع مع الأخذ في الاعتبار جميع حالات الطوارئ N-1. تتم مقارنة النتائج مع الأساليب التقليدية وكذلك تلك التي تم الحصول عليها من خلال طرق التحسين الحالية الأخرى الواردة في الأدبيات من أجل إظهار فعالية وتفوق التقنيات المعدلة المقترحة في تقليل وقت تشغيل التتابع لتحقيق التنسيق الأمثل لـ DOCRs.

الكلمات المفتاحية: أنظمة الطاقة؛ شبكة صغيرة. التنسيق الأمثل لـ DOCRs؛ نظام الحماية؛ خوارزمية التحسين؛ ميتايورستكس.

Acknowledgements

In the name of Allah, the Most Gracious and the Most Merciful Alhamdulillah, all praises to Allah for the strengths and His blessing in completing this thesis.

I would like to convey my heartfelt appreciation to my supervisor, Pr. Mohamed Bouchahdane, for his ongoing support of my PhD study.

My deepest appreciation also goes to professor Aissa Kheldoun for his patience, enthusiasm, and vast knowledge.

Thanks go to my many friends and colleagues, who over the years offered their kindness and encouragement.

I'd want to express my gratitude to all of the professors, teachers, personnel, and students at the Institute of Electrical and Electronic Engineering (IGEE) in Boumerdes, Algeria.

Finally, I am eternally thankful to my family members, especially my parents, for their patience, steadfast support, constant encouragement, and believe in me throughout my whole life. I would never have gotten this far without them at my side every step of the way.

Dedication

I dedicate this work

To my Beloved Mother and Father

To my Dear Sisters and Brother

To all my relatives and Friends

To all my teachers through my academic journey

Contents

Abstract. I
Acknowledgments IV
Dedication V
Table of contents VI
List of figures IX
List of tables XII
List of symbols XIV

Chapter 1 General introduction 17

1.1 Introduction 17
1.2 Literature review 18
1.3 Motivation 20
1.4 Thesis organization 21

Chapter 2 Protection system 22

2.1 Objectives 22
2.2 Protection System 23
2.3 Zones of Protection 26
2.4 Primary and Backup Protection 27
2.5 Overcurrent Protective Devices 27
2.5.1 Fuses: 27
2.5.2 Bimetallic Relays: 28
2.5.3 Overcurrent Protective Relays: 28
2.5.4 Instantaneous OCR (IOCR) 29
2.5.5 Definite Time OCR (DTOCR) 30
2.5.6 Inverse Time OCR (ITOCR) 31

2.6 Mixed Characteristic Curves 31
2.6.1 Definite-Time Plus Instantaneous 32
2.6.2 Inverse-Time Plus Instantaneous 32
2.6.3 Inverse-Time Plus Definite-Time Plus Instantaneous 32
2.6.4 Inverse-Time Plus Definite-Time 34
2.6.5 Inverse Definite Minimum Time (IDMT) 35
2.7 User-Defined Curves 35
2.8 Differentiating Between Time Dial Setting and Time Multiplier Setting 36
2.9 Overcurrent Relays Coordination 37

2.9.1 Relay Grading in Radial Systems 37
2.9.2 Directional Overcurrent Relays 39
2.9.3 Coordination of DOCRs 41

2.10 General Mechanism to Optimally Coordinate Directional Overcurrent Relays 42
2.11 Conclusion 43

Chapter 3 Optimal coordination of directional overcurrent relay in electrical power systems 44

3.1 Introduction 44
3.2 Problem formulation 45
3.2.1 Objective function 45
3.2.2 Relay characteristics 45
3.2.3 Constraints 46
3.3 Proposed optimization algorithm 47
3.3.1 The original marine predator algorithm 47
3.3.2 Elite Marine Predators Algorithm 51
3.4 Results and discussion 53
3.4.1 Test system 1: the 3-bus system 54
3.4.2 Test system 2: the 8-bus system 57
3.4.3 Test system 3: the 9-bus system 61

3.4.4 Test system 4: the 15-bus system.....65
3.5 Conclusion.....70

Chapter 4 optimal coordination of DOCRs in microgrids.....71

4.1 Introduction.....71
4.2 The adaptive microgrid protection scheme based on dual settings DOCRs.....72
4.2.1 Problem formulation.....72
4.2.2 proposed protection technique.....72
4.2.3 Test system and results:.....73
4.2.4 Results and discussion.....74
4.3 The adaptive Protection Coordination for microgrids utilizing user-defined DOCRs characteristics with different groups of settings.....77
4.3.1 Problem formulation.....77
4.3.2 Technical Constraints.....79
4.3.3 The proposed optimization method.....82

A. The original Hanger games search algorithm.....82
B. The modified hanger games search algorithm.....83
4.3.4 Simulation and results.....85
A. Test system.....85
B. Discussion.....101

4.4 Conclusion.....103

Chapter 5 General conclusion and future work.....104
References
List of Publications

List of figures

Figure 2-1: General representation of complete power system cycle. 23
Figure 2-2 Illustrated 1ϕ protection system. 25
Figure 2-3 Zones of protection. 26
Figure 2-4 Time-current characteristic curve of ITOCR/DCOCR. 29
Figure 2-5 Illustration of two-bus radial network. 30
Figure 2-6 Time-current characteristic curve of DTOCR. 31
Figure 2-7 OCR equipped with instantaneous and definite-time elements. 32
Figure 2-8 OCR equipped with instantaneous and inverse-time elements. 33
Figure 2-9 OCR equipped with instantaneous, definite-time, and inverse-time elements. 33
Figure 2-10 OCR equipped with instantaneous and definite-time elements. 34
Figure 2-11 Characteristic of inverse definite minimum time over current relay (IDMT OCR). .34
Figure 2-12: Radial system example. 37
Figure 2-13: Time grading for the radial system example. 37
Figure 2-14: Concept of current grading in radial systems. 38
Figure 2-15: Concept of inverse-time grading in radial systems. 39
Figure 2-16: Single-end fed power system of parallel feeders with only OCRs. 40
Figure 2-17: Single-end fed power system of parallel feeders with OCRs and DOCRs. 41
Figure 2-18 General flowchart to optimally coordinate DOCRs. 42
Figure 3-1. flowchart of the proposed algorithm 53
Figure 3-2. 3-bus system. 54
Figure 3-3**.** Graphical illustration of the total operating time of EMPA compared to the literature for 3-bus test system. 56
Figure 3-4**.** Convergence curve of the MPA vs EMPA algorithms in the 3-bus system. 56
Figure 3-5 . IEEE 8-bus system. 58
Figure 3-6**.** Graphical illustration of the total operating time of EMPA compared to the literature for 8-bus test system 60
Figure 3-7**.** Convergence curve of the MPA vs EMPA algorithms in the 8-bus system. 60

Figure 3-8. IEEE 9-bus system. 62
Figure 3-9. Graphical illustration of the total operating time of EMPA compared to the literature for 9-bus test system. 64
Figure 3-10. Convergence curve of the MPA vs EMPA algorithms in the 9-bus system. 65
Figure 3-11: IEEE 15-bus system. 66
Figure 3-12. Graphical illustration of the total operating time of EMPA compared to the literature for 15-bus test system. 69
Figure 3-13. Convergence curve of the MPA vs EMPA algorithms in the 15-bus system. 69
Figure 4-1. The adaptive protection scheme 73
Figure 4-2. IEEE 14 bus distribution system. 74
Figure 4-3. Relays coordination time interval (CTI) for the grid connected 14-bus distribution system. 76
Figure 4-4. Relays coordination time interval (CTI) for the islanded 14-bus distribution system. 77
Figure 4-5. Flowchart of the proposed technique. 81
Figure 4-6. Distribution network of the IEEE 14-bus test system. 86
Figure 4-7. Numerous contingencies and operating modes of the IEEE 14-bus test system's meshed distribution section. 87
Figure 4-8. Convergence curve of the HGS vs MHGS optimization algorithms under the main configuration (C1). 91
Figure 4-9. Convergence curve of the HGS vs MHGS optimization algorithms under an islanded system scenario (C4). 93
Figure 4-10. Convergence curve of the HGS vs MHGS optimization algorithms under a DG outage scenario (C 7) 95
Figure 4-11. Convergence curve of the HGS vs MHGS optimization algorithms under a line outage scenario (C 11) 98

List of tables

Table 2-1: Most popular standard coefficients for calculating the operating time of European and North American relays. 36
Table 3-1: Curve types of the IEC relays 45
Table 3-2**:** Short-circuit currents flowing through pairs of PR-BR relays in the 3-bus system 55
Table 3-3: Ct ratio 55
Table 3-4**:** Optimal settings and total operating time for the 3-bus system. 55
Table 3-5**:** P/B protection operational times for the IEEE 3-bus system 55
Table 3-6**:** Comparison of the results for the IEEE 3-bus system. 56
Table 3-7**:** Short-circuit currents flowing through pairs of PR-BR relays in the 8-bus system 58
Table 3-8: Optimal settings and total operating time for the 8-bus system. 59
Table 3-9**:** P/B protection operational times for the IEEE 8-bus system. 59
Table 3-10: Comparison of the results for the IEEE 8-bus system. 60
Table 3-11**:** Short-circuit currents flowing through pairs of PR-BR relays in the 9-bus system .62
Table 3-12**:** Optimal settings and total operating time for the 9-bus system. 63
Table 3-13**:** P/B protection operational times for the IEEE 9-bus system. 63
Table 3-14: Comparison of the results for the IEEE 9-bus system. 64
Table 3-15: CT ratio for 15 bus system relays 67
Table 3-16: Optimal settings and total operating time for the 15-bus system. 67
Table 3-17**:** P/B protection operational times for the IEEE 15-bus system. 68
Table 3-18: Comparison of the results for the IEEE 15-bus system. 69
Table 4-1: Short circuit current values in the main scenario (scenario1). 75
Table 4-2Table 4.2: Short circuit current values in scenario2. 75
Table 4-3: Relay settings and operation times for grid connected 14-bus distribution system. 76
Table 4-4: Relay settings and operation times for islanded 14-bus distribution system. 76
Table 4-5: Short circuit current values in the main scenario (C1). 88
Table 4-6: Near-end fault currents in different scenarios (C1-C15). 89
Table 4-7: Far-end fault currents in different scenarios (C1-C15). 90
Table 4-8: Optimized settings and operating times of DOCRs under scenario 1 (C1). 91
Table 4-9: Optimized settings and operating times of DOCRs under scenario 2 (C2). 92

Table 4-10: Optimized settings and operating times of DOCRs under scenario 3 (C3). 92
Table 4-11: Optimized settings and operating times of DOCRs under scenario 4 (C4). 93
Table 4-12: Optimized settings and operating times of DOCRs under scenario 5 (C5). 94
Table 4-13: Optimized settings and operating times of DOCRs under scenario 6 (C6). 94
Table 4-14: Optimized settings and operating times of DOCRs under scenario 7 (C7). 95
Table 4-15: Optimized settings and operating times of DOCRs under scenario 8 (C8). 96
Table 4-16: Optimized settings and operating times of DOCRs under scenario 9 (C9). 96
Table 4-17: Optimized settings and operating times of DOCRs under scenario 10 (C10). 97
Table 4-18: Optimized settings and operating times of DOCRs under scenario 11 (C11). 97
Table 4-19: Optimized settings and operating times of DOCRs under scenario 12 (C12). 98
Table 4-20: Optimized settings and operating times of DOCRs under scenario 13 (C13). 99
Table 4-21: Optimized settings and operating times of DOCRs under scenario 14 (C14). 99
Table 4-22: Optimized settings and operating times of DOCRs under scenario 15 (C15). 100
Table 4-23: results comparison of optimal operating times of primary relays for all possible configurations (N-1 contingency). 100

List of symbols

CT	Current transformer
CTI	Coordination time interval
DG	Distributed generator
DOCR	Directional overcurrent relay
DN	Distribution network
PS	Plug Setting Current
TDS	time deal setting
I	Inverse
V.I	Very inverse
E.I	Extremely inverse
RCT	Relay curve type
COP	Coordination optimization problem
$T_{op,pr}$	Total primary relay's operating time considering near end faults
MG	Microgrid
SG	Smart grid
ADN	active distribution network
HGS	hanger games search algorithm
MHGS	modified hanger games search algorithm
EG	Electrical grid
OF	Objective function
T_{op}	Total primary relay's operating time
m	Number of primary relays
FA	Firefly Algorithm
IF	Fault current
LP	Linear Programming
MILP	Mixed-integer linear programming
MINLP	Mixed integer nonlinear programming

NLP	Non-linear programming
SA	Simulated annealing algorithm
DE	Differential Evolution
MEFO	Modified Electromagnetic Field Optimization
HWOA	Hybrid whale optimization algorithm
MWCA	Modified Water Cycle Algorithm
MRFO	Manta ray foraging optimization
AFDBA	Adaptive fuzzy directional bat algorithm

Chapter 1 General introduction

1.1 Introduction

Transmission and distribution lines in the power system network are used to move produced power from the producing station to the customer. The crucial objective is to consistently deliver power to the consumer end in order to make income. Moreover, modern power systems are facing a very complicated problem, the steadily increasing of electrical power demand while decreasing the installation of fossil fuels power plants due to the climate challenges. Thus, decentralized distribution generation mostly known as microgrid has recently received much attention, however, as loads fluctuate indiscriminately, overcurrent may pass through the transmission line. In the other hand, the numerous modes of operation of the microgrid (grid-connected and islanded) generate a range of fault situations, which impact the selectivity, sensitivity, and speed of the protection system.

Many other things can go wrong, including load changes that cause overcurrent, wind and tree damage to overhead transmission and distribution lines, insulation failures, transformer winding fires, and more. Because it might injure the electrical power equipment that is installed, Relays, circuit breakers, isolators, and other protection devices are installed in the system to safeguard it from failures. Together, these components detect flows and pinpoint their locations.

Many research on the optimal protection of traditional electrical distribution networks, active distribution networks (ADNs), microgrids (MGs), and smart grids (SGs) have been conducted. MGs may operate in electric distribution networks in two modes: connected to the upstream network or islanded. Protection coordination for MGs in both islanded and grid-connected modes would face significant challenges.

As a result, the dependability of the system is guaranteed for the remaining portion of the system. The notion of a backup plan is employed to guarantee the dependability of the protection system.

Each overcurrent device in this design has a backup overcurrent device. If a fault occurs and the first device is unable to resolve it, the second device can be used to resolve the fault current and safeguard the system. The better coordination of direction overcurrent relays is essential for improved power system efficiency and to avoid the issue of equipment damage, but it is a time-consuming and difficult process. DOCRs are the results of combining the overcurrent relay (OCR) with the directional unit. DOCRs activate only when the amplitude of the current exceeds a certain threshold and flows in the same direction as the DOCR. DOCRs have two variable settings: The plug Setting (PS) and the time dial setting (TDS). These variables affect how long a relay operates. A proper TDS and PS are needed for DOCRs in a power system to operate in cooperation. Relays' TDS and PS must be chosen to retain the best possible sensitivity, selectivity, speed, and dependability. However, the complexity of the electrical distribution network makes the traditional analytical approaches time-consuming and not very effective to compute the relay settings.

1.2 Literature review

The primary goal of this study is to find variable values that reduce operating time. Optimization techniques are used in many fields of research, including manufacturing, renewable energy, control systems, computer science, coordination in protection, and so on[1]. Therefore, coordinating DOCR using various optimization techniques is a hot issue right now. The goal is to optimize TDS and PS values in order to preserve different limitations while still meeting the minimum needed operating time [2, 3].

Many optimization techniques have been used to solve the coordination problem of DOCRs. Fuzzy-based GA method, Hybrid whale optimization algorithm and grey wolf were use in [4] and [5] respectively. In [6], graph theory based methods was employed to develop a solution for the coordination problem . Also, trial and error technique is used in [5] for relay coordination, a bigger iterative procedure is used, causing the convergence process to be delayed. Some traditional techniques, such as curve fitting [7] and analytical method [8]also have been applied to solve the problem. The majority of work has tackled the nonlinear relay coordinating problem

by expressing it as a linear optimization problem [9], in which the TDSs of relays are created at random while keeping the plug setting multiplier (PSM) constant [4, 10, 11]. At the moment, population based approaches such as: genetic algorithm (GA) [4], particle swarm optimization (PSO) [12], Modified particle swarm optimizer (MPSO) [12], ant colony optimization (ACO) [13], differential evolution [14] are employed to ensure proper relay coordination. Other approaches include harmonic search algorithm (HAS) [11], chaotic firefly algorithm (CFA) [15], hybrid gray wolf optimization (GWO) [5], is also checked for the issue. In [7], author used the hybrid nonlinear programming based GA-NLP to get the optimal coordination. The same thing was done using the Firefly-based algorithm in [16]. Also, In [10], the author utilize the water cycle algorithm (WCA) to obtain the optimal settings of the protective relays in the coordination issue. Other works, such as hybridized whale optimization [17] enhanced firefly [18], improved moth-flame [19], modified African vultures optimization algorithm[20] created an improved version with respect to the original optimization algorithm to address the problems of relay coordination.

Considering N-1 contingencies, grid connected and islanded modes of operation, these techniques provide sub-optimal results. Therefore, the optimal selection of RCTs, in addition to other setup criteria, has been incorporated in the problem design in various researches [21-23]. The trip duration of the DOCR is determined by three configuration factors, namely, pick-up current setting (PCS), time dial setting (TDS), and relay curve type (RCT). The configuration parameters must be selected in such a way that the main relays (PRs) trip in the lowest time feasible [25].

If only the selectivity requirements of the basic grid-connected design were considered, various protection coordination failures emerge in different topologies [24, 25]. Both the islanded and grid-connected modes for coordinating DOCR pairings have been seen in [26, 27]. Despite this, if the network hosts several sources or a large number of distributed generations (DGs), the aforementioned issue worsens. MG/SG suffers additional operating modes as a result of component outage contingencies[28]. In the COP experiments, transient contingencies such as single line failures and DG outages were observed[29]. The structure of microgrids is influenced by a variety of factors. The definition of N-1 contingency is an outage of any generator or line. Furthermore, the grid-connected and islanding operating modes cause changes in microgrid topologies[30]. Some effort as [14,18] have been expended in the literature to establish

protective coordination of transmission systems or distribution systems based on line outages or contingency considerations of DG units that have been explored in [31, 32]. Authors in [22, 23, 33] proposed a strategy for optimizing the protection coordination of microgrids based on N-1 scenarios, which takes the DGs outage into account. However, none of these studies have evaluated all microgrid topologies due to distribution system contingencies, DG units and lines outage, grid connected and islanded modes utilizing a four user defined dual settings groups techniques when dealing with relay coordination problems. As a result, there is a lack of expertise in proposing the optimal microgrid protection plan under diverse system topologies utilizing user defined parameters of DOCRs features.

1.3 Motivation

Modern power systems are facing a very complicated problem, the steadily increasing of electrical power demand while decreasing the installation of fossil fuels power plants due to the climate challenges [1]. Thus, decentralized distribution generation, which constitute microgrid, has recently received much attention. During a fault, a dependable protection strategy would eliminate just the faulty component of the power system, leaving the healthy pieces of the feeder intact. In other words, a suitable protection mechanism would provide optimal power use with little loss during a fault state by isolating just the defective portion from the main supply[2]. DOCRs are among the most important protective devices in the electricity system that operate at medium voltage. The fundamental objective of the directional overcurrent relay (DOCR) in a microgrid is to detect and remove the faulty area with minimum possible duration and without any negative consequences such as tripping mechanism failure. Malfunction can arise in two ways; DOCRs do not work when the permanent fault is at their reach point or an unwanted trip happens. This requires the use of backup protective device to ensure dependable protective system. There is no systematic method for the selection of settings for both primary and backup protective devices. To this, the coordination of the DOCRs has been converted to an optimization problem, where the objective is to minimize the response of the protective system. DOCRs' decision variables (DVs) are the Plug setting (PS), the Time dial setting (TDS) and the curve settings (A and B). DOCRs in use today are DSP devices with novel characteristics such as multiple setting groups (MSGs), continuous parameters, and event monitoring. DGs are

intermittent sources and subsequently their contribution in terms of power generation strongly depends on the weather conditions. For instance, a wind energy conversion based DG generate electricity if the wind velocity is greater than the cut in speed. The DG will be disconnected whenever the speed goes below the cut in speed. This fact results in many changes of the configuration of the distribution system to which the DGs are connected. Therefore, each configuration has different appropriate protective system settings. The feature of the MSGs allows the DOCRs to have many setting clusters, with only one MSG active in the present network configuration [3]. The numerous modes of operation of the microgrid (grid connected mode, islanded mode and line or DG outage) generate a range of fault situations, which affect the selectivity, sensitivity, and speed of the protection system

1.4 Thesis organization

This thesis has four main chapters.

Chapter one provides the introduction and motivation behind the research work. Besides, a literature review of the previous works is well discussed.

Chapter two, provides a general review of the commonly protection schemes used in power systems against different faults and abnormal conditions.

Chapter three, presents a new optimization technique for optimal coordination of directional overcurrent relays, and a comparative study between other methods using different IEEE power systems.

Chapter four, discuss on the use of an adaptive protection scheme in microgrid considering deferent modes of operation.

Chapter 2 Protection system

2.1 Objectives

This chapter is intended to underscore the pivotal role of power system protection. It provides a taxonomy of open- and short-circuit faults, demarcates distinct protection zones, and elucidates the operational methodologies of primary and backup relays. Furthermore, the chapter introduces overcurrent relays along with their various categories and sub-categories. Fundamentally, the chapter seeks to illuminate the core tenets of protection and accentuates the imperative of harmonizing protective devices.

An electric power system fundamentally encompasses three cardinal parts:

1. Power generation
2. Power transmission
3. Power distribution

The interlinkages amongst these components can be graphically represented in Figure 2.1. Historically, the structure of these components was relatively uncomplicated, and challenges such as power outages and load shedding were not of substantial concern due to the limited reliance on electricity.

However, in the era of modern civilization, the demand for electricity has exponentially increased, powering a myriad of applications, from domestic appliances and street lights to industrial factories, transportation systems, and telecommunication networks. This has engendered a high level of dependency on electricity, rendering life without electrical energy virtually inconceivable. To cater to these burgeoning requirements, contemporary systems are designed and managed to ensure the economical and reliable delivery of energy to the points of

consumption. Consequently, modern systems are technologically sophisticated but also complex to operate and control without any failures, which are referred to as “faults” in the domain of protection engineering.

If a fault is not promptly addressed, it could precipitate a range of detrimental outcomes. These include the degradation of cable insulations due to the heat engendered by high current, damage to devices and equipment, and a shortfall in power delivery to consumers, among others.

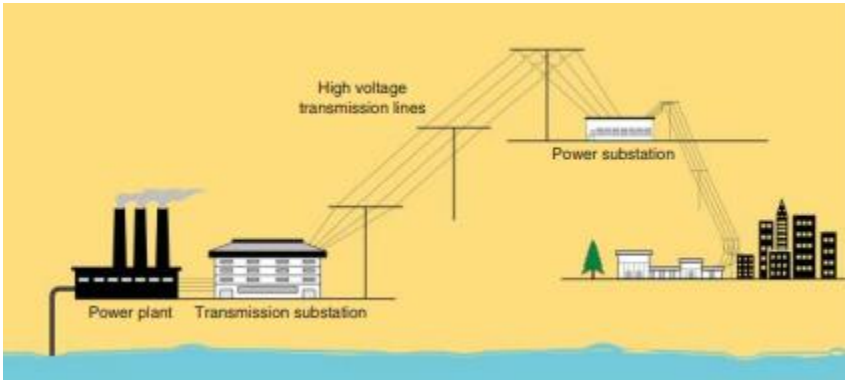

Figure 2-1: General representation of complete power system cycle.

2.2 Protection System

From an engineering standpoint, the complete eradication of all fault sources or causes is an unfeasible endeavor due to numerous factors such as uncontrollable/unforeseen abnormal events and the substantial cost associated with maintaining a highly secure and reliable system, especially when some of these faults are not predetermined or occur sporadically. A more pragmatic and economically viable approach is to nullify the effects of these causes (i.e., the faults themselves) through rapid detection and clearance actions. Consequently, any fault can be precluded from undermining system integrity, its impacts can be effectively mitigated, and the system can be shielded from any unstable operating conditions.

The apparatus typically utilized in power system protection comprise:

- Non-electrical relays (such as bimetallic, Buchholz, and pressure relief relays).
- Electrical relays (such as distance, overcurrent, differential, over/under voltage, over/under frequency, reverse power, and over flux relays).
- Reclosers.
- Sectionalizers.

- Fuses.

Faults can be promptly identified if the system voltages and/or currents are known. All the requisite information can be extracted from these two fundamental signals. Hence, these two fundamental signals need to be measured expeditiously and accurately. To fulfill this requirement, a current transformer (CT) and a potential transformer (PT2) are employed, as illustrated in Figure 2.2.

It is worth noting that there are two stages of step-down current and voltage quantities. The first stage, which involves a substantial stepping action, is executed through these primary transformers, while the second stage is conducted through what are referred to as auxiliary transformers. These diminutive transformers are positioned inside protective relays. Certain factors must be considered regarding the received signals, such as the effects of decaying DC components, harmonic, and CT saturation.

Protective relays can be categorized according to the technology as follows:

- Hardware-Based Protective Relays:
    - Electromechanical (or Electromagnetic) Relays
    - Solid-State (or Static) Relays
    - Digital Relays
- Numerical (or Software-Based) Protective Relays:
    - Microprocessor-Based Relays
    - DSP-Based Relays

From this classification, it is evident that electromechanical relays (such as moving coil, attracted armature, induction, and motor operated devices) represent the first generation of OCRs, having emerged in the early 1900s. Their use is constrained by the need for regular maintenance and calibration due to their mechanical moving parts. They possess a limited number of discrete values of PS and TMS, which means that the feasible search space is quite restricted, making it challenging to optimize feasibly. Additionally, their response is slower due to their over-shoot time caused by inertia. Their rudimentary technology renders them oblivious to each other, necessitating the use of three to four relays to safeguard all three phases plus the ground line, as depicted in Figure 2.5. However, these devices do offer some advantages, such as their stability and insensitivity to network conditions, and they continue to be in service due to their longevity.

Furthermore, their long lifespan has resulted in a wealth of experienced experts capable of coordinating these types of relays.

The second-generation OCRs were developed to leverage analog electronic technology to emulate the first generation. These relays are referred to as solid-state or static relays. The primary technical issue encountered with these relays is that their stability can be affected by ambient temperature. Also, accurate passive components (such as resistors, capacitors, and inductors) are necessary to minimize the total error.

Within a decade, the third-generation digital relays were introduced. Numerous manufacturers successfully developed new techniques to facilitate bidirectional communication between these relays through some standard protocols.

While all the inherent shortcomings of the electromechanical and solid-state relays can be permanently addressed by the third-generation relays, they remain hardware-based relays. Therefore, to have programmable relays, the fourth-generation numerical relays were conceived. As relay manufacturers discovered that the numerical relays share the same hardware (analog and digital inputs modules, auxiliary CTs and PTs, low pass filters, multiplexer, analog to digital converter, microprocessor, RAM and ROM, digital output module, communication card, power supply, etc.), some of these relays can function as general-purpose relays. These innovative relays are termed numerical relays, and due to their capabilities, some researchers regard them as intelligent electronic devices (IEDs). They are manufactured based on microcontrollers, microprocessors, or even digital signal processors (DSPs) for high computational applications. All the relay settings, instructions, and operations can be updated, modified, or even upgraded through some special software provided by their original equipment manufacturers (OEMs).

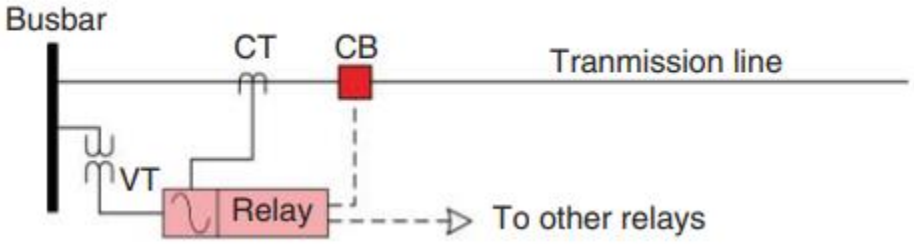

Figure 2-2 Illustrated 1ϕ protection system.

2.3 Zones of Protection

To ensure optimal protection designs, power systems are divided into several zones, each capable of being individually isolated against its specific faults. Faults occurring within the zone are termed as in-zone faults, while those outside are classified as out-zone faults. This strategy also contributes to minimizing the total number of isolated components. Figure 2.3illustrates the concept of protection zones using a basic system. It's important to highlight that the overlaps between the zones are vital to ensure all-encompassing protection

In practical terms, these zones are secured by deploying a combination of different protective relays. In addition to the general-purpose protective relays, there are numerous types of protective relays that can be categorized according to the operational principles:

- Distance relays
- Overcurrent relays
- Differential relays
- Over/under voltage relays
- Over/under frequency relays
- Reverse power relays
- Over flux relays
- etc.

For example, power transformers are protected by a collection of relays, such as differential, overcurrent, overflux, etc.

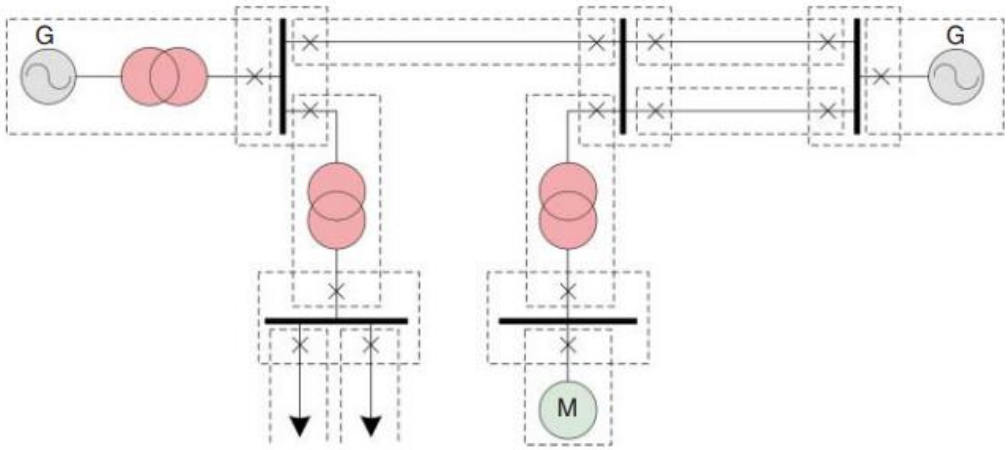

Figure 2-3 Zones of protection.

2.4 Primary and Backup Protection

Effective protection system designs can be established if each zone is equipped with a number of primary and backup relays. The initial set of relays serve as the first line of defense for in-zone faults, while the secondary set of relays provide a second layer of protection for out-zone faults. Backup relays could be positioned locally at the same site as the primary relays to monitor the same internal faults, known as local backup relays. Alternatively, they can be placed in different zones to observe the preceding faults as external faults, referred to as remote backup relays. These backup relays are crucial as there is always a possibility of failures occurring in any one of the primary protective relays. This implies that the second line of defense must always be prepared. Later, some examples will be provided to demonstrate how to choose the appropriate backup relays for each primary relay.

2.5 Overcurrent Protective Devices

Electric protective relays are extensively utilized in power systems. However, there exist other devices that can also serve to safeguard certain electrical components. These include Buchholz relays, pressure relief relays, fuses, and bimetallic relays. The latter protective devices are elaborated below.

2.5.1 Fuses:

A fuse is a safety apparatus in the electrical domain that functions to provide overcurrent protection to an electrical circuit. Its fundamental component is a metal wire or strip that liquefies when an excessive current passes through it, consequently disrupting the current. Fuses have been integral safety devices since the inception of electrical engineering. However, once a fuse has been activated, it becomes an open circuit and must be either replaced or rewired, contingent on its type. Furthermore, fuses are utilized in power systems up to 115,000 volts AC. High-voltage fuses are employed to safeguard instrument transformers used for electricity metering, or for minor power transformers where the cost of a circuit breaker is not justified.

2.5.2 Bimetallic Relays:

A bimetallic relay comprises a diminutive heater element wired in series with the motor and a bimetal strip that can function as a trip lever. The bimetal strip is fabricated from two different metals bonded together. When the current surpasses a certain threshold, the heat produced causes the bimetal strip to flex, instigating the trip mechanism. However, bimetallic relays have a slower response time in comparison to electronic relays and are more vulnerable to ambient temperature, which can influence their precision.

2.5.3 Overcurrent Protective Relays:

Overcurrent protection can be provided by using fuses or relays, Because coordination between diverse devices becomes difficult in big and complicated networks, OCRs are better suited for them. However, because fuses are inexpensive and accessible in a variety of time responses, they are still employed in conjunction with protective OCRs in certain big networks.

In comparison to other costly relays, OCRs may compromise between several design goals, which is why they are popular and frequently employed in power system protection.

Non-directional OCRs receive just currents from power networks. Current transformers (CTs) provide these input currents. The main parameter of OCRs is referred to as the plug setting (PS), which is also referred to as the current setting multiplier (CSM) in certain publications. The other setting is known as time multiplier setting (TMS), which is also referred to as time setting multiplier (TSM) in certain sources. It should be noted that there are two standards in play here: European and North American. As a result, the plug setting is also known as the pickup setting (Ip), pickup current setting (PCS), and current tap setting (CTS) in various sources. Time dial setting (TDS) and time lever setting (TLS) are alternate names for the time multiplier setting.

Another key distinction is that TMS has a different range than TDS. More details will be provided later in this Chapter when both standards are used to determine the appropriate relay settings.

The fault severity can be seen by OCRs via the following equation:

$$PSM = {I_{relay}}/{PS} \tag{2.1}$$

where PSM is the plug-setting multiplier and Irelay is the fault current sensed by the relay; refers to the secondary side of the CT. If PSM is 1, the system is fault-free.

OCRs are classified into three categories based on the relationship between fault current and relay operating time, which is known as the time-current characteristic curve (TCCC):

2.5.4 Instantaneous OCR (IOCR)

This sort of relay, also called as Definite Current OCR (DCOCR), contains just PS. Figure 2.4 shows the TCCC. It demonstrates that IOCR functions when the current surpasses the set Iins. As a result, it may be mathematically represented as follows:

$$T = \begin{cases} T_{ins} & , \quad if \quad I_{relay} \geq I_{ins} \\ \infty & , \quad \text{if} \quad \text{otherwise} \end{cases} \tag{2.2}$$

where *Iins* is the fixed value that the fault current must achieve and Tins is the intrinsic time delay that IOCR cannot overcome.

This form of relay cannot be used to discern between two defective sites if the source impedance is substantially greater than the impedance between these two points, i.e. ZS>>ZL. For example, if there are two faults, one at busbar A and the other at busbar B in Figure 2.5, the operating duration of the nearest fault will be about the same as that of the furthest fault.

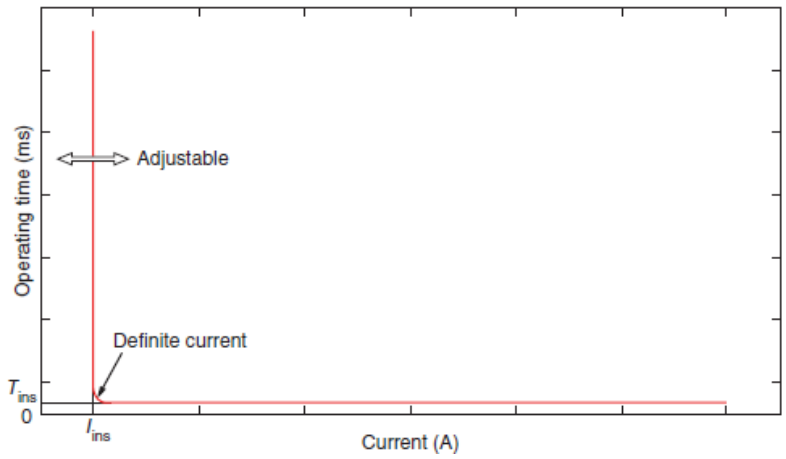

Figure 2-4 Time-current characteristic curve of ITOCR/DCOCR.

2.5.5 Definite Time OCR (DTOCR)

This type, in addition to PS, has a time delay setting (Tset). The relay only activates if the fault current exceeds the predetermined value and the fault duration lasts longer than the predefined delay. As a result, the defect at various sites may be clearly detected, as seen in Figure 2.6.
The biggest drawback of this kind, as seen in Figure 2.5, is when the defect is close to the source. Higher fault currents are predicted in this condition. Instead of acting immediately to clear that extremely severe fault, the relay will wait until Tset is reached. The following equation will determine whether or not DTOCR should operate based on that figure:

$$T = \begin{cases} T_{set} & , \quad if \quad I_{relay} \geq I_{set} \\ \infty & , \quad \text{if} \quad \text{otherwise} \end{cases} \tag{2.3}$$

here Iset is the specified value that the fault current must reach and Tset is the predetermined time delay that DTOCR must wait for.

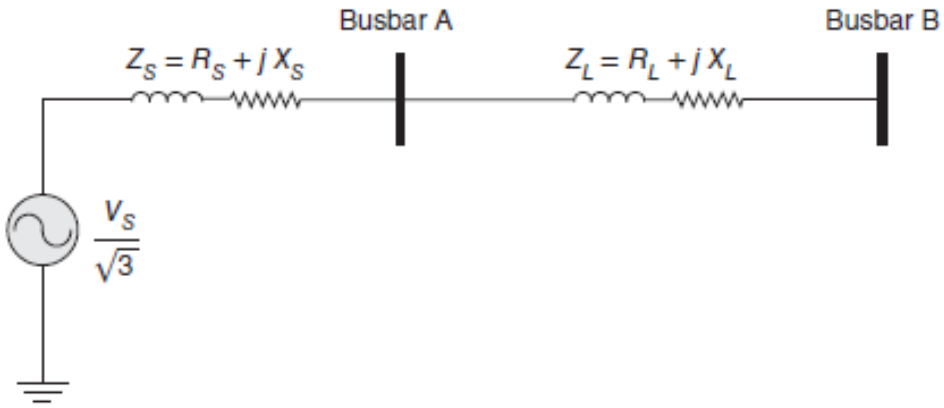

Figure 2-5 Illustration of two-bus radial network.

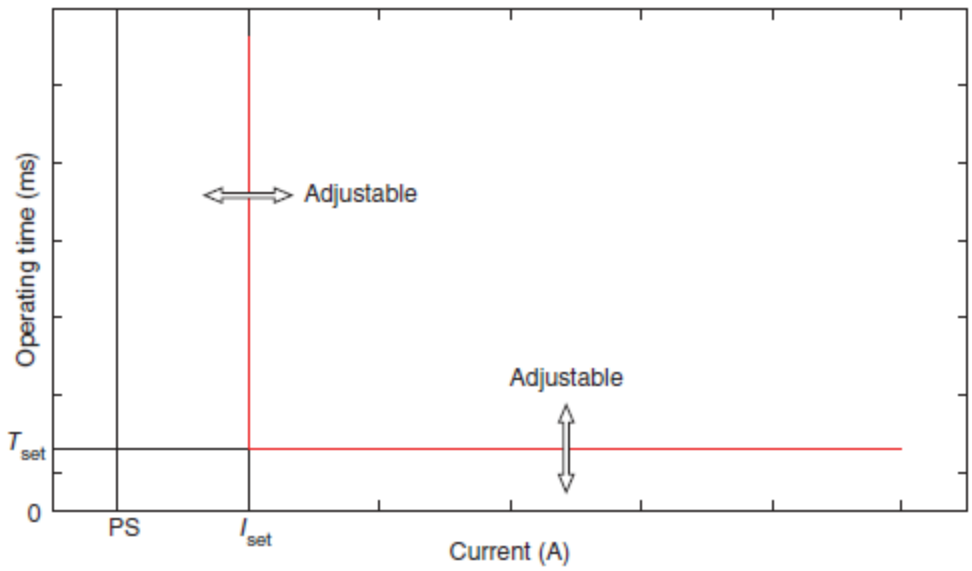

Figure 2-6 Time-current characteristic curve of DTOCR.

2.5.6 Inverse Time OCR (ITOCR)

PS and TMS are both present in this form of relay. Because its operation period is inversely proportional to the short-circuit current value, it can address the previous DTOCR problems:

$$T \propto \frac{1}{PSM} \tag{2.4}$$

Someone may inquire about (2.4)'s mathematical model! Many models have been proposed to simulate the real operation time of these types of OCRs. These models are critical for engineers to replicate the behavior of protective relays in computers in order to acquire appropriate and optimal settings. Previously, the most basic method for calculating the operation time of ITOCRs was to use certain standard log sheets given by OEMs.

2.6 Mixed Characteristic Curves

We've already seen the three main OCR curves. Each of them has advantages and disadvantages. The challenge here is if we can hybridize between these three curves such that the advantages may be combined and the downsides reduced. Yes, because these pieces are created as distinct units, we may do so. We have four hybrid setups to choose from, which are as follows:

2.6.1 Definite-Time Plus Instantaneous

Figure 2.7 depicts this combination of definite-current and definite-time components. It functions as a definite-time OCR for a narrow range of short-circuit currents between Iset and Iins.
The relay will take urgent action to clear the fault if Irelay reaches the maximum permitted limit (Iins).

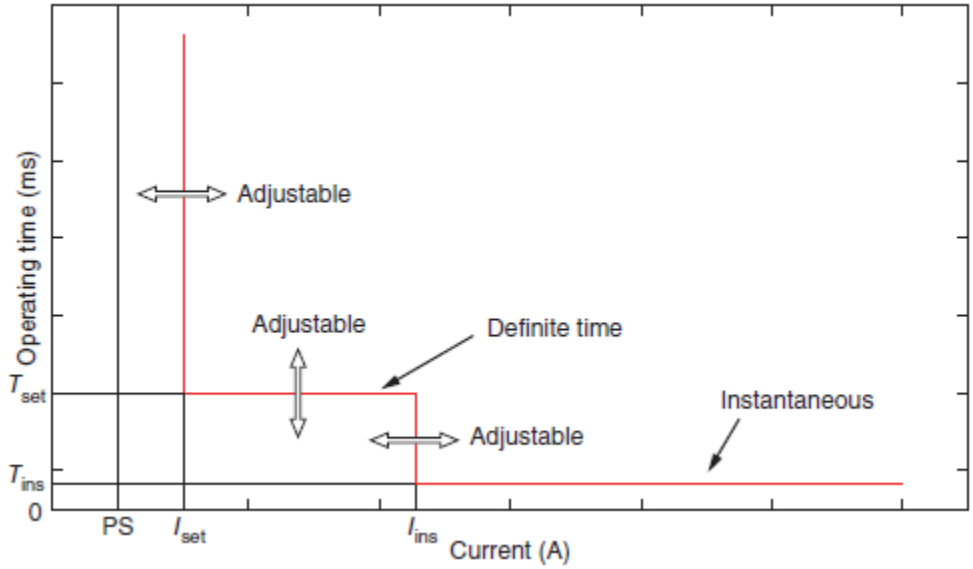

Figure 2-7 OCR equipped with instantaneous and definite-time elements.

2.6.2 Inverse-Time Plus Instantaneous

Figure 2.8 depicts the identical approach, except that the definite-time characteristic has been substituted with the inverse-time characteristic. As a result, the operating time reduces exponentially until it reaches Iins, at which point the relay is authorized to take rapid action to isolate the problematic component. It should be remembered that Iins is a programmable parameter.

2.6.3 Inverse-Time Plus Definite-Time Plus Instantaneous

Figure 2.9 depicts this distinctive curve. It is a sophisticated multi-stage model made up of three main parts. It is mostly employed in numerical relays.12 The operating time of OCR, as shown, begins at a high value when Irelay is close to PS and then declines exponentially as Irelay grows.

When Irelay reaches Iset, the operational time equals Iset. As a result, T will stay constant until the relay reaches the next threshold (Iins) when it may work instantly.

Someone could consider rearranging these components as follows:

Definite-Time ⇒ Inverse-Time ⇒ Instantaneous

Special relays of this type can be programmed in numerical relays that support customized TCCCs. This structure, however, contradicts the objective of employing the inverse-time characteristic.

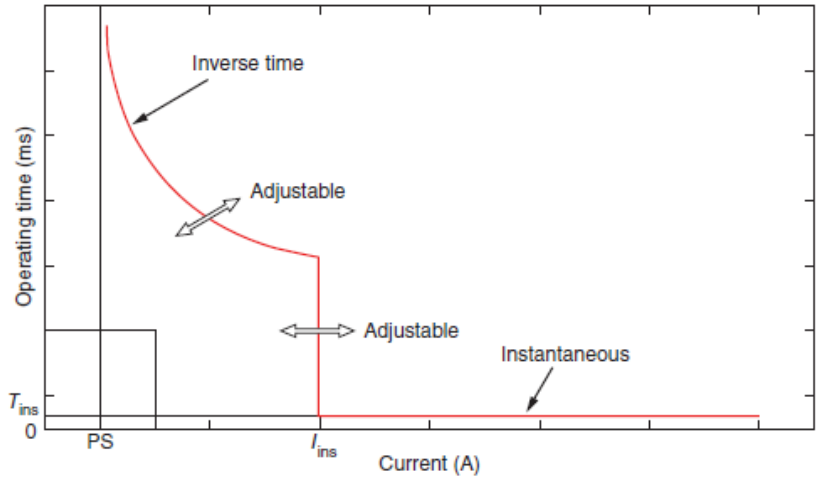

Figure 2-8 OCR equipped with instantaneous and inverse-time elements.

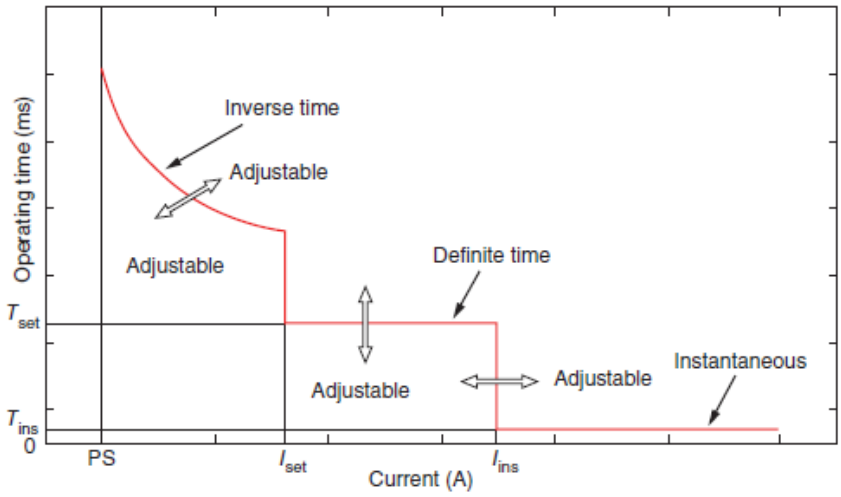

Figure 2-9 OCR equipped with instantaneous, definite-time, and inverse-time elements.

2.6.4 Inverse-Time Plus Definite-Time

Figure 2.10 depicts this configuration. As Irelay grows, T falls exponentially.

In contrast to Figure 2.8, the relay here will not respond immediately when Irelay hits the threshold (i.e. Iset). The operation time will instead be constant and equal to Tset.

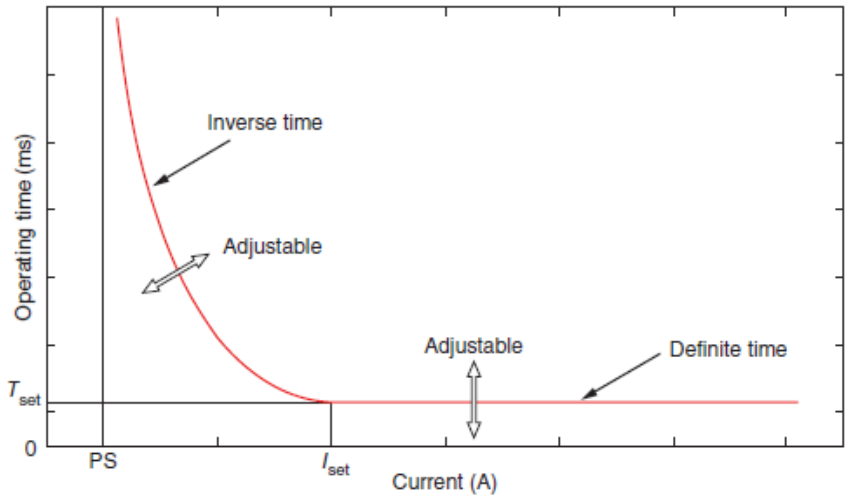

Figure 2-10 OCR equipped with instantaneous and definite-time elements.

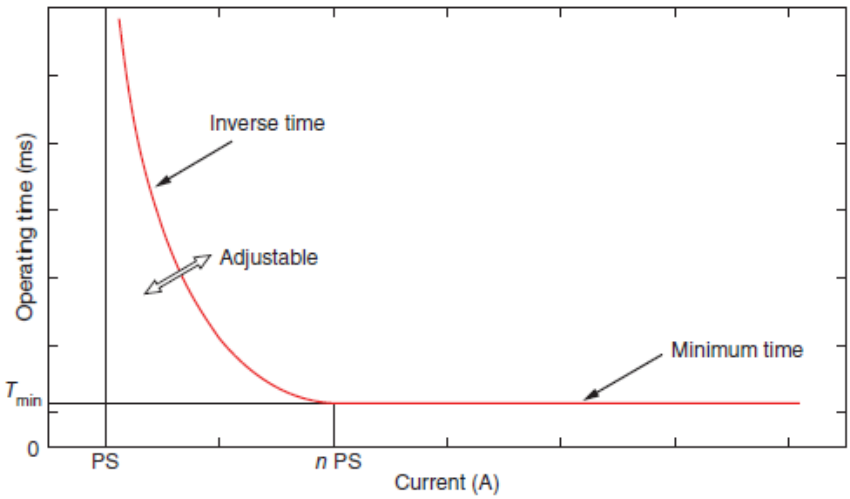

Figure 2-11 Characteristic of inverse definite minimum time over current relay (IDMT OCR).

Again, while we may switch the two pieces to get (definite-time + inverse-time), this arrangement is not advised since it renders the inverse-time feature useless.

2.6.5 Inverse Definite Minimum Time (IDMT)

It might be viewed as a realized version of the inverse-time curve or as a variant of the mixed curve depicted in Figure 2.10. Figure 2.11 depicts a popular and well-known curve known as the IDMT curve. We may think of it as a mixed (inverse-time + definite-time) curve where Iset equals certain multiples of PS and the operational time reaches an unmanageable number termed Tmin.

The rationale for obtaining this particular curve is that the inverse-time curve depicted in Figure 2.13 depicts an ideal relay that cannot be realized. The stepped-down current on the secondary side of CT grows as the fault current on the main side of CT increases. This will continue until the transformer gets saturated, at which point the secondary current will no longer grow.

At n multiples of PS, this phenomena will occur.After that point, the relay will not observe a rise in Irelay, and so T will not exceed the saturated limit.

2.7 User-Defined Curves

At this point, we've looked at how to simulate the operation of electromechanical/electromagnetic and solid-state/static inverse-time overcurrent relays. The narrative becomes more exciting with programmable relays! Assume we can program protective relays to accept any time-current characteristic curve defined by end users. This can be accomplished in two ways, Customized Formulas or Fixed Formula with User-Defined Parameters.

The fixed formula with user-defined paramerters may be accomplished simply by altering the parameters of the model used to compute operational time. For instance, consider the IEC standard model with user-defined A and B. This is the most commonly used because it is simple to program in optimization algorithms to efficiently coordinate protective relays without affecting the basic structure of the objective function being reduced.

2.8 Differentiating Between Time Dial Setting and Time Multiplier Setting

Table 2.1 summarizes the coefficients of the most prevalent overcurrent protection models. We can observe that the variable TDM's side restriction is not constant. As a result, we must include an if-statement in optimization methods to change the lower and higher boundaries dependent on the model used to imitate overcurrent relays.

Table 2-1: Most popular standard coefficients for calculating the operating time of European and North American relays.

Type of curve	**Standard**	**TDS/ TMS**	α	β	γ	ξ
IEC Standard Inverse (SI)	IEC/A	TMS	0.02	0.14	0	1
IEC Very Inverse (VI)	IEC/B	TMS	1	13.5	0	1
IEC Extremely Inverse (EI)	IEC/C	TMS	2	80	0	1
IEC Ultra-Inverse (UI)	IEC	TMS	2.5	315.2	0	1
IEC Long Time Inverse (LTI)	IEC/UK	TMS	1	120	0	1
IEC Short Time Inverse (STI)	IEC/FR	TMS	0.04	0.05	0	1
IEEE Long Time Inverse	IEEE	TDS	0.02	0.086	0.185	1
IEEE Long Time Very Inverse	IEEE	TDS	2	28.55	0.712	1
IEEE Long Time Extremely Inverse	IEEE	TDS	2	64.07	0.25	1
IEEE Moderately Inverse	IEEE (IEC/D)	TDS	0.02	0.0515	0.114	1
IEEE Very Inverse	IEEE (IEC/E)	TDS	2	19.61	0.491	1
IEEE Extremely Inverse	IEEE (IEC/F)	TDS	2	28.2	0.1217	1
IEEE Short Time Inverse	IEEE	TDS	0.02	0.167 58	0.118 58	1
IEEE Short Time Extremely Inverse	IEEE	TDS	2	1.281	0.005	1
US Moderately Inverse (U1)	US	TDS	0.02	0.0104	0.2256	1
US Inverseb)(U2)	US	TDS	2	5.95	0.18	1
US Very Inverse (U3)	US	TDS	2	3.88	0.963	1
US Extremely Inverse (U4)	US	TDS	2	5.67 (ISA, 2011), 5.64 (SEL, 2013)	0.0352 0.024 34	1
US Short Time Inverse (U5)	US	TDS	0.02	0.003 42	0.002 62	1
CO short time inverse (CO2)	CO	TDS	0.02	0.023 94	0.016 94	1
CO long time (CO5)	CO	TDS	1.1	4.842	1.967	1
CO definite minimum time (CO6)	CO	TDS	1.4	0.3164	0.1934	1
CO moderately inverse time (CO7)	CO	TDS	0.02	0.0094	0.0366	1
CO time inverse (CO8)	CO	TDS	2	5.95	0.18	1
CO very inverse time (CO9)	CO	TDS	2	4.12	0.0958	1
CO extremely inverse time (CO11)	CO	TDS	2	5.57	0.028	1
UK Rectifier Protection	RECT	TDS	5.6	45 900	0	1
BNP (EDF)	EDF	TMS	2	1000	0.655	1
RI	RI	TMS	−1	−4.2373	0	1.436 44

2.9 Overcurrent Relays Coordination

The purpose of this section is to provide a basic understanding of relay coordination. This topic is addressed by introducing broad principles of relay grading utilizing various forms of overcurrent relays (OCRs), such as definite-time overcurrent relays (DTOCRs), definite-current overcurrent relays (DCOCRs), and inverse-time overcurrent relays (ITOCRs). Beginning with current and time gradings, the significance of inverse-time grading is addressed by solving various radial systems.

The technical challenge linked with the basic approach utilized to improve relay settings is explored in the next sections.

2.9.1 Relay Grading in Radial Systems

Previously in this Chapter, we looked at many sorts of OCRs and associated TCCCs. The relays in radial systems may be simply coordinated to guarantee that the key devices run first. This may be accomplished by selecting the appropriate parameters. The three most common relay grading techniques are briefly detailed in the sections that follow.

A. Time Grading

The aim here is to have the nearest circuit breaker (CB) open first. As a result, as the relay is positioned more away from the source, the operational time decreases, and vice versa.

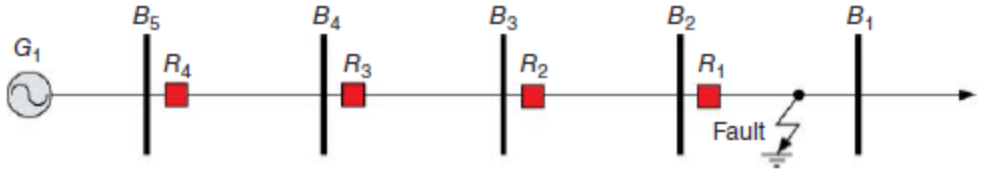

Figure 2-12: Radial system example.

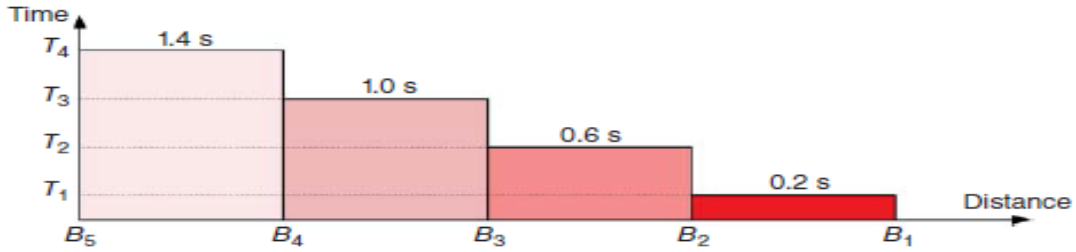

Figure 2-13: Time grading for the radial system example.

B. Current Grading

Because fault current is related to fault distance, the goal here is to safeguard the zones of radial systems based on fault current values. In other words, the operational time of protective relays is determined by their distance from the source. Figure 2.14 explains the overall concept underlying the present grading process. In contrast to Figure 2.13, the current magnitude is utilized here to indicate the severity of the fault.

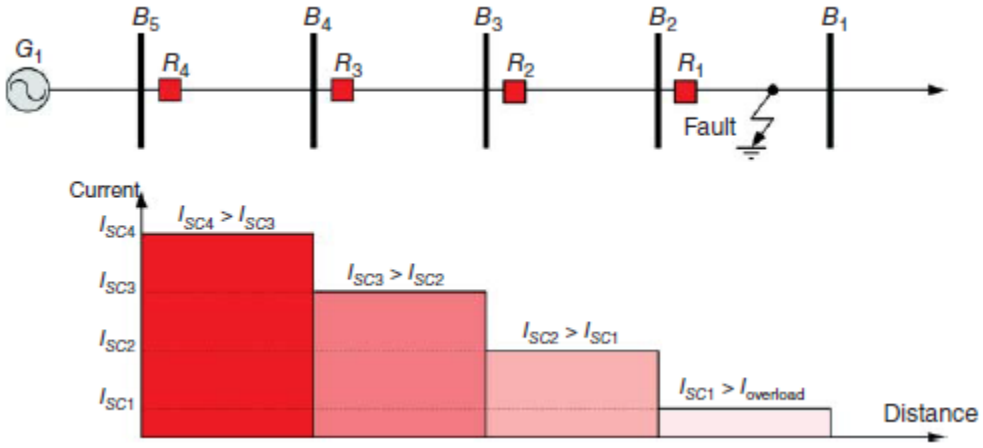

Figure 2-14: Concept of current grading in radial systems.

C. Inverse-Time Grading

To address the fundamental weakness of the preceding relay grading, the protective relay should be capable of distinguishing between in-zone and out-of-zone errors. Its operation time should also be inversely proportionate to the location of the problem. Figure 2.15 depicts the basic notion of this grading technique.

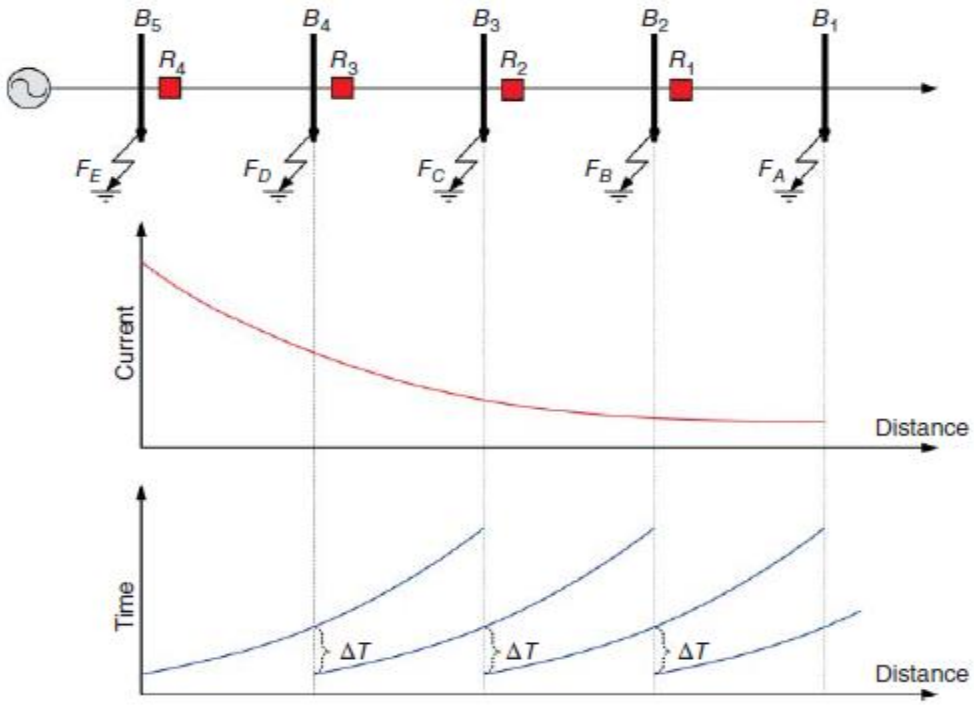

Figure 2-15: Concept of inverse-time grading in radial systems.

2.9.2 Directional Overcurrent Relays

Non-directional OCRs identify fault currents based only on their magnitudes, and trip signals are subsequently transmitted to the relevant CBs to clear the faults. Consider the parallel line radial circuit depicted in Figure 2.16 to understand the main issue with these OCRs. Assume in this example that a fault (F) has occurred on line 2 near busbar B. If only non-directional OCRs are employed, the third and fourth relays, R3 and R4, will perceive the same fault current magnitude, causing their trip signals to be relayed to CB3 and CB4 at the same time. Furthermore, R2 will trip B2 after a time delay in order to thoroughly remove the fault from the system.

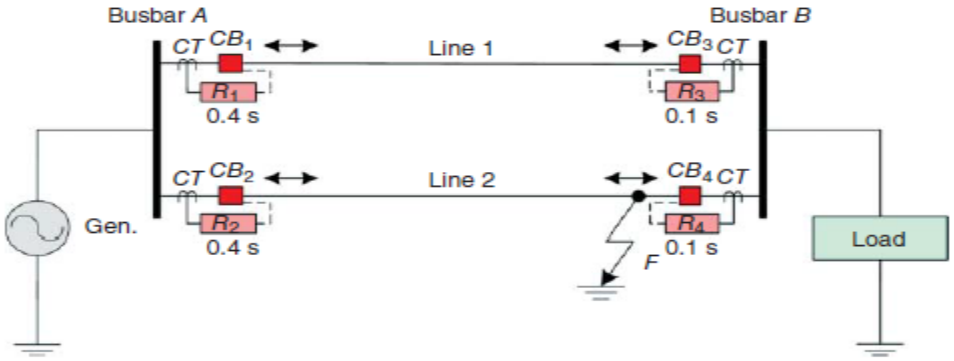

Figure 2-16: Single-end fed power system of parallel feeders with only OCRs.

The difficulty with this protection approach is that the load and line 1 will be disconnected needlessly, rendering the protection system unstable and unselective.

To address this issue, an extra directional unit is used in conjunction with OCRs to determine the fault current directions in relation to a reference signal. Based on this, both the current magnitude and direction are examined in order to trip the problematic element as quickly and selectively as possible while allowing the rest elements of the network to function correctly.

This unique protection device is known as a directional overcurrent relay (DOCR), and it will be the focus of the following chapters while exploring typical ORC difficulties. The reference signal4 is typically a voltage that may be supplied via PT. In some applications, current is also employed as a polarizing signal to reduce overall costs. With the exception of non-inverse-time OCRs, these relays have both PS and TMS, and their TCCCs are comparable to non-directional OCRs. Suppose that R3 and R4 are directional OCRs, i.e. DOCRs, and that they function depending on both the current magnitude and direction, as seen in Figure 2.17. R4 will trip CB4 in this situation because it detects both the amplitude and the right direction of the short-circuit current. Similarly, after a time delay, R2 will trip CB2, clearing the fault from both ends of line 2.

R3, on the other hand, will restrict (i.e. not operate) since the fault current direction is different from the tripping direction, despite the fact that the fault current magnitude is comparable to that detected by R4. As a result, the supply to the load is maintained via the healthy line, which is line 1. Thus, DOCRs can be utilized as the primary protection for interconnected sub-transmission and distribution systems, as well as the backup protection for transmission systems, in actual applications.

If R4 fails to function for the fault F, R1 will serve as a distant backup to clear F by tripping CB1 after a sufficient time delay. As a result, selectivity and dependability requirements are critical in the field of power system protection.

Using just non-directional OCRs in other intricate networks, such as multi-loop systems, ring feeder systems, or even double-end fed power systems, is a difficult undertaking that may not meet the reliability and selectivity standards.

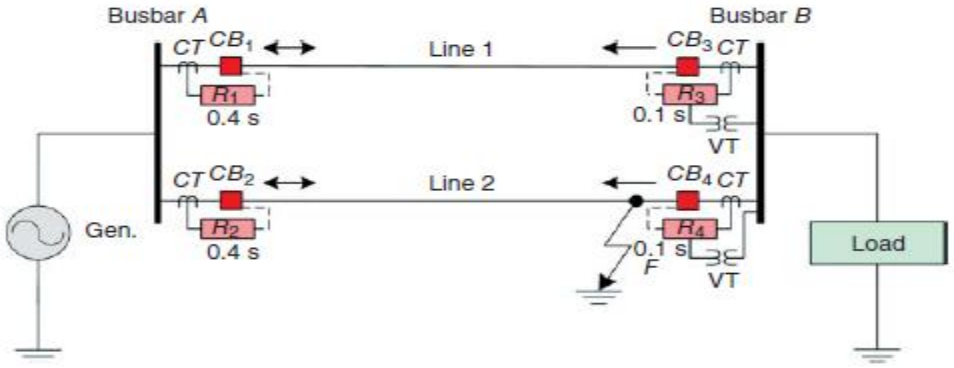

Figure 2-17: Single-end fed power system of parallel feeders with OCRs and DOCRs.

2.9.3 Coordination of DOCRs

It is a critical stage in any protection design. Correct relay coordination entails choosing the appropriate relay configuration to ensure that faults in the protected zone are cleared first by the associated main relays, and that if they fail, the corresponding backup relays act after a coordination time interval5 (CTI), which may be calculated as:

$$CTI = T_{CB} + T_{OS} + TSM \quad (5.3)$$

where T_{CB} is the CB's operating time after receiving a trip signal from the primary relay, T_{OS} is the over-shoot time, and TSM is a safety margin supplied to the model to allow for mismatches due to relay timing error, CT-ratio error, current magnitude measurement error, and so on. CTI values range from 0.2 and 0.5 s.

With the exception of some radial network specific situations, the coordination issue may be modeled as a highly restricted MINLP problem, where TMS is continuous and PS is discrete.7 An expert protection engineer is required to address such a situation logically, where all fault possibilities, system contingencies, and anomalies are examined and planned. Alternatively, it is simple to solve using optimization methods.

2.10 General Mechanism to Optimally Coordinate Directional Overcurrent Relays

The historical chronology of the ORC issue has been described based on the literature study. In addition, several foundations have been discussed in this Chapter, which are critical for individuals seeking to understand the optimal coordination of DOCRs. This issue may be solved numerically, and the optimal (or near-optimal) solution can be reached by employing a variety of optimization techniques. The purpose of this section is to demonstrate how to construct the coordination issue of DOCRs into a mathematical model that can subsequently be addressed using any available n-dimensional optimization approach.

General Program Requirements: The stages outlined in Figure 2.18's flowchart must be met in order to develop a program as a numerical ORC solver to optimally coordinate all the relays amongst each other.

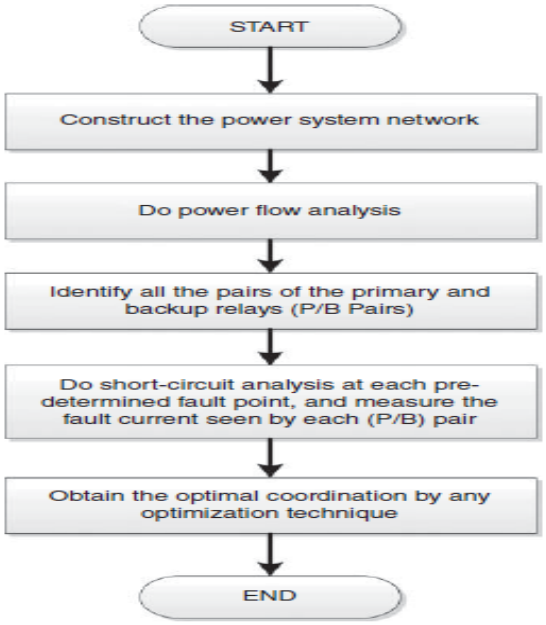

Figure 2-18 General flowchart to optimally coordinate DOCRs.

2.11 Conclusion

This chapter has provided a comprehensive overview of the power network, offering insights into various protection systems and methodologies essential for addressing electrical failures. The discussion has delved into diverse methods and techniques employed in safeguarding the power system, with a particular emphasis on the principles of optimal coordination. While the current chapter has laid the foundation, a more detailed exploration of advanced techniques and additional intricacies will be undertaken in the forthcoming chapters, namely Chapter 3 and Chapter 4.

Chapter 3 Optimal coordination of directional overcurrent relay in electrical power systems

3.1 Introduction

The improvement of technology in the previous several decades has enabled a significant presence of renewable power sources in the distribution network (DN). The integrating of such resources has had a significant influence on DN by reducing power loss and enhancing network dependability. Aside from that, the current protection system has met coordination issues as a result of bidirectional power flow, varied types and capacities of generating sources, and variations in fault levels as a result of network operating modes (grid-connected or islanded). Therefore, an effective and optimum coordination strategy is required to deal with relays coordination problem.

The coordination problem of the directional overcurrent relays (DOCRs) is a restricted and nonlinear optimization issue that involves determining appropriate time dial settings (TDS) and plug setting (PS) to reduce relays operating time while maintaining the sensitivity and the selectivity characteristics. Currently, a various nontraditional optimization strategies have been presented to overcome this challenge. In this paper, a modified version of the marine predators algorithm (MPA) referred to as Elite marine predator (EMPA) is developed for the optimal coordination of DOCRs. Therefore, the EMPA method is used to find out the optimal settings for the DOCRs problem. The suggested algorithm's performance is evaluated using standard test systems, including 3-bus, 8-bus, 9-bus, and 15-bus. The findings are compared with the traditional MPA and with other recent optimization methods presented in the literature to prove the efficiency and superiority of the proposed EMPA in reducing relay operation time for optimal DOCRs coordination.

3.2 Problem formulation

3.2.1 Objective function

One of the effects of a malfunction on the electrical networks is the rapid rise in the fault current to risky levels. Finding the settings (PS , TDS) that reduce the operating time of the primary relays is the goal of the optimal coordination of DOCRs [34],[35]–[36]. The speed criteria directly affect the ideal settings. Therefore, the Objective Function (OF) employed by the optimization algorithm can be formulated as follow [37] :

$$\text{Minimize, } T_{op} = \sum_{i=1}^{m} W_i \, T_{pr\,i} \tag{3.1}$$

Where T_{op} is the total operating time, m denotes the overall number of primary relays and T_{pri} denotes the main relay's operational time of the relay(R_i), W represents the likelihood of a power system malfunction and is often interpreted as "1."

3.2.2Relay characteristics

The operating time of DOCRs is inversely correlated to input current. The short-circuit current determines how long the relay operates. It implies that when the fault current diminishes, the operational time increases. Additionally, the directional element distinguishes the fault current's direction and is only sensitive to a certain fault direction. Thus, selectivity may be achieved in meshed systems. Otherwise, the overcurrent relay's characteristic function is represented by the equation below [38]

$$T_{i,j} = \frac{A_i \times TDS_i}{\left[\left(\frac{I_{scj}}{PS_i}\right)^{N_i} - 1\right]} \tag{3.2}$$

where $T_{i,j}$ is the relay's operational time (R_i) for a malfunction at location j. The TDS_i and PS_i of R_i are, respectively, TDS_i and PS_i. Iscj is the degree of short-circuit that Ri observes for a defect at j. The IEC defined curve forms of R_i are connected to the constants A_i and N_i. These constants are shown in the table below.

Table 3-1: Curve types of the IEC relays

Curve type	A	N
I	0.14	0.02
V.I	13.50	1.00
E.I	80.00	2.00

3.2.3 Constraints

The OF in Eq.1 is subject to the following restrictions:

a) The first aspect that must be taken into account are the coordination constraints, the optimum coordination of DOCR sets the proper settings to ensure that the faults are eradicated in the protected regions with the associated main relays. In the event that this scenario fails, it is anticipated that the pertinent backup relays will fix the issue after a coordination lag. Inadequate coordination of the primary /backup relays is avoided by using the constraint specified in Eq. 3.3.

$$T_{bc\,i} - T_{pr\,i} \geq CTI \tag{3.3}$$

The coordination time interval, or CTI, is measured in seconds and relies on the system factors such as the speed of the circuit breakers, the kind of relay (electromechanical or microprocessor-based), and the selectivity. Typically, electromechanical and microprocessor-based relays have CTIs of 0.3–0.4 and 0.1–0.2 s, respectively [39].

b) Relays need a minimum amount of operating time to run, if the relay runs slowly, irreparable equipment damage and power system instability may result. The limitations are represented as follows

$$T_{i,min} \leq T_i \leq T_{i,max} \tag{3.4}$$

Where: $T_{i,min}$is the amount of time that R_i must be active for in order to serve as the primary form of defense. The relay manufacturer will determine this duration, it is typically 0.05 s [40]to 0.2 s [7].

When serving as primary protection, R_i must remain functioning for a maximum amount of time, or $T_{i,max}$ regarded as 1 s as shown in [40].

c) the objective function is subjected to other Constraints depending on the variable settings. The relay must let the system to operate normally, therefore, even in a mild overload

scenario; the plug setting should be higher than the maximum projected load through the relays. Also, the plug setting should be less than the smallest fault current that the corresponding relay can detect. In any other case, the relay is not susceptible to that error. Additionally, PS and TDS need to be within each relay's range. To reach these requirements, PS and TDS boundaries of the ith relay can be expressed as in (3.5) and (3.6) , The typical ranges for the lowest and highest available TDS and PS are 0.05 to 1.1 and 0.1 to 5, respectively [7, 40].

$$TDS_{i,min} \leq TDS_i \leq TDS_{i,max} \tag{3.5}$$

$$PS_{i,min} \leq PS_i \leq PS_{i,max} \tag{3.6}$$

Where: The minimum and maximum PS_i values are designated as $PS_{i,min}$ and $PS_{i,max}$, respectively. The lowest and maximum TDS accessible for R_i are, respectively, $TDS_{i,min}$ and $TDS_{i,max}$.

3.3 Proposed optimization algorithm

In this work, deferent optimization algorithm have been used to tackle the relays coordination optimization problem.

Then the MPA algorithm has been modified for improving its performance in terms of convergence speed and solution quality.

3.3.1The original marine predator algorithm

A metaheuristic (MH) algorithm called the MPA uses the survival of the fittest approach. Because the predator searches for the prey that is searching for food, both of prey and predator act as search agents in the MPA [41]. As all MH techniques are based on how animals forage,

MPA uses a stochastic that determines the search space then obtains initial solutions that are distributed randomly. The answers are then adapted based on the main framework of the algorithm, with the next location (solution) dependent on the present position. Depending on the availability of prey, marine predators switch between the Lévy and Brownian search techniques while looking for prey. Predators adopt a Lévy movement when there is less food available, and a Brownian movement when an abundance of prey [41].

The starting solutions are chosen randomly, and Equation (3.7) is used to evaluate the position updates:

$$X_0 = X_{min} + rand * (X\_max - X\_min) \tag{3.7}$$

Where: rand is a random vector [0,1] , $X_{\_max}$ and $X_{\_min}$ are the upper and lower bounds of the design variable respectively.

The two primary matrices in the MPA are the Elite matrix and Pray matrix, as shown in Equations (3.8) and (3.9):

$$\text{Elite} = \begin{bmatrix} X_{11}^1 & X_{12}^1 & \dots & X_{1d}^1 \\ X_{21}^1 & X_{22}^1 & \dots & X_{2d}^1 \\ \dots & \dots & \dots & \dots \\ X_{n1}^1 & X_{n2}^1 & \dots & X_{nd}^1 \end{bmatrix} \tag{3.8}$$

It organizes the Elite matrix using a vector of predators that was repeated n times. Where n and d respectively, correspond to the quantity and size of the agents. After each cycle, The Elite is modified by replacing the predators with superior ones. The Elite matrix's dimensions are the same as those of the Prey matrix, which serves as the foundation for updating the placements of the predators. The following is how the Prey matrix is displayed :

$$\text{Prey} = \begin{bmatrix} X_{11} & X_{12} & \dots & X_{1d} \\ X_{21} & X_{22} & \dots & X_{2d} \\ \dots & \dots & \dots & \dots \\ X_{n1} & X_{n2} & \dots & X_{nd} \end{bmatrix} \tag{3.9}$$

X_{ij} is the j-th dimension for the i-th prey in this scenario. To keep the optimizer from becoming stuck in local minima while searching, the MPA enforces random variables and operators throughout iterations [41].

1) PHASES OF MPA

The MPA is founded on mimicking the whole life cycle of the predator and prey. The MPA's most important control parameter throughout iterations is the speed ratio of the prey to a predator. MPA is split into three primary stages depending on the amount of this parameters, there will be a high-speed ratio, a unity ratio, and sub-unity ratios in the three phases respectively. For each determined phase, a number of iterations is provided. Each phase's specifics are shown in [41]and are described in the section that follows.

a) PHASE 1 : THE EXPLORATION STAGE .

Prey is faster than predator in the exploring phase, with a speed ratio larger than 10. In the initial third of iterations, this phase occurs. As the prey moves quickly to grab their meal, the smallest predators remain still at this period. Eqs. (3.10) and (3.11) [41]serve as a mathematical representation of this step.

For $Iter < \frac{1}{3} Iter_{max}$

$$\overrightarrow{step\ size_i} = \overrightarrow{R_B} \otimes \left(\overrightarrow{Elite_i} - \overrightarrow{R_B} \otimes \overrightarrow{prey_i}\right) \tag{3.10}$$

Where i=1,2,3,….n

$$\overrightarrow{prey_i} = \overrightarrow{prey_i} + P.\vec{R} \otimes \overrightarrow{stepsize_i} \tag{3.11}$$

where R_B, which represents the Brownian movement, is a random vector with a normal distribution. The vector multiplications are indicated by the notation $\otimes$, P is a fixed value of 0.5, and R is a uniformly random vector within the range [0, 1]. The current and maximum iterations are designated as $Iter$ and $Iter_{max}$, respectively.

b) PHASE 2: TRANSITION STAGE

At this point, the speed of the predator and the prey is almost equal. Exploitation in this phase is done by the prey (the other half of the population), while exploration is done by the predator. According to Eqs. (3.12) and (3.13), the first half of the population (exploitation) is reflected, and the second half of the population (exploration) is reflected by Eqs. (3.12)–(3.13) [41]:

For the group that relies on exploitation:

For $\frac{1}{3} Iter_{max} < Iter < \frac{2}{3} Iter_{max}$

$$\overrightarrow{step\ size_i} = \overrightarrow{R_L} \otimes (\overrightarrow{Elite_i} - \overrightarrow{R_L} \otimes \overrightarrow{prey_i}) \tag{3.12}$$

Where i = 1,2,3,….n/2

$$\overrightarrow{prey_i} = \overrightarrow{prey_i} + P.\vec{R} \otimes \overrightarrow{stepsize_i} \quad (3.13)$$

Where $\overrightarrow{R_L}$ is a vector of different and random numbers corresponding to the Lévy distribution.
The exploration-based on population:

$$\overrightarrow{step\ size_i} = \overrightarrow{R_B} \otimes (\overrightarrow{R_B} \otimes \overrightarrow{Elite_i} - \overrightarrow{prey_i}) \quad (3.14)$$

Where i=n/2,….n/2

$$\overrightarrow{prey_i} = \overrightarrow{Elite_i} + P.CF \otimes \overrightarrow{stepsize_i} \quad (3.15)$$

Where CF is a tunable control parameter for the predator's step size, it is stated as follows:

$$CF = \left(1 - \frac{Iter}{Iter_{max}}\right)^{\left(2 * \frac{Iter}{Iter_{max}}\right)} \quad (3.16)$$

c) PHASE 3 : EXPLOITATION STAGE

The predator travels more quickly than the victim during the last stage of the MPA. The mathematical model is used in this rule as indicated [41]:

For $Iter > \frac{2}{3} Iter_{max}$

$$\overrightarrow{step\ size_i} = \overrightarrow{R_L} \otimes (\overrightarrow{R_L} \otimes \overrightarrow{Elite_i} - \overrightarrow{prey_i}) \quad (3.17)$$

Where, i=1,2,3…n

$$\overrightarrow{prey_i} = \overrightarrow{Elite_i} + P.CF \otimes \overrightarrow{stepsize_i} \quad (3.18)$$

2) RUNNING FROM LOCAL MINIMA

Fish Aggregating Devices (FADs) or Eddy formation in marine life have an impact on the behavior of marine predators. The FADs are local minima in mathematics. Applying Eq. (3.19) prevents MPA from becoming stuck in non-globally optima [41].

$$\overrightarrow{prey_i} = \begin{cases} \overrightarrow{prey_i} + CF\left[\overrightarrow{X_{min}} + R \otimes \left(\overrightarrow{X_{max}} - \overrightarrow{X_{min}}\right)\right] \otimes \vec{U} \\ if\ r \le FAD \\ \overrightarrow{prey_i} + [FAD \times (1-r) + r]\left(\overrightarrow{prey_{r1}} - \overrightarrow{prey_{r1}}\right) \\ if\ r \ge FAD \end{cases} \tag{3.19}$$

Where $\vec{U}$ is a ones and zeros vector, $\overrightarrow{X_{max}}$ and $\overrightarrow{X_{min}}$ are vectors representing the dimensions' upper and lower bounds, and subscripts (r1 and r2) stand for the indices of the Prey matrix. Typically, FAD is given an amount of 0.2 [41].

3.3.2 Elite Marine Predators Algorithm

In this part, we will demonstrate the basic concept of the proposed Elite marine predators algorithm (EMPA) for DOCRs coordination problem. As previously stated, MPA is a novel metaheuristic algorithm that has demonstrated performance in addressing real-world engineering challenges. It has been modified and improved to address a variety of optimization problems, including parameter estimation of photovoltaic models in [42], optimal design of hybrid renewable energy systems in [43], economic dispatch problem[44] [45], Wireless Sensor Network Coverage Optimization Problem[46], covid 19 detecting [47, 48] and medical image synthesis [49]. Furthermore, To solve the problem that the MPA is not applicable in binary scenarios; a binary version of MPA is proposed in [50] .also [51] used IMPA for solving the shape optimization models and An automatic arrhythmia classification is presented in [52].

Since the standard Marine Predators algorithm proved to be able to handle a wide range of engineering applications, the Current research focuses on applications and enhancements of the performance of the MPA in relay coordination optimization problem. Finding the optimal operating time of DOCRs is a significant challenge, especially given the enormous number of variables and the associated large number of constraints involved in practical power systems. As

a result, the standard MPA scheme might well be vulnerable to local minima stagnation. Moreover, the standard movement is carried out with respect to the global best solution along most of the iterative process. In this way, the search agents may overlook the different promising regions within the search space. To resolve this matter, an elite vector that includes the three global best solutions and their average, is constructed and gets updated each iteration. Instead of conducting the movement with respect to the global best solution only, for each agent now, a member of the vector is chosen for the movement, a flowchart of the EMPA is presented in Fig.3.1. The Elite vector is constructed as follows :

$$Elite = [Gbest1, Gbest2, Gbest3, Gavg] \tag{3.20}$$

Where

$$Gavg = \frac{Gbest1 + Gbest2 + Gbest3}{3} \tag{3.21}$$

For each agent, a member from the elite vector is randomly chosen for the movement as follows:

$$EM(i) = Elite(r) \tag{3.22}$$

Where $r = 1,2,3,4$

The operation of the principal modified part of the EMPA is provided in the following pseudo code:

Calculate the fitness and construct the Elite vector
$for\ i = 1{:}N$
$EM(i) = Elite(r)$
$if\ \ Iter < Max_{Iter}/3$
$Stepsize(i) = RB((EM(i) - RB * Prey(i))$
$Prey(i) = Prey(i) + P * RB * Stepsize(i)$
$Else\ if\quad Max_{Iter}/3 < Iter < 2Max_{Iter}/3$
$if\ i < N/2$
$Stepsize(i) = RL(EM(i) - RL * Prey(i))$
$Prey(i) = Prey(i) + P * RB * Stepsize(i)$
$Else$
$Stepsize(i) = RB(RB * EM(i) - Prey(i))$
$Prey(i) = EM(i) + P * CF * Stepsize(i)$

End if

Accomplish memory saving and update elite vector

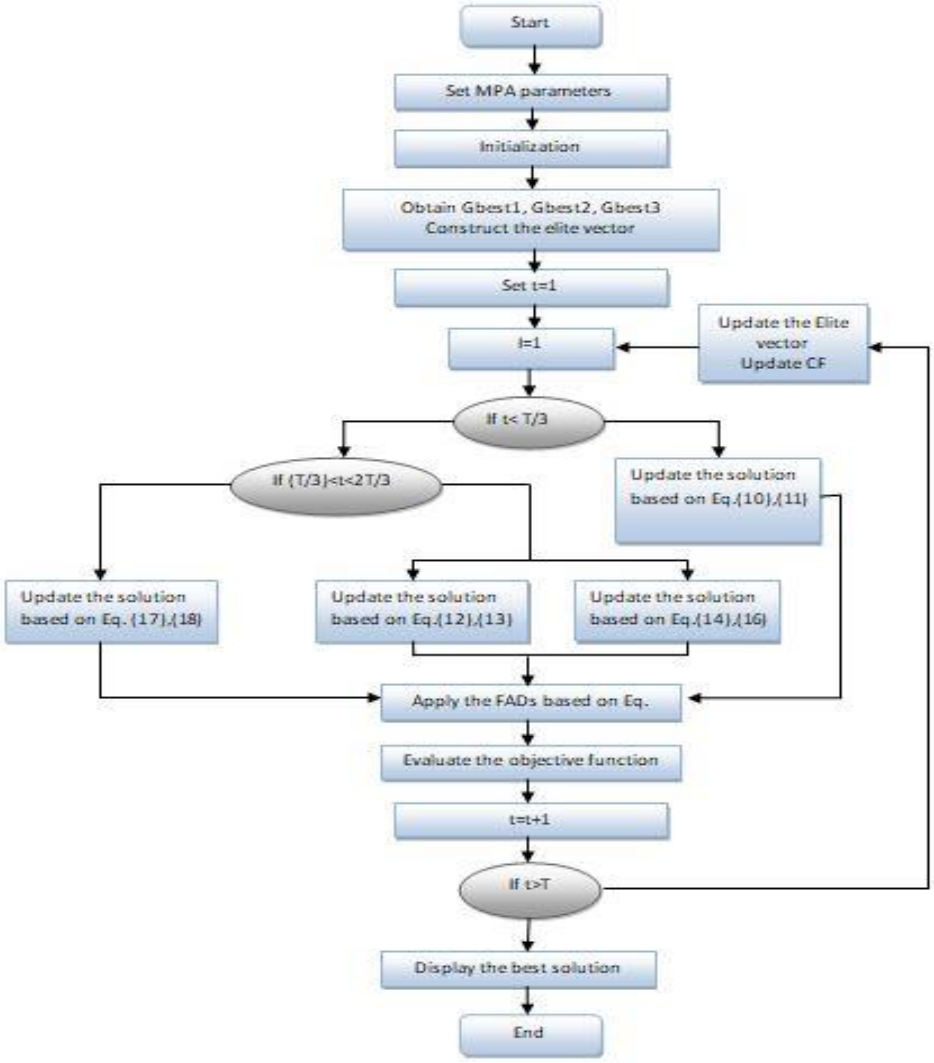

Figure 3-1. Flowchart of the proposed algorithm (EMPA)

3.4 Results and discussion

The efficiency of the suggested method was examined using four Benchmark test systems. The suggested method was applied to the optimal coordination issue of DOCRs in four reference systems: 3-bus, 8-bus, 9-bus and 15-bus to demonstrate its better performance to previous similar algorithms. Because this optimization challenge is frequently related to transmission and sub-transmission systems, all systems are set up in a ring topology. However, the problem is mathematically modeled using the same method as radial and ring networks[53]. The obtained

simulation results are compared with those of other techniques reported in literatures that use the same: system topology; types and locations of faults; primary/backup relay pairs; continuous PS and TDS, DOCRs curve type and fault levels. The suggested approach is implemented using MATLAB R2018a running on a Windows 10, 64-bit platform with an 8 GB RAM Core i5 computer.

3.4.1Test system 1: the 3-bus system

According to Fig. 3.2, the IEEE 3-bus test system comprises of three generators, three lines, six DOCRs, and six primary/backup relay pairs. The six relays' best settings needed to be determined. Here, the 12 control variables (TDS1–TDS6 and PS1–PS6) should be adjusted to their optimal values. TDS and PS have upper and lower limits of 0.05 to 1.1 and 0.1 to 5 respectively. A 0.2 second CTI min was chosen. Tables 3.2 and 3.3 [40] include the short circuit currents values (IF) and the CT rating that correspond to the system. The Data of this system can be found in [54].

To finish the examination, Table 3.4 shows the optimal TDS and PS values obtained with MPA and the enhanced MPA. Table 3.5 lists the operation times of primary and backup relays as well as CTI values. Tables 3.4 and 3.5 show that the EMPA meets all of the operational limitations of relay settings while minimizing the overall operating time of the relays. Table 3.6 compares the proposed EMPA to MPA and other approaches that have been published; a graphical illustration of the total operating time of EMPA compared to existing strategies in the literature is shown in fig.2. The EMPA convergence characteristic achieved during the simulation is depicted in Fig. 3.3. The network setup employed by the published methodologies is comparable to the one used in the current work.

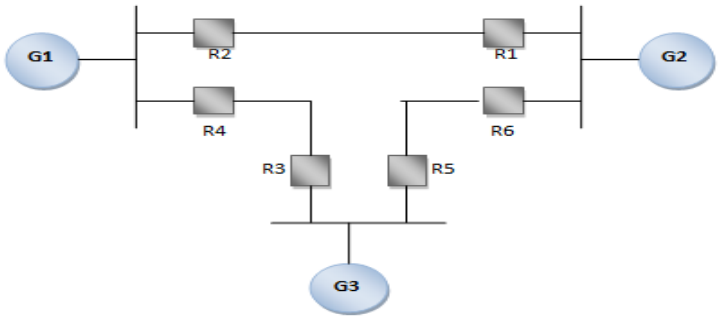

Figure 3-2. 3-bus system.

*T*able 3-2**:** Short-circuit currents flowing through pairs of PR-BR relays in the 3-bus system

Relay	BR	*IFpr*	*IFbc*
1	5	1978.9	175
2	4	1525.7	545
3	1	1683.9	617.22
4	6	1815.4	466.17
5	3	1499.7	384
6	2	1766.3	145.34

Table 3-3: Ct ratio

relays	CT ratio
1,4	300/5
2,3,5	200/5
6	400/5

Table 3-4**:** Optimal settings and total operating time for the 3-bus system.

Relays	MPA		EMPA	
	TDS	PS	TDS	PS
1	0.1000	4.0025	0.2483	0.2068
2	0.1061	2.1279	0.1	0.7548
3	0.1	4.7529	0.120	1.1972
4	0.1	2.1336	0.1	1.4291
5	0.1	1.9819	0.1	1.1767
6	0.1	2.0035	0.1	1.2454
of	1.6621		1.3793	

Table 3-5**:** P/B protection operational times for the IEEE 3-bus system

relays		MPA			EMPA		
R_{pr}	R_{bc}	Top pr	Top bc	CTI	Top pr	Top bc	CTI
1	5	0.3249	0.8771	0.5522	0.3257	0.5261	0.2004
2	4	0.2502	0.4762	0.2260	0.1715	0.3717	0.2001
3	1	0.3139	0.7345	0.4205	0.2278	0.4278	0.2000
4	6	0.2570	0.6487	0.3917	0.2224	0.4466	0.2241
5	3	0.2311	0.9888	0.7576	0.1953	0.3954	0.2001
6	2	0.2847	1.3820	1.0972	0.2365	0.4386	0.2021

Table 3-6**:** Comparison of the results for the IEEE 3-bus system.

Method	$sum(T_{pr\ i})$
TLBO(MOF) [55]	6.972
TLBO [55]	5.3349
MDE[40]	4.7806
AFDBA [53]	2.5287
MPSO[56]	1.9258
SA [54]	1.599
BBO-LP[57]	1.5987
WOA [58]	1.5262
HBA[58]	1.5029
SCA [8]	1.4419
HBA	**1.4793**
GTO	**1.6156**
EWCA	**1.3990**
MPA	**1.6621**
EMPA	**1.3793**

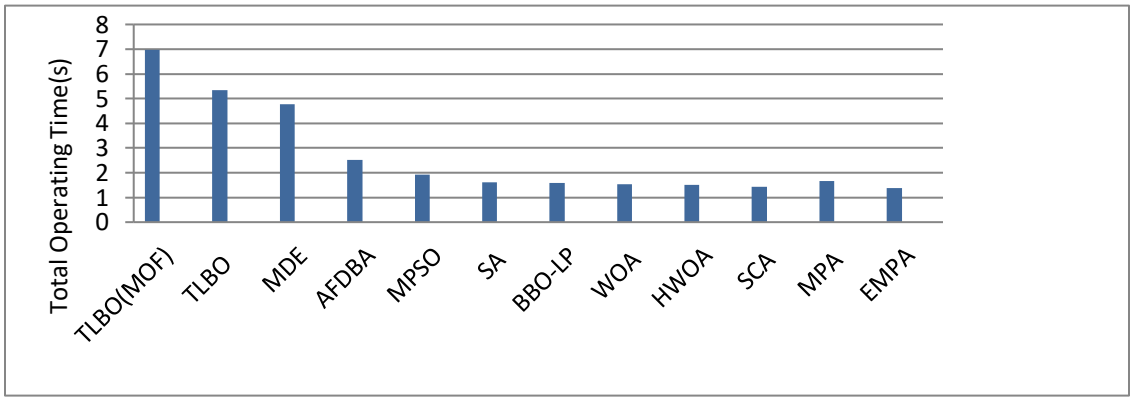

Figure 3-3**.** Graphical illustration of the total operating time of EMPA compared to the literature for 3-bus test system.

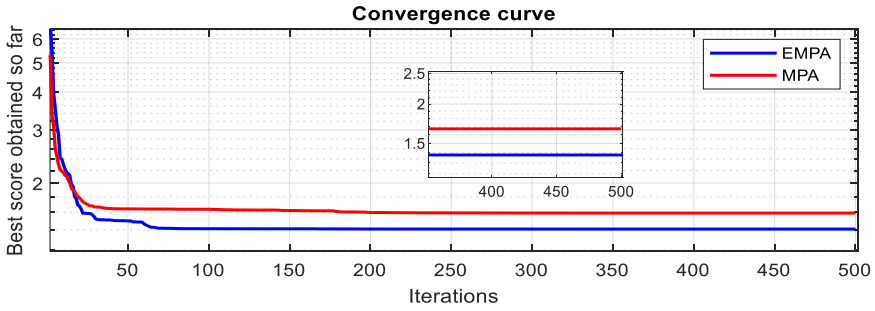

Figure 3-4**.** Convergence curve of the MPA vs EMPA algorithms in the 3-bus system.

3.4.2Test system 2: the 8-bus system

The second test system considered in this section is the 8-bus system. It consists of two generators, two transformers, seven lines, fourteen relays, and twenty primary/backup relay pairs. The 8-bus test system is shown in (Fig. 3.5), each relay has two variable settings TDS and PS, therefore, 28 decision variables (TDS1-TDS14 and PS1-PS14)must be found. The TDS varied between 0.1 and 1.1, while the PS values were between 0.5 and 5. The CT ratio was 800/5 for R3, R7, R9, and R14 and 1200/5 for the remaining relays, with the CTImin set at 0.2 s. The fault current values and primary/backup relay pairs for the 8-bus test system are shown in Table 3.7 [54]. The DOCRs coordination problem in the 8-bus test system was optimized using the MPA and the suggested EMPA method. Table 3.8 presents the ideal values for the TDS and PS control variables as well as a comparison of the proposed algorithm's objective function to the original marine predator algorithms. Furthermore Tables 3.9 displays the operating time(OT) and the coordination time interval (CTI) values for 20 primary/backup relay pairs. The findings demonstrate that the suggested strategy greatly decreased the total OT of the major relays and all results are within acceptable bounds. The original MPA method achieved an OF value of 7.4711s, whereas the EMPA algorithm achieved an OF value of 5.3635s. Table 3.10 provides a comparison of the outcomes produced by various optimization approaches. The top values for the objective function are shown in this table. The best value achieved by the IMPA approach is the lowest value when compared to the other procedures, as can be seen in the graphical illustration of the total operating time in fig.3.6. Where fig.3.7, displays the convergence characteristic of an 8-bus test system. The chart clearly shows that EMPA has a fast convergence speed compared to the original method.

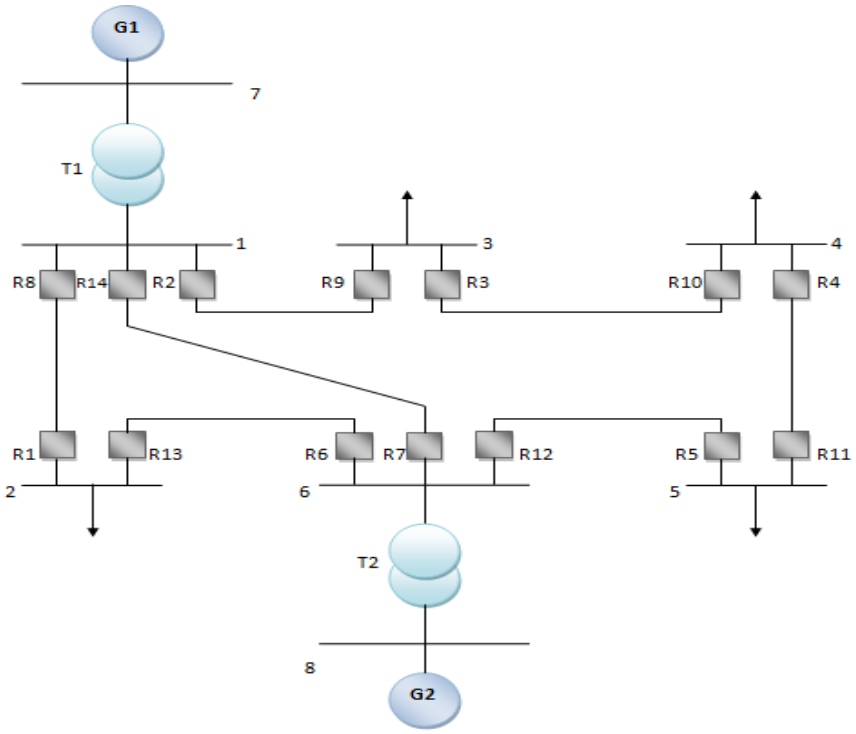

Figure 3-5 . IEEE 8-bus system.

Table 3-7**:** Short-circuit currents flowing through pairs of PR-BR relays in the 8-bus system

Primary Relay	Back-up Relay	Primary Fault Current	Back-up Fault Current
1	6	3232	3232
2	1	5924	996
2	7	5924	1890
3	2	3556	3556
4	3	3783	2244
5	4	2401	2401
6	5	6109	1197
6	14	6109	1874
7	5	5223	1197
7	13	5223	987
8	7	6093	1890
8	9	6093	1165
9	10	2484	2484
10	11	3883	2344
11	12	3707	3707
12	13	5899	987
12	14	5899	1874
13	8	2991	2991
14	1	5199	996
14	9	5199	1165

Table 3-8: Optimal settings and total operating time for the 8-bus system.

Relays	MPA		EMPA	
	TDS	PS	TDS	PS
1	0.0986	1.9313	0.0514	2.8349
2	0.1142	4.2955	0.0853	4.9995
3	0.1772	1.4116	0.0807	4.4156
4	0.0659	3.9226	0.0522	4.2436
5	0.0144	4.2248	0.0539	2.5084
6	0.0893	4.3859	0.0553	4.4675
7	0.1547	2.3955	0.0733	4.8375
8	0.1451	1.5533	0.0636	3.9510
9	0.0520	4.1082	0.0542	3.7139
10	0.0898	2.7660	0.0634	3.5751
11	0.1439	1.6138	0.0547	4.4921
12	0.1198	4.2049	0.0826	4.9980
13	0.0655	2.4552	0.0442	2.3657
14	0.1873	1.7089	0.0686	4.9845
OF	7.4711		5.3635	

Table 3-9**:** P/B protection operational times for the IEEE 8-bus system.

Relays		MPA			EMPA		
R_{pr}	R_{bc}	Top pr	Top bc	CTI	Top pr	Top bc	CTI
1	6	0.3486	0.5516	0.2030	0.1389	0.3470	0.2081
2	1	0.4494	0.8956	0.4461	0.3683	0.5748	0.2064
2	7	0.4494	0.6679	0.2185	0.3683	0.5698	0.2014
3	2	0.4379	0.6379	0.2000	0.3441	0.5441	0.2000
4	3	0.3272	0.5281	0.2009	0.2749	0.4834	0.2084
5	4	0.1162	0.4883	0.3720	0.2192	0.4227	0.2034
6	5	0.3496	0.6083	0.2586	0.2186	0.4444	0.2257
6	14	0.3496	0.6683	0.3186	0.2186	0.5575	0.3389
7	5	0.3807	0.6083	0.2275	0.2436	0.4444	0.2008
7	13	0.3807	0.8844	0.5036	0.2436	0.5574	0.3138
8	7	0.3747	0.6679	0.2932	0.2568	0.5698	0.3129
8	9	0.3747	0.632	0.2579	0.2568	0.4572	0.2004
9	10	0.2702	0.470	0.2000	0.2135	0.4136	0.2000
10	11	0.3497	0.5498	0.2000	0.2899	0.4900	0.2000
11	12	0.4362	0.6362	0.2000	0.3067	0.5067	0.2000
12	13	0.4666	0.8844	0.4177	0.3572	0.5574	0.2002
12	14	0.4666	0.6683	0.2016	0.3572	0.5575	0.2003
13	8	0.2777	0.4777	0.2000	0.1834	0.3836	0.2001
14	1	0.4322	0.8956	0.4633	0.2514	0.5748	0.3233
14	9	0.4322	0.6326	0.2003	0.2514	0.4572	0.2057

Table 3-10: Comparison of the results for the IEEE 8-bus system.

Method	$sum(Tpr\ i)$	Method	$sum(Tpr\ i)$
GA [59]	11.001	FA [60]	6.6463
LM [61]	11.0645	MWCA [62]	6.4
HGA-LP[59]	10.9499	MEFO [63]	6.349
BBO-LP [57]	8.7555	VNS [64]	6.328
SA [54]	8.4270	HWOA[58]	5.8563
MILP [65]	8.001	IHSA-NLP[66]	5.4505
MPA	**7.4711**	**EMPA**	5.3635
GTO	**7.8813**		

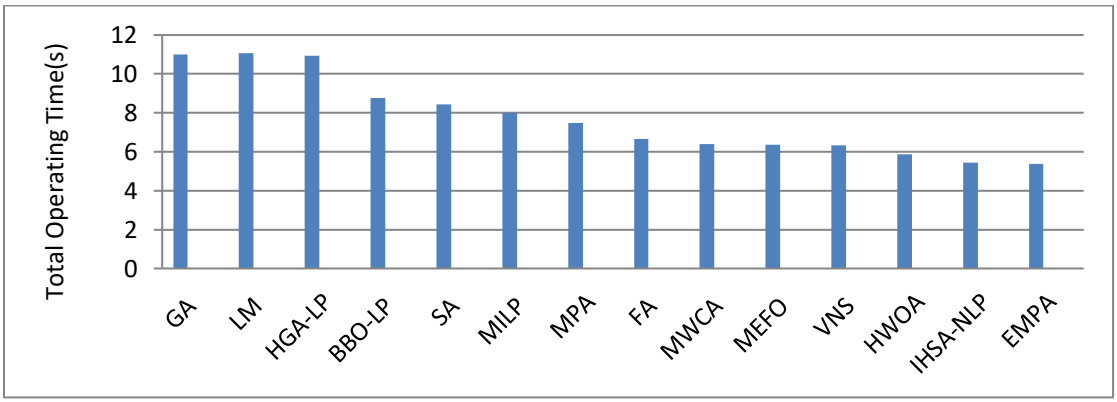

Figure 3-6. Graphical illustration of the total operating time of EMPA compared to the literature for 8-bus test system.

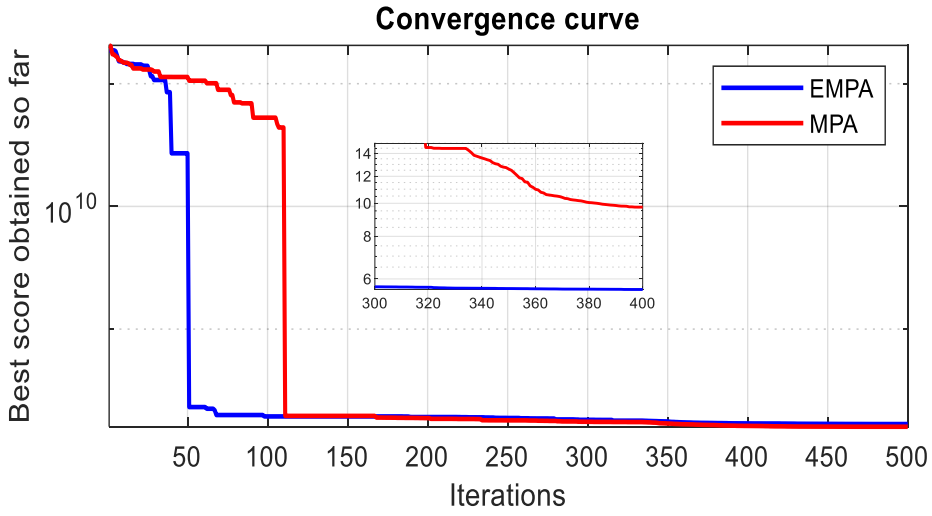

Figure 3-7. Convergence curve of the MPA vs EMPA algorithms in the 8-bus system.

3.4.3Test system 3: the 9-bus system

A single-line schematic of the 9-bus test system is depicted in Fig.3.8 and the short circuit currents are listed in Table 3.11. This system consists of 32 primary/backup relay pairs, 12 lines, and 24 DOCRs. The main objective was to reduce the total OT of all the principal relays, and the goal was to adjust the settings of 24 relays. The CTI_{min} was set to 0.2 seconds; Relays R3, R7, R9, and R14 have CT ratios of 800:5, whereas relays R1, R2, R4, R5, R6, R8, R10, R11, R12, and R13 have CT ratios of 1200:5. The results of TDS and PS are given in Table 3.12

The ideal settings for protection coordination are accomplished by decreasing the OF utilizing the modified marine predator algorithm (EMPA). The outcomes are compared with the original marine predators algorithm (MPA) results in order to demonstrate the usefulness of the EMPA in the coordination of protection. Table 3.13 presents a comparison of the operating time (OT) and the coordination time interval (CTI) values for the corresponding algorithms. The thirty-two selectivity criteria for primary/backup relay pairs should be set within bounds to allow for successful coordination of DOCRs. As a result, it is clear from a detailed analysis in Table 3.13 that all CTI values obtained by EMPA algorithm are within allowable bounds. In Table 3.14, a comparison between results obtained by EMPA method and other recent techniques was made, primary relays total operating time is computed as 2.698 sec using EMPA method and it's clear from the graphical illustration in fig.3.9.that the proposed optimization process gives the least value of the operating time of all primary relays compared to other techniques. Also, The EMPA convergence characteristic achieved during the simulation is depicted in Fig.3.10.where it can be seen that the EMPA converges rapidly.

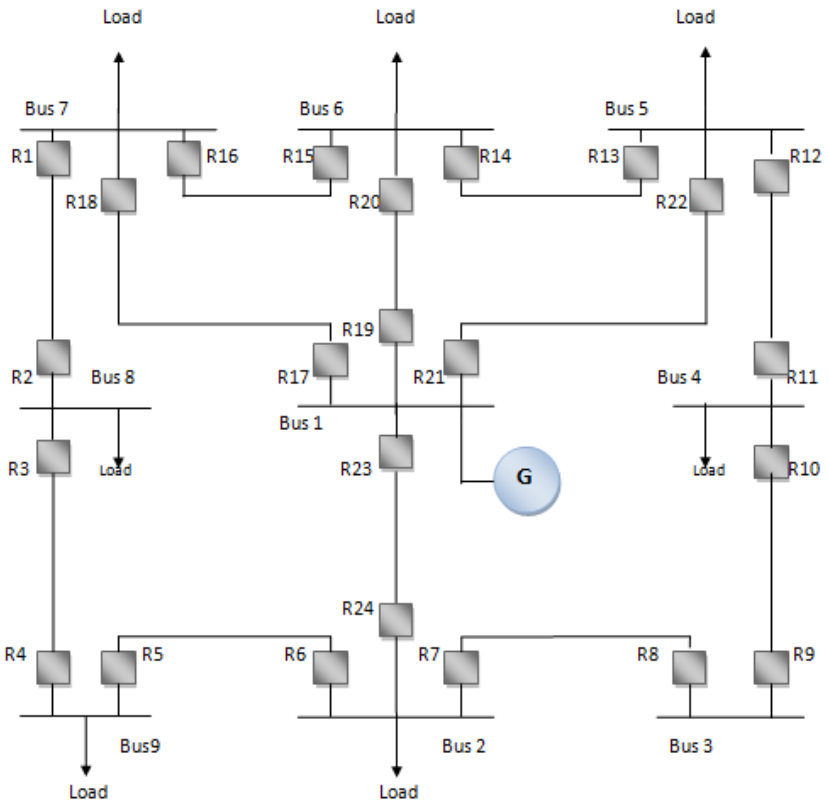

Figure 3-8. IEEE 9-bus system.

Table 3-11: Short-circuit currents flowing through pairs of PR-BR relays in the 9-bus system

PR	BC	I_{PR}	I_{BC}	PR	BC	I_{PR}	I_{BC}
1	15	4863.6	1168.3	14	16	4172.5	1031.7
1	17	4863.6	1293.9	14	19	4172.5	1264.1
2	4	1634.4	1044.2	15	13	4172.5	1031.7
3	1	2811.4	1361.6	15	19	4172.5	1264.1
4	6	2610.5	1226	16	2	3684.5	653.6
5	3	1778	1124.4	16	17	3684.5	1293.9
6	8	4378.5	711.2	17	0	7611.2	0
6	23	4378.5	1345.5	18	2	2271.7	653.6
7	5	4378.5	711.2	18	15	2271.7	1168.3
7	23	4378.5	1345.5	19	0	7435.8	0
8	10	1778	1124.4	20	13	2624.2	1031.7
9	7	2610.5	1226	20	16	2624.2	1031.7
10	12	2811.4	787.2	21	0	7611.2	0
11	9	1634.4	1044.2	22	11	2271.7	653.6
12	14	2811.4	1168.3	22	14	2271.7	1168.3
12	21	2811.4	1293.9	23	0	7914.7	0
13	11	3684.5	653.6	24	5	1665.5	711.2
13	21	3684.5	1293.9	24	8	1665.5	711.2

Table 3-12**:** Optimal settings and total operating time for the 9-bus system.

Relays	MPA		EMPA		Relays	MPA		EMPA	
	TDS	PS	TDS	PS		TDS	PS	TDS	PS
1	0.2083	0.3419	0.0323	1.2368	13	0.1857	0.2693	0.0105	1.6100
2	0.2022	0.2234	0.0265	0.6641	14	0.2169	0.1939	0.0383	0.9878
3	0.1404	0.6480	0.0155	1.5900	15	0.2295	0.2192	0.0241	1.3529
4	0.1800	0.3741	0.0383	0.8964	16	0.1930	0.2523	0.0172	1.4227
5	0.2546	0.1625	0.0255	0.7435	17	1.0349	0.3458	0.1050	0.4645
6	0.1534	0.5066	0.0228	1.5560	18	0.0788	0.4223	0.0100	0.1000
7	0.1197	0.6259	0.0181	1.5902	19	0.9978	0.5188	0.0276	2.4366
8	0.1535	0.2623	0.0679	0.2848	20	0.0103	0.3706	0.0222	0.1002
9	0.1872	0.2272	0.0172	1.4410	21	0.8044	0.5836	0.1844	0.4937
10	0.2187	0.1910	0.0100	1.8835	22	0.1226	0.3438	0.0100	0.3969
11	0.1176	0.3230	0.0335	0.5154	23	0.4718	0.4023	0.0678	0.5397
12	0.1704	0.2522	0.0349	0.6272	24	0.0879	0.1287	0.0100	0.1000
OF	11.2015		2.698						

Table 3-13**:** P/B protection operational times for the IEEE 9-bus system.

Relays		MPA			EMPA			Relays		MPA			EMPA		
pr	bc	Top pr	Top bc	CTI	Top pr	Top bc	CTI	pr	bc	Top pr	Top bc	CTI	Top pr	Top bc	CTI
1	15	0.4212	0.663	0.2419	0.1077	0.3077	0.2000	13	11	0.3801	0.5808	0.2007	0.0476	0.2502	0.2026
1	17	0.4212	3.5280	3.1067	0.1077	0.4207	0.3130	13	21	0.3801	3.7253	3.3452	0.0476	0.7666	0.7190
2	4	0.5137	0.7206	0.2069	0.1145	0.3145	0.2000	14	16	0.3886	0.6298	0.2411	0.1231	0.3231	0.2000
3	1	0.4452	0.6885	0.2432	0.0850	0.2850	0.2000	14	19	0.3886	4.3414	3.9527	0.1231	5.2473	5.1242
4	6	0.4657	0.6707	0.2049	0.1496	0.3500	0.2003	15	13	0.4257	0.6257	0.2000	0.0912	0.2958	0.2045
5	3	0.5602	0.7803	0.2201	0.1123	0.3128	0.2005	15	19	0.4257	4.3414	3.9156	0.0912	5.2473	5.1561
6	8	0.3664	0.6251	0.2587	0.0909	0.2909	0.2000	16	2	0.3872	0.7875	0.4002	0.0721	0.2721	0.2000
6	23	0.3664	1.7050	1.3386	0.0909	0.2909	0.2000	16	17	0.3872	3.5280	3.1408	0.0721	0.4207	0.348
7	5	0.3092	0.8043	0.4950	0.0734	0.2734	0.2000	18	2	0.2268	0.7875	0.5606	0.0176	0.2721	0.2548
7	23	0.3092	1.7050	1.3958	0.0734	0.2909	0.2175	18	15	0.2268	0.6632	0.4363	0.0176	0.3077	0.2900
8	10	0.4016	0.6058	0.2042	0.1836	0.3943	0.2106	20	13	0.0266	0.6257	0.5991	0.0377	0.2958	0.2580
9	7	0.4052	0.6053	0.2000	0.0928	0.2929	0.2001	20	16	0.0266	0.6298	0.6031	0.0377	0.3231	0.2854
10	12	0.4376	0.6396	0.2020	0.0633	0.2633	0.2000	22	11	0.3241	0.5808	0.2566	0.0280	0.3090	0.2222
11	9	0.3476	0.5780	0.2304	0.1249	0.3250	0.2001	22	14	0.3241	0.5950	0.2708	0.0280	0.2721	0.2810
12	14	0.3725	0.5950	0.2225	0.1090	0.3090	0.2000	24	5	0.1832	0.8043	0.6210	0.0192	0.2909	0.2716
12	21	0.3725	3.7253	3.3527	0.1090	0.7666	0.6575	24	8	0.1832	0.6251	0.4418	0.0192	0.3090	0.2222

Table 3-14: Comparison of the results for the IEEE 9-bus system.

Method	$sum(T_{pr\ i})$
GA [67]	14.5426
HS [63]	9.838
DE [67]	8.6822
WOA [58]	8.3849
HWOA [58]	8.1968
AFDBA [53]	7.3493
EFO [63]	6.050
MEFO [63]	5.225
BBO [62]	5.243
VNS [64]	4.800
MWCA [62]	3.7074
MRFO [68]	2.99
HBA	**4.2094**
EWCA	**3.3118**
MPA	**11.2015**
EMPA	**2.698**

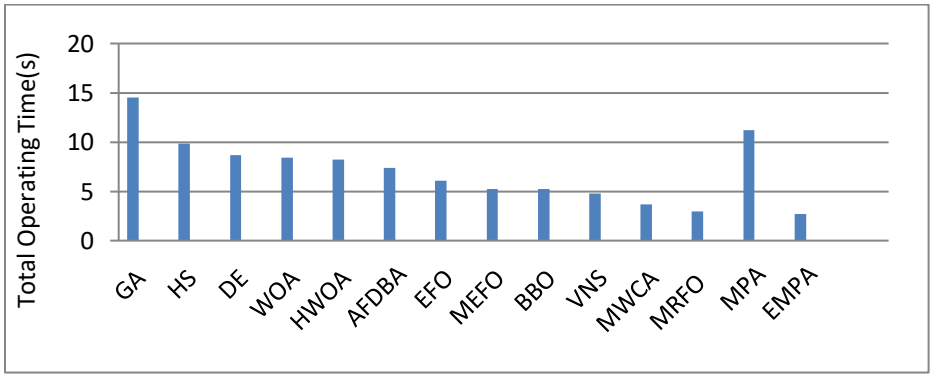

Figure 3-9. Graphical illustration of the total operating time of EMPA compared to the literature for 9-bus test system.

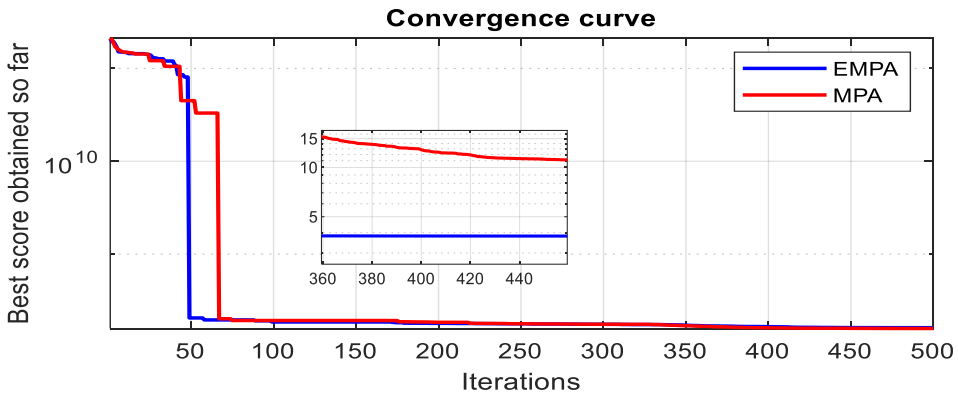

Figure 3-10**.** Convergence curve of the MPA vs EMPA algorithms in the 9-bus system.

3.4.4Test system 4: the 15-bus system

For more confirmation of the effectiveness of the EMPA approach, the proposed technique has been applied on a very large and highly penetrated distribution network with a variety of DG units. Fig. 3.11 shows the single-line diagram of the 15-bus test system as well as the relay placements. This electric system contains a total of 7 DG units. Twenty-one lines and forty-two relays make up the fifteen-bus test system. The primary parameters of the power system as the short circuit current values are available in [69] and the CT ratio in table 3.16 . The TDS and PS values are set between 0.1 to 1.1 and 0.1 to 5 respectively. the CTI value is chosen as a minimum of 0.2 sec , in order to determine the best relay settings . The relay coordination issue in the 15 bus test system has 84 variables and 164 constraints. Table 3.17 illustrates the optimal TDS and PS for DOCRs achieved by the proposed EMPA, whereas Table 3.18 displays the relative result of the proposed EMPA with an existing recent published method. The comparison validates the effectiveness of the proposed method in the DOCR Coordination scheme. Table 3.18 displays a comparison between the suggested method and other ones found in the literature and their graphical illustration is depicted in fig.3.12. The findings demonstrate that the suggested technique outperforms the other algorithms. Using MWCA [62], for example, decreases the entire operating time of DOCRs to 13.3 s, whereas the suggested technique reduces this time to 10.9610 s. This time decrease is equivalent to reducing the total ROT of DOCRs to the desired 17.58 %. The convergence curve of the 15-bus test system is shown in fig.3.13. The

chart clearly shows that the EMPA converges rapidly than the original method. As a result, the suggested technique outperforms others in determining appropriate ROT settings.

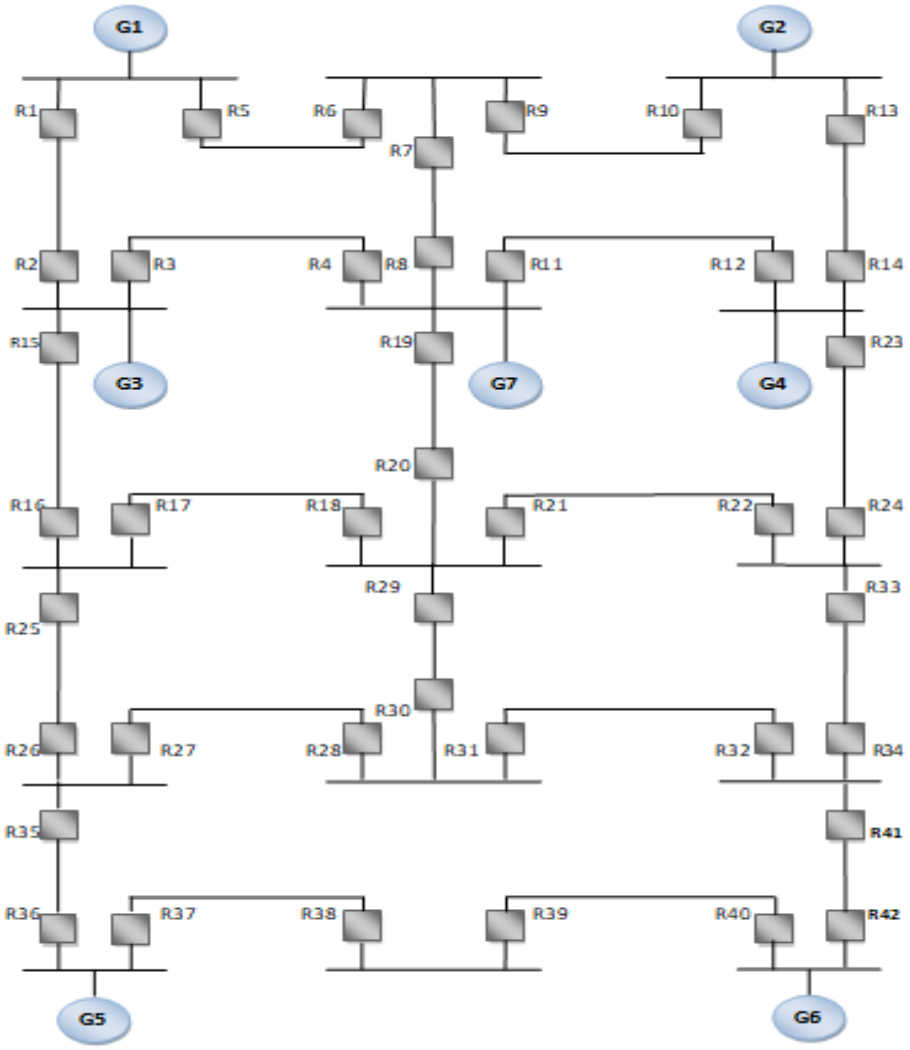

Figure 3-11: IEEE 15-bus system.

Table 3-15: CT ratio for 15 bus system relays

Relays	CT Ratio
18, 20, 21, 29	1600/5
2, 4, 8, 11, 12, 14, 15, 23	1200/5
1, 3, 5, 10, 13, 19, 36, 37, 40, 42	800/5
6, 7, 9, 16, 24, 25, 26, 27, 28, 31, 32, 33, 35	600/5
17, 22, 30, 34, 38, 39, 41	400/5

Table 3-16: Optimal settings and total operating time for the 15-bus system.

Relays	MPA		EMPA		Relays	MPA		EMPA	
	TDS	PS	TDS	PS		TDS	PS	TDS	PS
1	0.27610	1.0719	0.0645	2.3758	22	0.1846	2.1331	0.0717	2.4999
2	0.1607	2.6231	0.0517	2.2518	23	0.2707	1.1878	0.05	2.2903
3	0.3768	1.4950	0.0978	2.4927	24	0.3033	1.1052	0.0867	1.5493
4	0.3505	1.6145	0.0685	2.2299	25	0.2767	1.2551	0.0854	2.4730
5	0.2650	2.3566	0.0920	2.4851	26	0.2871	2.2499	0.1048	1.6863
6	0.3753	0.5041	0.0814	2.5	27	0.2802	1.2178	0.1028	1.9407
7	0.3550	1.4922	0.0919	2.278	28	0.4149	1.1364	0.1014	2.4999
8	0.2523	0.8813	0.0902	1.9397	29	0.3430	0.9891	0.0795	2.0374
9	0.2424	1.7314	0.1049	2.3360	30	0.3094	1.2318	0.0863	2.4997
10	0.3158	0.9893	0.0832	2.4939	31	0.2279	1.3672	0.0972	1.8904
11	0.2195	1.8948	0.0759	1.4850	32	0.2245	1.6414	0.1029	1.5435
12	0.2939	2.0623	0.0647	2.3731	33	0.4647	0.2869	0.1013	2.4924
13	0.3449	1.3592	0.0907	1.595	34	0.3200	1.1698	0.1026	2.4756
14	0.3584	1.1798	0.0500	2.5	35	0.3457	0.6668	0.0913	2.2809
15	0.2081	0.9671	0.0947	1.0926	36	0.1913	2.3974	0.0982	1.9462
16	0.2909	1.0704	0.0648	2.4970	37	0.3320	0.8371	0.0990	2.4997
17	0.4535	0.3259	0.0880	2.4898	38	0.3104	0.9684	0.1100	2.3142
18	0.3356	1.2852	0.0505	2.4991	39	0.2812	1.2220	0.1057	2.0398
19	0.3559	0.6740	0.0968	1.7741	40	0.2590	1.4051	0.1039	2.5
20	0.2982	1.3217	0.0669	2.3300	41	0.1765	2.3396	0.1042	2.4999
21	0.2752	1.8617	0.0997	1.1720	42	0.2148	1.2480	0.0697	2.5
OF	29.89717		10.96104						

Table 3-17**:** P/B protection operational times for the IEEE 15-bus system.

Relays		MPA			EMPA			Relays		MPA			EMPA		
pr	bc	Top pr	Top bc	CTI	Top pr	Top bc	CTI	pr	bc	Top pr	Top bc	CTI	Top pr	Top bc	CTI
1	6	0.6145	0.8456	0.23108	0.1960	0.3974	0.201	20	30	0.6999	0.9626	0.3991	0.1964	0.4257	0.2911
2	4	0.5549	1.8092	1.2543	0.1655	0.4679	0.3023	21	17	0.7096	0.9815	0.2719	0.2177	0.5535	0.3358
2	16	0.5549	1.1401	0.5852	0.1655	0.4950	0.3294	21	19	0.7096	0.9548	0.2452	0.2177	0.4236	0.2059
3	1	0.9116	1.1856	0.2739	0.2908	0.5547	0.2639	21	30	0.7096	1.0991	0.3895	0.2177	0.4875	0.2697
3	16	0.9116	1.1401	0.2284	0.2908	0.4950	0.2041	22	23	0.5177	1.5175	0.9997	0.2156	0.6029	0.3872
4	7	0.9872	1.3370	0.3498	0.2234	0.4525	0.2290	22	34	0.5177	0.9358	0.4180	0.2156	0.4450	0.2294
4	12	0.9872	1.8784	0.8912	0.2234	0.4759	0.2524	23	11	0.6471	1.2909	0.6437	0.1563	0.3689	0.2126
4	20	0.9872	1.4162	0.4290	0.2234	0.524	0.3007	23	13	0.6471	1.5070	0.8598	0.1563	0.4419	0.2855
5	2	0.8346	2.9385	2.1038	0.2972	0.6742	0.377	24	21	0.7236	2.3891	1.6655	0.2354	0.5458	0.3103
6	8	0.6694	0.8699	0.2004	0.2560	0.5192	0.2632	24	34	0.7236	0.9358	0.2122	0.2354	0.4450	0.2096
6	10	0.6694	1.1186	0.4491	0.2560	0.5690	0.3130	25	15	0.6928	1.0053	0.3124	0.2868	0.5006	0.2137
7	5	0.9186	1.3983	0.4797	0.2845	0.5062	0.221	25	18	0.6928	1.9916	1.2988	0.2868	0.7027	0.4158
7	10	0.9186	1.1186	0.2000	0.2845	0.5690	0.2845	26	28	0.9181	1.3110	0.3929	0.2947	0.5078	0.2131
8	3	0.5523	1.4524	0.9001	0.2669	0.5314	0.2645	26	36	0.9181	1.2481	0.3299	0.2947	0.5346	0.2399
8	12	0.5523	1.8784	1.3260	0.2669	0.4759	0.2089	27	25	0.7287	1.0625	0.3338	0.3268	0.5315	0.2047
8	20	0.5523	1.4162	0.8639	0.2669	0.5242	0.2572	27	36	0.7287	1.2481	0.5193	0.3268	0.534	0.2078
9	5	0.6234	1.3983	0.7749	0.3052	0.5062	0.2010	28	29	0.9665	1.3455	0.3789	0.3264	0.534	0.2080
9	8	0.6234	0.8699	0.2465	0.3052	0.5192	0.2140	28	32	0.9665	1.2281	0.2616	0.3264	0.5367	0.2103
10	14	0.6879	1.7384	1.0505	0.2602	0.5172	0.2569	29	17	0.7101	0.9815	0.2714	0.2128	0.5535	0.3407
11	3	0.6659	1.4524	0.7865	0.2073	0.5314	0.3241	29	19	0.7101	0.9548	0.2447	0.2128	0.4236	0.2108
11	7	0.6659	1.3370	0.6711	0.2073	0.4525	0.2451	29	22	0.7101	0.9626	0.2525	0.2128	0.4257	0.2129
11	20	0.6659	1.4162	0.7503	0.2073	0.5242	0.3168	30	27	0.7336	0.9806	0.2469	0.2738	0.4743	0.2004
12	13	0.9425	1.5070	0.5645	0.2224	0.4419	0.2194	30	32	0.7336	1.2281	0.4944	0.2738	0.5367	0.2629
12	24	0.9425	1.2017	0.2592	0.2224	0.4278	0.2053	31	27	0.5420	0.9806	0.4385	0.2617	0.4743	0.2125
13	9	0.8542	1.0570	0.2028	0.2389	0.5664	0.3275	31	29	0.5420	1.3455	0.8034	0.2617	0.5344	0.2727
14	11	0.8748	1.2909	0.4160	0.1682	0.3689	0.2007	32	33	0.6527	0.8923	0.2396	0.2915	0.5157	0.2241
14	24	0.8748	1.2017	0.3268	0.1682	0.4278	0.2596	32	42	0.6527	0.9788	0.3260	0.2915	0.5916	0.3001
15	1	0.4696	1.1856	0.7159	0.2229	0.5547	0.3318	33	21	0.7418	2.3891	1.6473	0.3403	0.5458	0.2054
15	4	0.4696	1.8092	1.3396	0.2229	0.4679	0.2449	33	23	0.7418	1.5175	0.7757	0.3403	0.6029	0.2625
16	18	0.6939	1.9916	1.29769	0.2217	0.7027	0.4809	34	31	0.7418	0.9843	0.2361	0.3257	0.5288	0.2031
16	26	0.6939	1.6415	0.9476	0.2217	0.4828	0.2610	34	42	0.7481	0.9788	0.2307	0.3257	0.5916	0.2659
17	15	0.7113	1.0053	0.2939	0.2687	0.5006	0.2318	35	25	0.7173	1.0625	0.3451	0.3078	0.5315	0.2237
17	26	0.7113	1.6415	0.9302	0.2687	0.4828	0.2140	35	28	0.7173	1.3110	0.5937	0.3078	0.5078	0.2000
18	19	0.7548	0.9548	0.2000	0.1467	0.4236	0.2768	36	38	0.6104	0.8718	0.2613	0.2851	0.4858	0.2006
18	22	0.7548	0.9626	0.2078	0.1467	0.4257	0.2789	37	35	0.7023	0.9715	0.2692	0.3217	0.5259	0.2041
18	30	0.7548	1.0991	0.3443	0.1467	0.4875	0.3407	38	40	0.7287	0.9723	0.2435	0.3727	0.5727	0.2000
19	3	0.6649	1.4524	0.7874	0.2496	0.5314	0.2818	39	37	0.7136	0.9573	0.2437	0.3334	0.5363	0.2028
19	7	0.6649	1.3370	0.6720	0.2496	0.4525	0.2028	40	41	0.6697	0.8824	0.2126	0.3460	0.5474	0.2014
19	12	0.6649	1.8784	1.2134	0.2496	0.4759	0.2262	41	31	0.5127	0.9843	0.4716	0.3116	0.5288	0.2172
20	17	0.6999	1.0991	0.2815	0.1964	0.4875	0.3571	41	33	0.5127	0.8923	0.3796	0.3116	0.5157	0.2040
20	22	0.6999	0.9815	0.2626	0.1964	0.553	0.2293	42	39	0.5216	0.8692	0.3476	0.2267	0.4275	0.2007
									OF	29.89717			10.96104		

Table 3-18: Comparison of the results for the IEEE 15-bus system.

Method	$sum(Tpr\ i)$
GA [67]	18.9033
EFO [63]	17.906
MEFO [63]	13.953
MWCA [62]	13.3
SA [54]	12.227
IHSA [66]	12.1122
SCA [8]	11.9535
MILP [70]	11.908
VNS [64]	11.779
MRFO with MOF [68]	11.7789
DE [67]	11.7591
IHSA-NLP [66]	11.6699
WOA[58]	11.2670
MPA	29.89717
EMPA	10.9610

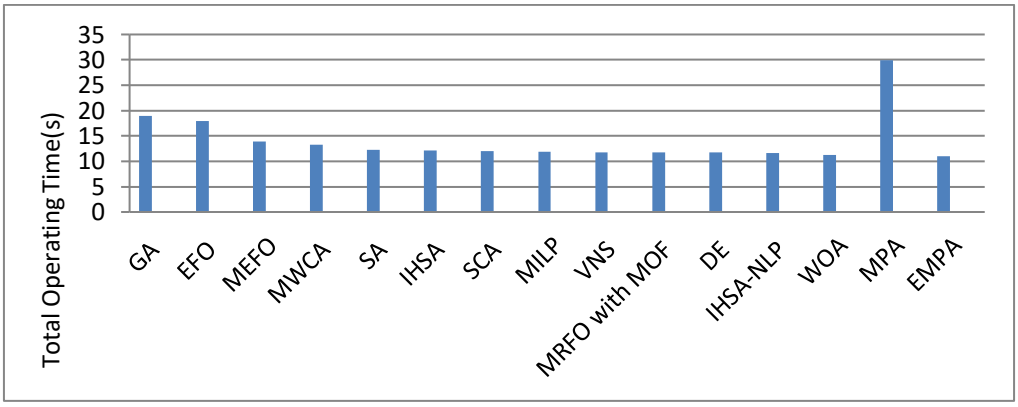

Figure 3-12. Graphical illustration of the total operating time of EMPA compared to the literature for 15-bus test system.

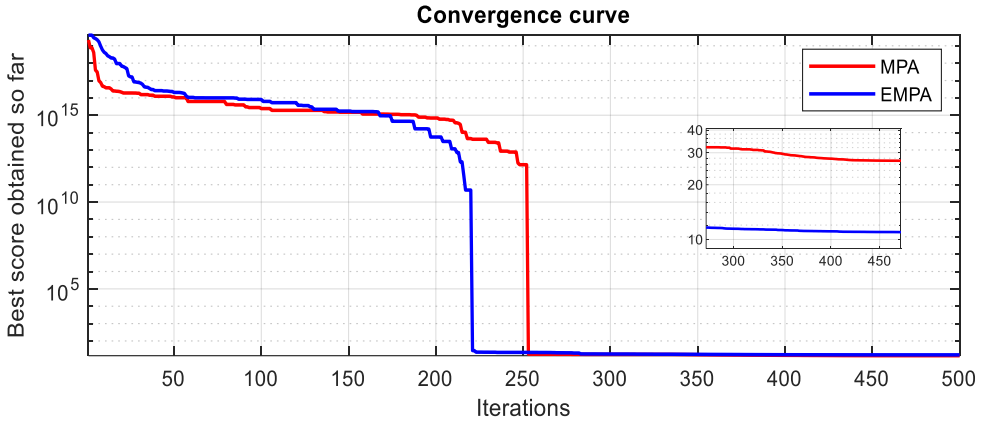

Figure 3-13. Convergence curve of the MPA vs EMPA algorithms in the 15-bus system.

3.5 Conclusion

The DOCRs optimum coordination issue was tackled in this research using an updated version of the marine predators optimization technique. To assess the effectiveness of the suggested technique, it has been verified for relay coordination problem with four distinct systems, which include the 3-bus, 8-bus, 9-bus, and 15- bus test systems. Results are compared with most recently published optimization algorithms (SA, DE, MILP, HS, IHSA-NLP, MEFO, HWOA, MWCA and MRFO). The findings demonstrate that the suggested EMPA technique is an effective and dependable tool for coordinating directional overcurrent relays. Moreover, the obtained results using EMPA clearly show that the suggested approach outperforms a variety of well-known optimization strategies documented in the literature. The Elite marine predators algorithm can be extended and adapted to deal with the optimal coordination problem of DOCRs in more complicated and highly penetrated systems

Chapter 4 Optimal coordination of DOCRs in microgrids

4.1 Introduction

Due to the increased integration of distributed generation (DG) in electric power systems, optimal coordination of overcurrent relays has become a key problem in power distribution systems. However, there is a lack of expertise in the creation of optimum microgrid coordination that takes into account all modes of operations including the grid connected mode, the islanded mode and all the N-1 scenarios through the nonstandard relay characteristics. This work presents a novel technique for optimal coordination of directional overcurrent relays (DOCRs) in terms of relay curve settings (A and B), time dial setting (TDS) and plug setting (PS) to achieve the shortest running time and attain optimal settings. The optimization is carried out using metaheuristic algorithms that ends with a modified version of the Hanger Games Search algorithm (MHGS). The performance of the proposed method is assessed using the 14 bus distribution system while considering all the N-1 contingencies including the grid connected and islanded modes of operations. DIgSILENT software was utilized to perform the required power system analysis, such as power flow and short circuit analysis. The MHGS method is used to determine the best settings for the DOCRs problem. The results are compared to the traditional HGS as well as those obtained by other current optimization approaches provided in the literature in order to demonstrate the effectiveness and superiority of the proposed MHGS in lowering relay operation time for optimum DOCRs coordination.

4.2 The adaptive microgrid protection scheme based on dual settings DOCRs

4.2.1Problem formulation

the Objective Function (OF) employed by the optimization algorithm can be formulated as in chapter 3 where the main objective function is to minimize the total operating time of all primary relays.

Relay characteristics and all the constraints related to the objective function are all the same as previously stated in chapter 3.

4.2.2 proposed protection technique

In Fig 4.1 the proposed protection technique is displayed, the load flow and short circuit analysis are calculated using DIgSILENT software with both grid connected and islanded scenarios and the optimization process was done in the MATLAB environment using the same objective function as in the previous chapter. The relays group of settings is reactivated with each change of the system configuration.

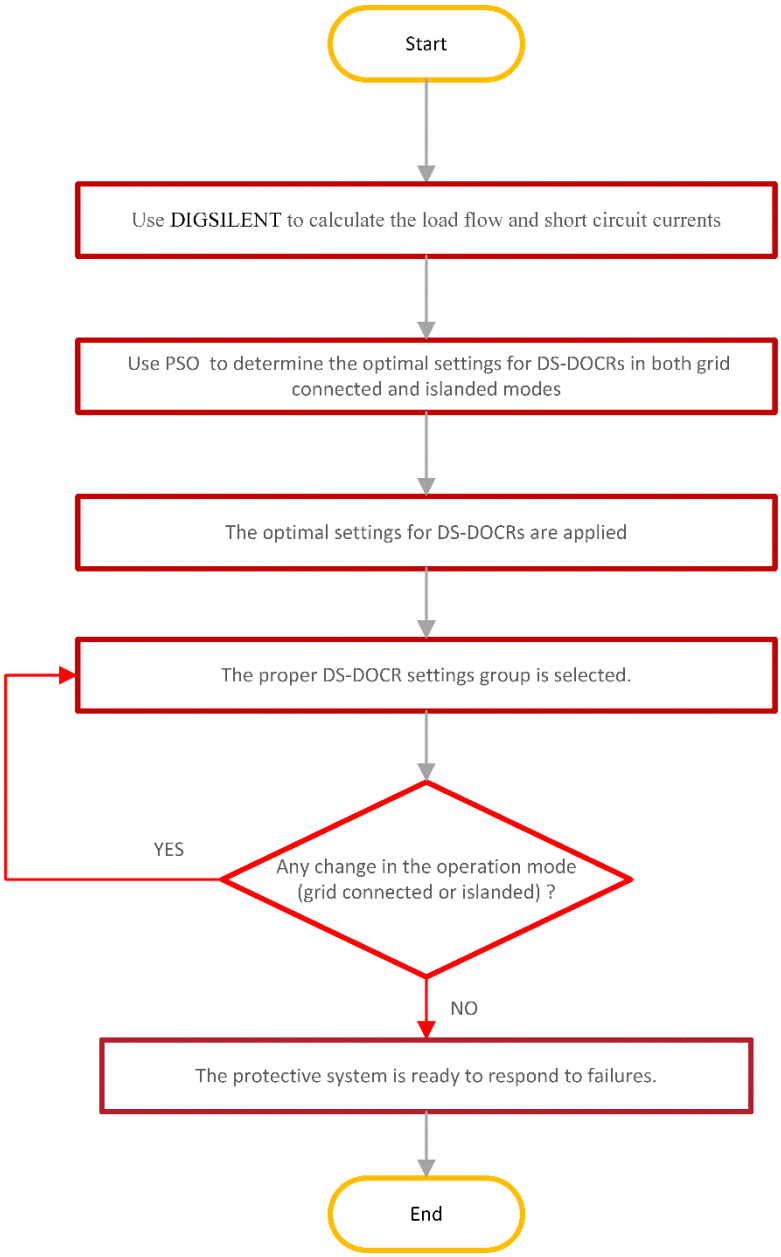

Figure 0-1. The adaptive protection scheme

4.2.3 Test system and results:

The proposed DSDOCR-based protection system is tested on the distribution network of the IEEE 14-Bus test system in this study. Fig.4.2 depicts the selected system's single line diagram (SLD). The IEEE 14-bus system is connected to the grid through two 132 kV/33 kV transformers (T1 and T2). Furthermore, this system has seven buses, 16 protection relays and three DG units,

each with a capacity of 20 MVA, are linked to this network. The rest of the system's data are in [23]. The created approach will be tested in two different scenarios:

Scenario 1: Grid connected mode

Scenario 2: Islanded mode of operation

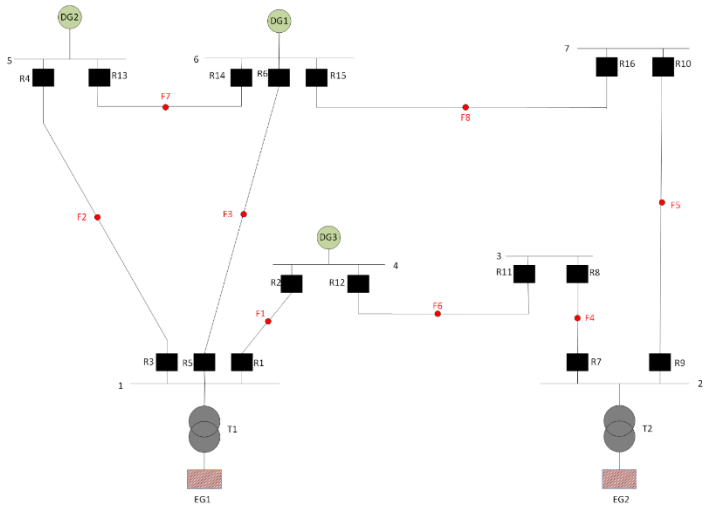

Figure 0-2. IEEE 14 bus distribution system.

4.2.4 Results and discussion

This section discusses the optimal relay settings and total operating time for failures at middle points F1 - F8 in two different operating modes. For comparative analysis and assessment, the dual-setting design technique is used on the IEEE 14 bus distribution test system illustrated in Fig. 4.2. The following settings for both design methodologies are examined in grid-connected and islanded modes of operation.

Table 4.1 and table 4.2 shows the short circuit currents of the first and second scenarios respectively. The data were calculated using DIgSILENT software, the optimization process was done using PSO algorithm and the findings are summarized in table 4.3 and 4.4 for the grid connected and islanded mode respectively, where all relays settings (TDS and PS settings) and the overall operating time of all primary relays are displayed. The validation of the results is shown in figure 4.3 and figure 4.4 where the coordination time interval between the operating times of the primary and backup relays is shown. The CTI is kept in a range of [0.2, 0.3], so it is

clear that the protection coordination scheme is working properly, no miscoordination between the relays and with minimum operating times for both grid connected and islanded modes.

Table 0-1: Short circuit current values in the main scenario (scenario1).

Fault location	Short-circuit currents (A)					
	Primary Relays		1st back-up relay		2nd back-up relay	
F1	R1	6021	R4	965	R6	1566
	R2	3815	R11	2166		
F2	R3	5462	R2	1696	R6	593
	R4	3033	R14	1450		
F3	R5	6477	R2	2012	R4	483
	R6	4080	R13	1046	R16	1275
F4	R7	5902	R10	1392		
	R8	3206	R12	3206		
F5	R9	4878	R8	1574		
	R10	2278	R15	2278		
F6	R11	3886	R7	3886		
	R12	4617	R1	3050		
F7	R13	3446	R3	1819		
	R14	4707	R5	2196	R16	1094
F8	R15	4479	R5	2312	R13	1026
	R16	2417	R9	2417		

Table 0-2Table 4.2: Short circuit current values in scenario2.

Fault location	Short-circuit currents (A)					
	Primary Relays		1st back-up relay		2nd back-up relay	
F1	R1	2707	R4	1142	R6	1566
	R2	2148	R11	295		
F2	R3	2432	R2	1313	R6	1122
	R4	2337	R14	602		
F3	R5	2288	R2	1357	R4	936
	R6	2876	R13	753	R16	260
F4	R7	1211	R10	1211		
	R8	2426	R12	2426		
F5	R9	1756	R8	1756		
	R10	1663	R15	1663		
F6	R11	894	R7	894		
	R12	3262	R1	1530		
F7	R13	2303	R3	497		
	R14	2664	R5	587	R16	329
F8	R15	3039	R5	770	R13	815
	R16	974	R9	974		

Table 0-3: Relay settings and operation times for grid connected 14-bus distribution system.

Relay	TDS	PS	Relay	TDS	PS
1	0.0593	2.6197	9	0.0967	5
2	0.2798	1.2746	10	0.4137	0.2091
3	0.2733	5	11	1.1	0.1
4	0.2310	1.7667	12	0.2669	3.5336
5	0.1353	4.9984	13	0.7383	2.0821
6	0.0205	3.7644	14	0.2685	5
7	0.1654	3.1630	15	0.7170	0.7864
8	0.5487	0.1	16	0.5661	0.1041
OF	11.4638				

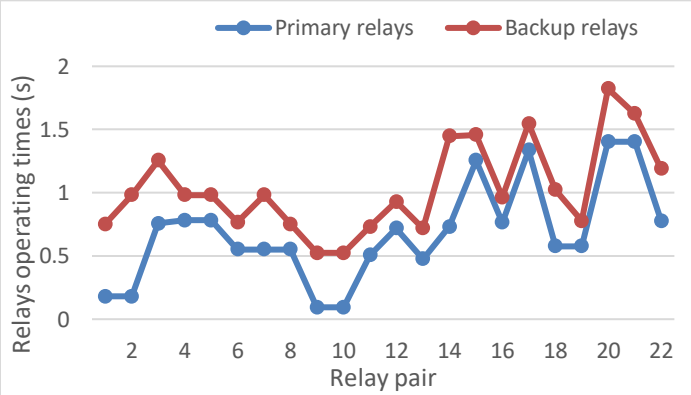

Figure 0-3. Relays coordination time interval (CTI) for the grid connected 14-bus distribution system.

Table 0-4: Relay settings and operation times for islanded 14-bus distribution system.

Relay	TDS	PS	Relay	TDS	PS
1	0.1119	2.4051	9	0.1620	1.8897
2	0.1581	0.5371	10	0.2698	1.0520
3	0.2916	1.2506	11	0.1856	0.8421
4	0.2152	0.7837	12	0.4601	0.9890
5	0.1161	1.5850	13	0.1845	3.9728
6	0.1265	1.1487	14	0.2170	2.0986
7	0.2483	0.6902	15	0.1285	2.1839
8	0.5214	0.3924	16	0.1886	0.6820
OF	9.8872				

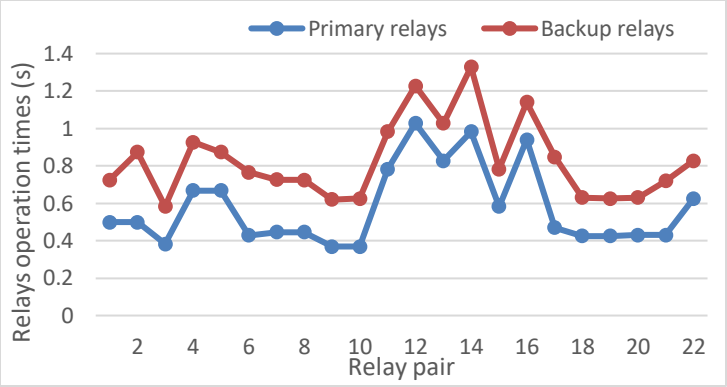

Figure 0-4. Relays coordination time interval (CTI) for the islanded 14-bus distribution system.

4.3 The adaptive Protection Coordination for microgrids utilizing user-defined DOCRs characteristics with different groups of settings

4.3.1 Problem formulation

1.1. Objective Function

This study proposes a novel adaptive protection system for DS-DOCRs with an unrestricted number of setting groups taking into account the various operating modes and topologies of MG. For a particular relay, the values of the curve settings (A and B) are fixed. The traditional COP does not take these parameters into account. The proposed research would optimize the time Multiplier settings (TDS), the plug settings (PS) and the curve settings (A and B) of the DOCRs. This research also focuses on minimizing the optimization problem's coordination restrictions, employing an adaptive strategy, and considering different setting groups for various network configurations. The suggested relay coordination issue minimize the overall time of operation of all relays by optimizing the four continuous variables, TMS, PS, A, and B. Therefore, the problem may be formulated using Eq.(4.1):

$$\text{Minimize, OF} = \sum_{i=1}^{m} W_{1i}\, T_{pr\,i} + W_{2i}\, T_{bc\,i} + W_{3i} CTI_i \qquad (4.1)$$

Where m is the number of all relays in the system under study, W_1, W_2, and W_3 are weight factors and their total is frequently taken as 1. The suggested OF takes into account the running

time of primary relays, backup relays and the coordination time interval (CTI). When the input current of a directional overcurrent relay (DOCR) exceeds a predefined value; the relay functions and sends a trip signal in which it is located. Moreover, the directional element distinguishes the direction of the fault current and is only sensitive to a single fault direction. Selectivity can therefore be achieved in meshed systems. Besides, obtaining selectivity in meshed systems using simply non-directional overcurrent relays is very difficult. The time-current characteristics of an (IEC) IDMT relay are described by the Eq. (4.2) [71] :

$$T_{i,j} = A_i \frac{TDS_i}{\left[\left(\frac{I_{scj}}{PS_i}\right)^{B_i} - 1\right]} \tag{4.2}$$

Where $T_{i,j}$ is the time relay i (R_i) takes to operate for a failure at location j. TDS_i and PS_i represent R_i's settings. I_{scj} is the amount of short-circuit detected by R_i for a fault at location j. The constants Ai and Bi are connected to the IEC defined curve types of R_i. TDS, PS, A, and B of all relays in the simulated system are regarded as variables for optimum relay coordination. In a relay coordinating issue with m relays, the optimization process requires 4*m variables for optimal relay coordination in a network with m relays.[21]

Traditional protective systems that simply address the basic network design may not be sufficient for ADNs, MGs, and SGs. This is primarily because, unlike traditional passive distribution networks, ADNs, MGs, and SGs may operate in islanded mode and different network configurations other than grid-connected operating mode. As a result, some miscoordinations are expected to take place if the coordination constraints addressing the islanded mode and other network designs are not concerned with the ideal protection system. The rising penetration of DGs emphasizes the significance of evaluating alternative network architectures and accompanying selectivity limits.

4.3.2Technical Constraints

a) Relay operational time limits

The restrictions in Eq. (4.3) are linked to the minimum and maximum operating times permitted. Although relays should run as quickly as possible, they only need a short period of time to do so. Yet, if the DOCRs take too long to function, irreparable equipment damage and power system instability may occur. This set of restrictions is represented as follows:

$$T_{i,min} \leq T_i \leq T_{i,max} \tag{4.3}$$

Where $T_{i,min}$ and $T_{i,max}$ are the minimum and maximum operational times for R_i while acting as main protection. This time varies depending on the relay designer and the heat constraints of the protected device, and it is often set to 0.05 and 1 respectively.

b) Coordination time interval

The coordination limitations are one of the constraints that must be considered by the algorithm. The coordination time interval, which is calculated using Eq. (4.4), corresponds to the time delay during which the backup relay (BR) must trip. The CTI depend on the type of the employed relay. Numerical relays have a CTI of 0.2sec while electromechanical relays have a CTI of 0.3 sec.

$$T_{bc\,i} - T_{pr\,i} \geq CTI \tag{4.4}$$

Where $T_{pr\,i}$ / $T_{bc\,i}$ are the primary and backup relays operating time for relay i (R_i)

c) Pickup current and time dial settings

This limitation is determined by the operating parameters of both the relay and the power system. As the pickup current is the smallest current at which the relay must trip, it must be larger than the highest current detected by the relay. Otherwise, it may result in erroneous and/or premature tripping. Fault currents in power networks with high impedance faults or high penetration of DG units based on grid-tie inverters tend to be low, that is, frequently rated at the load current. In this regard, the pickup current should not be too high such that the relay becomes overly sensitive. As a result, the inequality established in Eq.(4.5) must be followed by [72] :

$$PS_{i,min} \leq PS_i \leq PS_{i,max} \tag{4.5}$$

Where $PS_{i,min}$ and $PS_{i,max}$ are the minimum and maximum pickup currents of the relay, respectively. Furthermore, the goal function is subject to additional limitation based on the TDS limits, which are described below in Eq. (4.6).

$$TDS_{i,min} \leq TDS_i \leq TDS_{i,max} \tag{4.6}$$

Where $TDS_{i,min}$ and $TDS_{i,max}$are lower and upper limits of *TDS* of the *ith* relay

d) User defined Relay curve settings (A and B)

The constant variables are calculated to give additional flexibility inside numerical DOCRs by providing operation with a broader range of characteristics that are not confined to standard time-current characteristics. Both constants A and B are treated as variables in the relay coordination issue in the suggested technique. Setting the upper and lower bounds in the specified issue yields the optimal and feasible values for these variables. The lower and upper bounds of both variables are specified as follows:

$$A_{i,min} \leq A_i \leq A_{i,max} \tag{4.7}$$

$$B_{i,min} \leq B_i \leq B_{i,max} \tag{4.8}$$

Where the minimum and maximum values of the continuous variables A and B examined in this paper are [0.14,80] and [0.02,2] respectively [21] . Fig.4.5 depicts the flowchart of the suggested technique for optimizing the adaptive protection system of MG and ADNs. DIgSILENT is utilized to imitate the system understudy and distinct the needed inputs of the optimization issue, such as the current traveling through the distribution lines in various operating modes (before a fault occurs) and short circuit currents. The proposed technique addresses the presented COP by employing relays coordination with four user defined settings (TDS, PS, A, B). The optimization algorithm is written in the MATLAB programming language.

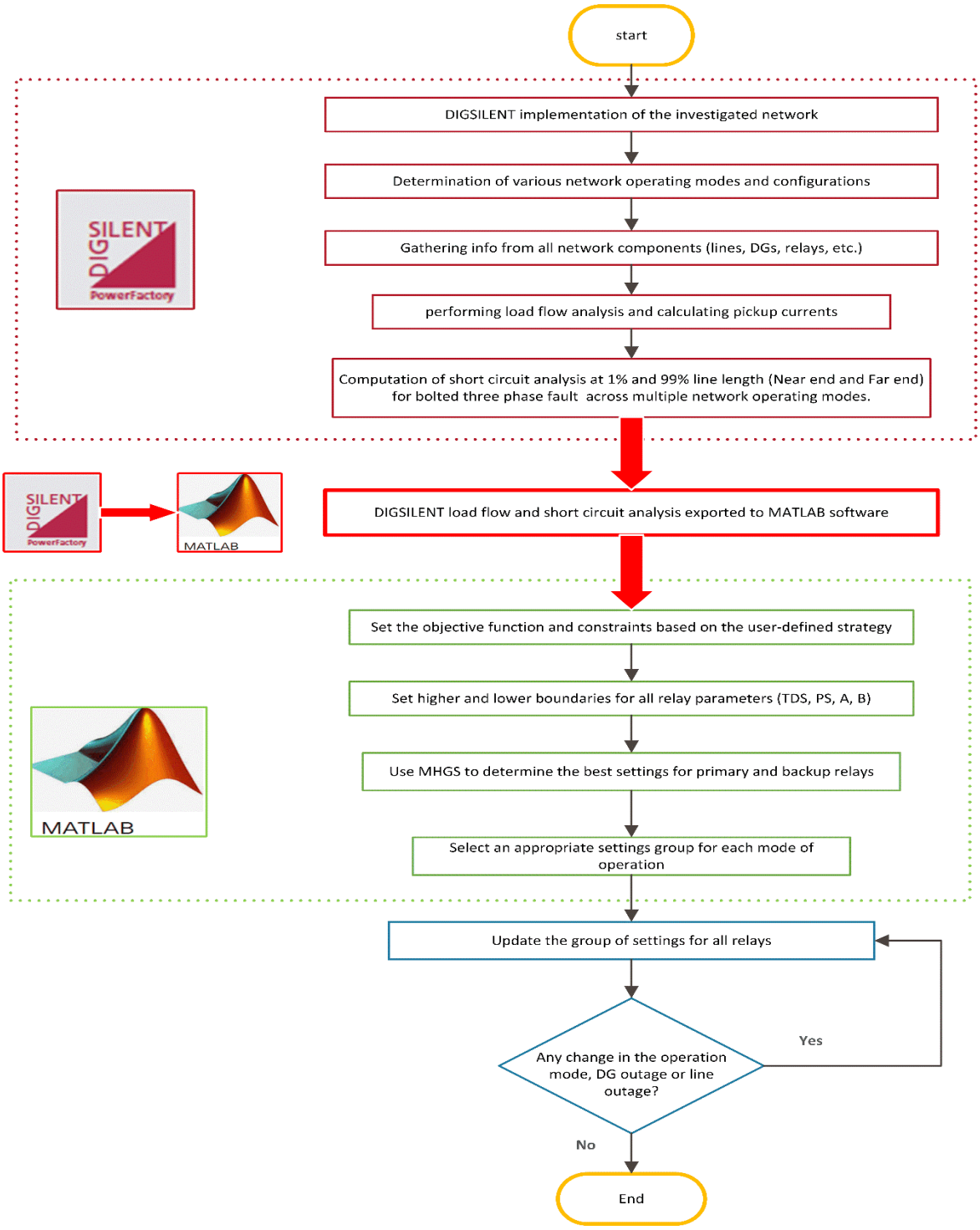

Figure 0-5. Flowchart of the proposed technique.

4.3.3 The proposed optimization method

A. The original Hanger games search algorithm

The hunger games search (HGS) optimizer is a meta-heuristic algorithm that has been introduced by Y. Yang *et al.* [73].So far it has not been employed in recent research for coordination protection problems. HGS mimics the starvation driven actions and behavior of animals. While looking for food, animals employ two social strategies: the first involves the animals 'cooperation as a group. Whereas, the second strategy appears when few individuals or animals are separated and refuse to participate in the collaboration. The last individuals rely on their talents to collect food (self-reliance). Therefore, when searching for food, animals adopt a logic of games according to their level of hunger. Mathematically, this logic of games is represented by a set of equations, as expressed by Eq.(4.9). These equations model the cooperation and separation of individuals of HGS.

$$\overrightarrow{Y(t+1)} = \begin{cases} G_1: \overrightarrow{Y(t)}.\left(1+rd(1)\right), 1 < u \\ G_2: \overrightarrow{W_1.Y_b(t)} + \overrightarrow{RF}.\overrightarrow{W_2}.\left|\overrightarrow{Y_b} - \overrightarrow{Y(t)}\right|, r_1 > u, r_2 > C \\ G_3: \overrightarrow{W_1.Y_b(t)} - \overrightarrow{RF}.\overrightarrow{W_2}.\left|\overrightarrow{Y_b} - \overrightarrow{Y(t)}\right|, r_1 > u, r_2 > C \end{cases} \quad (4.9)$$

Where:

- r_1 and r_2 are arbitrary values in the range of [0,1], G1, G2, and G3 represent various game strategies while *rd*(1) creates random numbers from a normal distribution. The parameter u was added to improve the method, and $\overrightarrow{Y(t)}.\left(1+rd(1)\right)$ represents the animal's capacity to look for food in the domain while hungry. C is a variation control for all position and RF is a variable that is defined within the interval [-a, a] and can rely on the number of iterations as in Eq.(4.10):

$$RF = 2 \times s \times rd - s, \quad s = 2 \times \left(1 - \frac{t}{T}\right) \quad (4.10)$$

- W_1 and W_2 reflect the hunger weights which are provided by Eq.(4.11) and Eq.(4.12) respectively:

$$W_1 = \begin{cases} H_i \times \frac{N}{SH} \times r_4, r_3 < u \\ 1, r_3 > u \end{cases} \quad (4.11)$$

$$W_2 = (1 - e^{(-|H_i - SH|)}) \times r_5 \times 2 \quad (4.12)$$

- N is the total number of individuals, while SH denotes the overall hunger affliction of each animal.

- r_3, r_4, r_5 are arbitrary values in the range of [0,1].

Eq. (4.13) is often used to compute the term Hi.

$$\mathrm{H}_i = \begin{cases} 0, & Fitn_i = Best\ fitness \\ H_i + H_n, & otherwise \end{cases} \quad (4.13)$$

Where:

- $Fitn_i$ is the fitness of every creature in the current iteration and H_n is hunger parameter which is computed using Eq.(4.14):

$$H_n = \begin{cases} LH \times (1 + r), & Hr < LH \\ Hr, & otherwise \end{cases} \quad (4.14)$$

- Hr is a hunger ratio that is determined by the amount of food consumed to overcome hunger and the total searching capabilities for food. Hr is represented in Eq.(4.15) where the term r_6 is an arbitrary value in the range of [0,1] and the minimum and maximum limitations define the individual's level of hanger.

$$Hr = 2\ \frac{Fitn_i - Best\ fitness}{Fitn_w - Best\ fitness} \times r_6 \times (upper\ bound - lower\ bound) \quad (4.15)$$

B. The modified hanger games search algorithm

In the early phases of the optimization process, the original HGS optimizer has a property to converge early. This is due to the algorithm's greedy approach, which means it always selects the solution that is closer to the optimum at each stage. This might cause the algorithm to become trapped in a local minimum. The faster is nothing but a suboptimal solution that cannot be the best feasible result.

The modified HGS algorithm (MHGS) overcomes this drawback by incorporating a number of improvements. Hanger weights and best Positions determine the transformation range, this means that any change to these terms flutters the optimizer during calculation and may prohibit local optima. To balance the exploration and exploitation phases, the examined population-based algorithm realized statistical patterns (games). Therefore, this optimizer may combine the possibilities of a global optimal solution with the capacity to handle multimodal challenges.

In the proposed enhanced algorithm, the suggested improvement on the parameters can be expressed as follows:

- Weight considerations to reinforce solutions: This step guarantees that the algorithm continues to seek the global optimum even if a local minimum is found, the modifications of $W_1\ and\ W_2$ are mentioned in Eq.(4.16) and Eq.(4.17) .

$$W_1 = \begin{cases} H_i \times \frac{N}{SH}, r_3 < l \\ 1, r_3 > l \end{cases} \quad (4.16)$$

$$W_2 = (1 - e^{(-|H_i - SH|)}) \times 2 \quad (4.17)$$

- Randomly distributed choice approach for selecting two solutions: the individuals in classical HGS choose between three games (G1, G2 and G3). Equation of G1 simulate the evolution of positions of Individuals who rely on their skills (self-reliance) to search for food. Equations of G2 and G3 simulate the cooperation of individuals within the search space while looking for food. Therefore, the last game is extremely important to perform the first stage of the algorithm that is exploration. In other words, failing to accomplish this stage, the algorithm is likely to converge to local optima. In this work, a modification in the update of individual of G2 and G3 is suggested. This method ensures that the algorithm does not always choose the most comparable solutions, and subsequently can help avoiding the algorithm from becoming trapped in a local minimum as it is mentioned in Eq.(4.18).

$$\overrightarrow{Y(t+1)} = \begin{cases} G_1: \overrightarrow{Y(t)}.\left(1 + rd(1)\right), 1 < u \\ G_2: \overrightarrow{W_1}.\overrightarrow{Y_b(t)} + \overrightarrow{(RF \times rd)}.\overrightarrow{W_2}.\left|\overrightarrow{Y_b} - \overrightarrow{Y(t)}\right|, r_1 > u, r_2 > C \\ G_3: \overrightarrow{W_1}.\overrightarrow{Y_b(t)} - \overrightarrow{(RF \times rd)}.\overrightarrow{W_2}.\left|\overrightarrow{Y_b} - \overrightarrow{Y(t)}\right|, r_1 > u, r_2 > C \end{cases} \quad (4.18)$$

These modifications contribute to the MHGS method being quicker and more efficient than the original HGS optimizer. The MHGS method converges faster and is less vulnerable to get trapped in local minima. This indicates that the MHGS algorithm is more likely to identify the global optimum, or optimal solution.

The MHGS method is not only faster and more economical, but it also generates good results. The MHGS method was able to reach the best operating time of DOCRs in a power system with a high number of variables and restrictions in the problem formulation. This demonstrates that the MHGS algorithm is a potential method for determining the optimal coordination of DOCRs in real-world power systems.

4.3.4 Simulation and results

A. Test system

One of the most important problems with every newly established technique and its programming is determining the dependability of the computations, the efficacy and applicability of the suggested protection settings method.

The employed system in this research depends on the distribution system component of the IEEE 14-bus system [34], as illustrated in Fig. 4.6**.** The system is powered by a 500-MVA utility grid with an X/R ratio of 6. Two 60-MVA 132 kV/33 kV transformers linked at buses 1 and 2 connect the considered system to utility grid. Three synchronous-based distributed power generations are spread at some feeders. The rating of the Distributed Generators (DGs) is chosen such that it can provide the local load in the event of islanded operating mode. Each unit has a 20 MVA rating. This system is outfitted with identical 16 DOCRs. The rest of the data for the system under consideration is taken from [74]. According to [22, 23, 33], the distribution system of the IEEE 14-bus test bench comprises a number of 15 network configurations based on N-1 contingency. Fig.4.7 displays all the possible scenarios.

Scenario 1 : normal operation or Grid-connected mode.

Scenarios 2-to-3 : Loss of power from the upstream grid (Upstream grid outage).

Scenario 4 : Disconnected from the main power grid (Islanded mode).

Scenarios 5-to-7 : Loss of distributed generation (DG outage).

Scenarios 8-to-15 : Loss of a transmission line (Line outage).

Fig.4.7 shows the various topologies that are taken into account in this study, one test system was chosen (a benchmark case study in [22]). The procedure described in [22] was used to replicate the available outputs. If the reported findings in the accessible reference are identical to the achieved results, the calculations and programming will be confirmed. Furthermore, a parametric comparison of the suggested approach as well as other references that have the same case study is important to demonstrate the performance and the advantages of this research. As a consequence, the acquired findings using the suggested approach are compared to those published in the accessible reference. Besides, the Near-end faults(the highest short circuit current traveling through the primary and backup DOCRs), Far-end faults on the other hand, are also essential, and coordination constraint violations may occur if they are not included in

protective system design [75]. As a result, additional evaluations have been performed to evaluate the performance of the proposed technique against far-end faults to other current methods. Table 4.5 displays the near/far-end faults for scenario 1 whereas tables 4.6 and 4.7 summarize the findings of all configurations considering near / far end faults respectively.

Since all the findings in [22] are approximately the same, the comparison test results have approved the calculations and applied programming. Furthermore, the technique of [27] (by employing dual setting DOCRs, taking into account only grid-connected and islanded modes) and the proposed method (adaptive protective scheme based on independent changes in setting groups, considering N-1 contingency) were both applied to the IEEE 14-bus distribution system. Table 4.23 shows a comparison of test results of several methodologies.

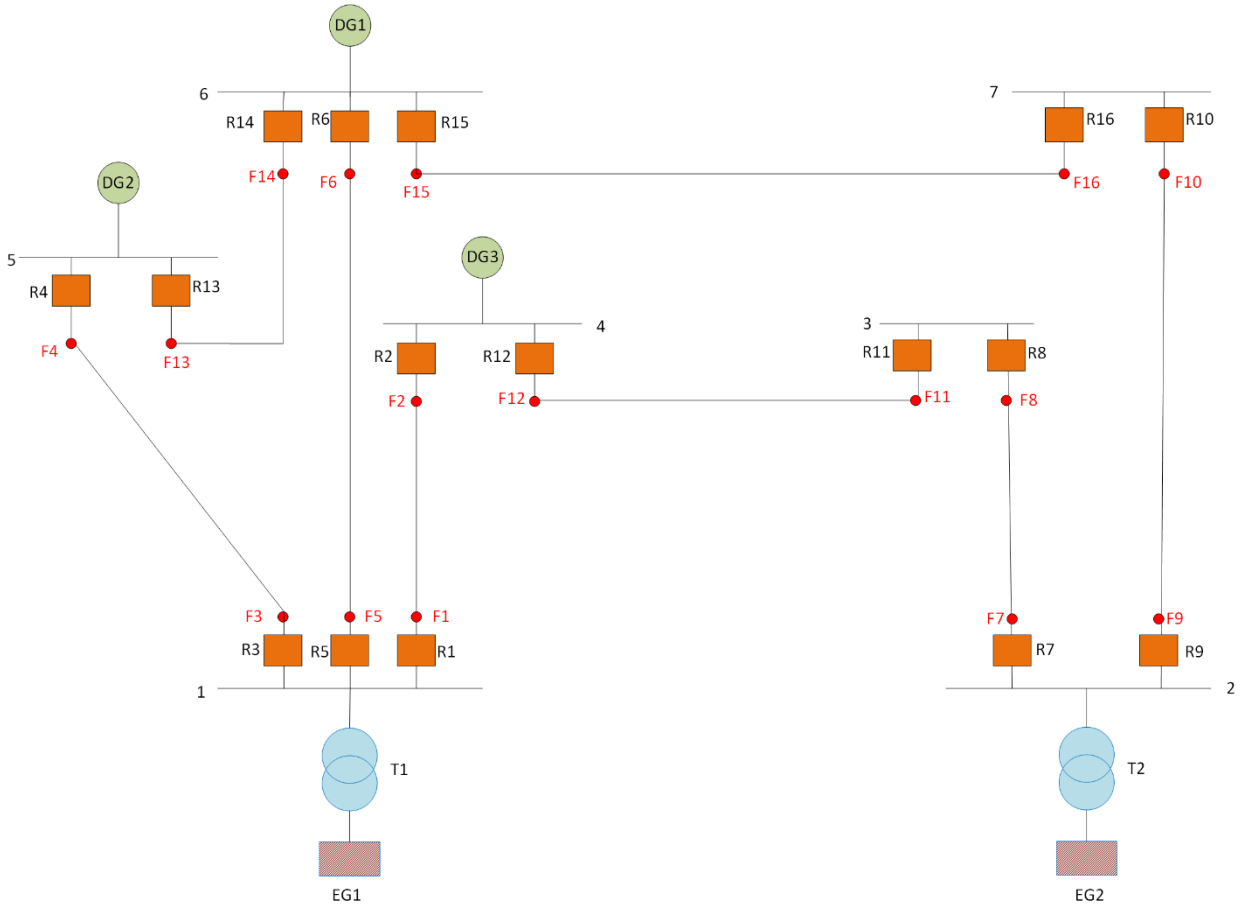

Figure 0-6. Distribution network of the IEEE 14-bus test system.

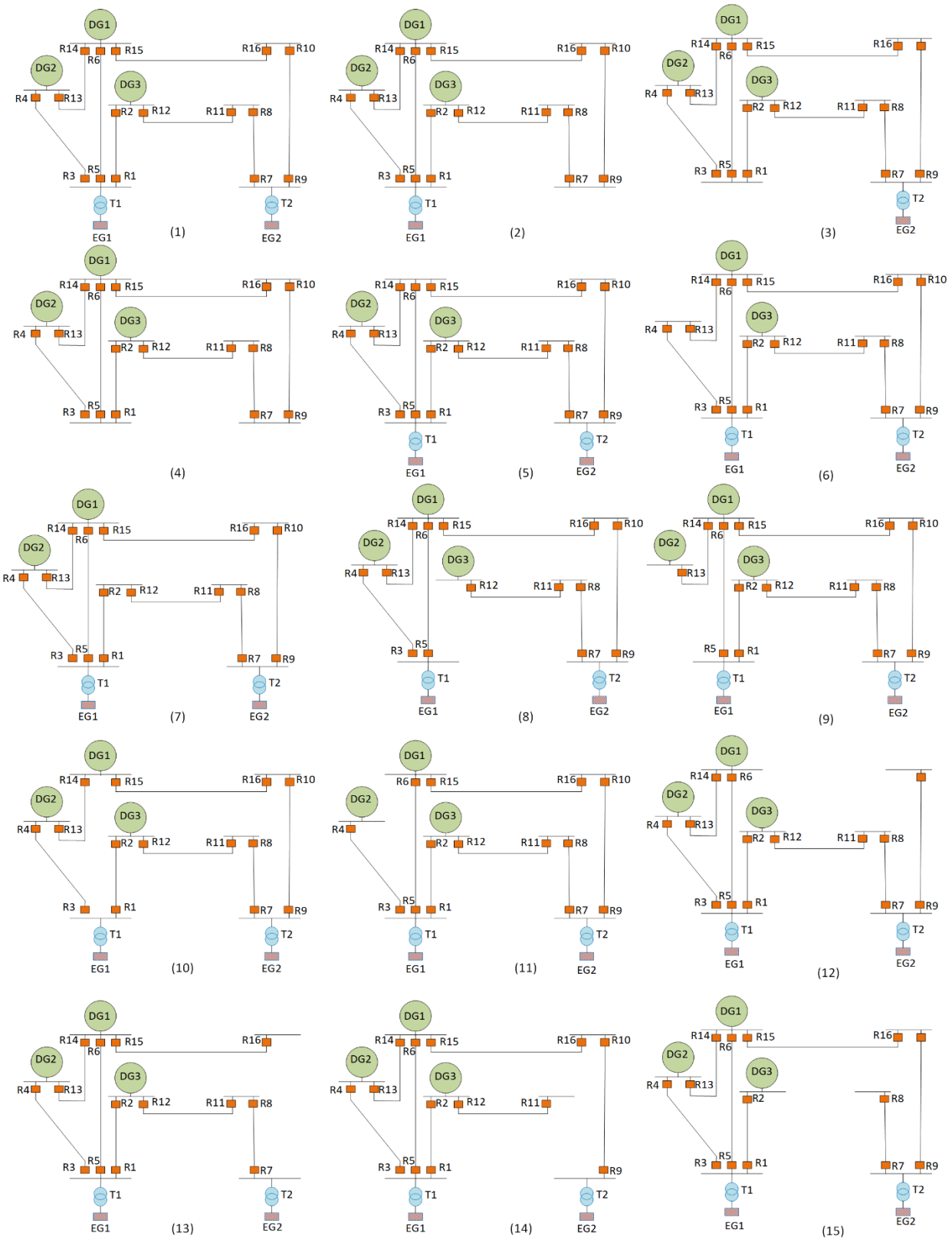

Figure 0-7. Numerous contingencies and operating modes of the IEEE 14-bus test system's meshed distribution section.

Table 0-5: Short circuit current values in the main scenario (C1).

Fault locations	Fault currents (A)					
	Primary Relays		1st back-up relay		2nd back-up relay	
F1	R1	9641	R4	1515	R6	2721
	R2	2897	R11	1468		
F2	R2	5111	R11	3035		
	R1	4341	R4	690	R6	921
F3	R3	10662	R2	2834	R6	2682
	R4	1570	R14	71		
F4	R4	4831	R14	2860		
	R3	3425	R2	1383	R6	826
F5	R5	9554	R2	2855	R4	1505
	R6	2783	R13	137	R16	978
F6	R6	5650	R13	1932	R16	1679
	R5	4670	R2	1546	R4	473
F7	R7	6913	R10	1715		
	R8	2900	R12	2900		
F8	R8	3548	R12	3548		
	R7	5137	R10	1136		
F9	R9	8012	R8	2852		
	R10	1735	R15	1735		
F10	R10	2942	R15	2942		
	R9	3460	R8	941		
F11	R11	5092	R7	5092		
	R12	3572	R1	2276		
F12	R12	6344	R1	4282		
	R11	3071	R7	3071		
F13	R13	5430	R3	3355		
	R14	2925	R5	874	R16	879
F14	R14	8292	R5	4568	R16	1670
	R13	1983	R3	511		
F15	R15	8485	R5	4555	R13	1918
	R16	1704	R9	1704		
F16	R16	3412	R9	3412		
	R15	2979	R5	1427	R13	699

Table 0-6: Near-end fault currents in different scenarios (C1-C15).

Fault locations	Relays	Fault currents for each scenario (A)														
		C1	C2	C3	C4	C5	C6	C7	C8	C9	C10	C11	C12	C13	C14	C15
F1	R1	9641	8674	4262	3506	8020	7965	9309	/	8716	7673	9417	8639	8777	9436	9513
	R4	1515	1388	1524	1397	1265	567	1409	/	/	2505	1604	1381	1301	1495	1490
	R6	2721	2093	2739	2110	1573	2216	2631	/	3548	/	2633	2064	2064	3035	2882
F2	R2	5111	3043	4929	2726	4960	5045	3043	/	5128	5235	5098	4983	4667	2096	1970
	R11	3035	959	2850	636	2882	2967	3043	/	3053	3161	3021	2905	2635	1	/
F3	R3	2834	8885	5570	2098	9439	10139	9587	8239	/	8286	10606	10324	9960	9557	9483
	R2	10662	1639	2855	1652	2749	2808	1830	/	/	3104	2831	3163	2944	1657	1586
	R6	2682	2069	2715	3750	1540	2176	2599	3078	/	/	2628	2019	2019	2995	2847
F4	R4	4831	4482	4171	3615	4304	2872	4706	4669	/	4469	2093	4546	4307	4568	4557
	R14	2860	2477	2169	1568	2313	2872	2724	2690	/	2445	/	2555	2492	2685	2692
F5	R5	9554	8241	4383	3048	9215	8568	8533	6801	8103	/	9652	9736	9340	8494	8372
	R2	2855	1646	2868	1655	2765	2829	1841	/	2904	/	2849	3188	2962	1667	1594
	R4	1505	1380	1518	1393	1253	552	1489	1585	/	/	1609	1367	1367	1567	1482
F6	R6	5650	4597	5032	3811	3592	4775	5439	5777	5418	/	3799	4037	4080	5545	5530
	R13	1932	1815	1430	1263	1935	1063	1847	1732	1660	/	/	2000	1736	1672	1655
	R16	1679	734	1549	483	1664	1650	1548	2003	1689	/	1725	/	0.00	1845	1660
F7	R7	6913	1721	6517	1306	6514	6779	6818	7224	6924	6791	6848	5040	4858	/	6902
	R10	1715	1721	1301	1306	1485	1573	1617	2051	1728	1595	1647	1	/	/	1910
F8	R8	3548	3457	2774	2632	3364	3377	2693	1720	3500	3553	3548	3535	3575	/	0
	R12	3548	3457	2774	2632	3364	3377	2693	1720	3500	3553	3548	3536	3575	/	/
F9	R9	8012	2878	7387	2229	7688	7873	7357	6773	7983	8093	8014	7927	/	4828	4969
	R8	2852	2878	2207	2229	2693	2706	2192	1580	2824	2934	2854	2939	/	/	2
F10	R10	2942	2768	2399	2108	2581	2734	2833	3006	2944	2408	2789	0	/	2928	2907
	R15	2942	2768	2399	2108	2581	2734	2833	3006	2944	2408	2789	/	/	2929	2908
F11	R11	5092	1494	4810	1112	4838	4998	5029	5395	5103	5088	5056	4006	3890	0	/
	R7	5092	1494	4810	1112	4838	4998	5029	5395	5103	5088	5056	4007	3891	/	/
F12	R12	6344	6047	4621	4183	5952	5956	4292	2095	6185	6039	6344	6016	6091	6317	/
	R1	4282	3980	2545	2101	3884	3888	4292	/	4123	3974	4282	4270	4343	4404	/
F13	R13	5430	5069	4221	3568	3070	3367	5231	4985	2094	5686	/	4795	4777	4808	4780
	R3	3355	2986	2136	1477	5148	3367	3152	2903	/	3627	/	3207	3201	3208	3196
F14	R14	8292	6852	5950	4159	6227	7856	7793	7714	8531	4024	/	6651	6849	7870	7881
	R5	4568	4042	2336	1586	4574	4149	4186	3680	4796	/	/	4771	4683	4459	4399
	R16	1670	733	1545	484	1657	1646	1541	1992	168	1961	/	/	0.00	1635	1650
F15	R15	8485	7843	5807	4893	6459	7249	8028	7440	8442	5006	7394	/	8424	7918	7843
	R5	4555	4022	2341	1585	4565	1062	4175	3688	4759	/	5348	/	4666	4462	4403
	R13	1918	1801	1428	1261	1924	4148	1834	1727	1639	3025	/	/	1982	1662	1646
F16	R16	3412	1777	3199	1379	3317	3360	3238	3339	3412	3530	3417	/	0	2673	2714
	R9	3412	1777	3199	1379	3317	3360	3238	3339	3412	3530	3417	/	/	2674	2715

Table 0-7: Far-end fault currents in different scenarios (C1-C15).

Faults locations	Relays	Fault currents for each scenario (A)														
		C1	C2	C3	C4	C5	C6	C7	C8	C9	C10	C11	C12	C13	C14	C15
F1	R2	2897	1678	2893	1671	2805	2867	1870	/	2943	3159	2892	3222	2988	1677	1602
	R11	1468	0042	1464	49	1355	1430	1870	/	1526	1793	1462	1879	1640	40	/
F2	R1	4341	4035	2576	2126	3936	3940	4340	/	4179	4023	4341	4442	4395	4460	4495
	R4	690	631	1012	974	611	198	690	/	/	1115	844	710	1013	1096	1089
	R6	921	493	1565	1155	363	772	919	/	1367	/	767	1061	1061	1461	1844
F3	R4	1570	1436	1555	1421	1313	610	1548	1636	/	2544	1625	1431	1343	1537	1532
	R14	71	257	90	278	411	610	100	67	/	1234	/	264	236	165	197
F4	R3	3425	3050	2185	1517	3135	3421	3219	2964	/	3678	4226	3335	3265	3271	3259
	R2	1383	761	1913	1185	1445	1384	890	/	/	1178	1128	1718	2175	1293	1352
	R6	826	873	423	393	1314	834	707	313	/	/	1047	1282	1282	602	1027
F5	R6	2783	2148	2774	2138	1616	2266	2690	3162	3604	/	2679	2105	2123	2943	2929
	R13	137	31	128	307	473	552	161	63	1227	/	/	331	254	123	158
	R16	978	65	976	61	1143	1063	847	1546	842	/	995	/	0	1435	1244
F6	R5	4670	4124	2392	1624	4657	4243	4279	3764	4870	/	5460	4962	4777	4559	4498
	R2	1546	615	2120	1123	1529	1063	884	/	1482	/	1327	2064	2324	1413	1429
	R4	473	335	369	528	473	1650	375	257	/	/	977	562	562	409	725
F7	R8	2900	2899	2246	2244	2738	2752	2228	1597	2870	2979	2902	2985	3018	/	0
	R12	2900	2899	2246	2244	2738	2752	2228	1597	2870	2979	2902	3008	3041	/	/
F8	R7	5137	1501	4853	1118	4880	5042	5073	5440	5148	5130	5100	4034	3917	/	5147
	R10	1136	1501	768	1118	949	1010	1054	1544	1151	1130	1088	59	/	/	1395
F9	R10	1735	1731	1321	1315	1503	1592	1663	2064	1747	1609	1655	0	/	1937	1924
	R15	1735	1731	1321	1315	1503	1592	1636	2064	1747	1609	1655	/	/	2003	1989
F10	R9	3460	1795	3244	1394	3363	3408	3283	3379	3460	3577	3465	3461	/	2702	2743
	R8	941	1795	537	1394	850	841	618	788	942	1155	952	1185	/	/	88
F11	R12	3572	3479	2793	2647	3387	3401	2710	1725	3524	3576	3573	3557	3597	3676	/
	R1	2276	2160	1314	1134	2046	2061	2710	/	2219	2279	2278	2629	2685	2603	/
F12	R11	3071	975	2884	649	2918	3003	3070	3441	3089	3195	3057	2714	2659	0	/
	R7	3071	975	2884	649	2918	3003	3070	3441	3089	3195	3057	2764	2709	/	/
F13	R14	2925	2573	2222	1611	2369	2921	2786	2752	3890	2475	/	2498	2547	2744	2751
	R5	874	918	395	364	1363	870	752	343	2187	/	/	1320	1184	1147	1049
	R16	879	299	964	227	1008	880	819	1232	767	1088	/	/	0	1011	967
F14	R13	1983	1859	1471	1295	1976	1106	1896	1783	1670	3074	/	1795	1777	1719	1702
	R3	511	362	336	498	505	1106	407	279	/	1878	/	773	744	767	754
F15	R16	1704	757	1571	500	1685	1678	1573	2020	1715	1983	1747	/	0	1658	1674
	R9	1704	757	1571	500	1685	1678	1573	2020	1715	1983	1747	/	/	1734	1750
F16	R15	2979	2802	2428	2133	2612	2768	2869	3038	2982	2432	2824	/	3027	2963	2941
	R5	1427	1193	701	316	1784	1444	1281	1506	1426	/	1892	/	1821	1964	1927
	R13ù	699	680	639	606	844	370	687	705	691	1379	/	/	726	621	617

Table 0-8: Optimized settings and operating times of DOCRs under scenario 1 (C1).

Relays	HGS				MHGS			
	TDS	PS	A	B	TDS	PS	A	B
1	1.1	0.100	0.140	0.0229	1.100	1.996	3.8733	1.1325
2	0.529	1.4316	8.2282	1.1788	1.1000	1.486	3.2527	1.1779
3	0.0732	0.3042	24.854	0.5927	1.0999	1.311	11.623	1.6712
4	1.0767	1.41604	1.5475	0.5134	1.0929	2	3.4910	1.2266
5	0.9844	2	3.5458	0.9900	1.0996	2	6.0342	1.1469
6	0.0511	0.1001	0.1400	0.0992	0.5728	0.100	0.2455	2
7	1.0999	1.9740	2.0132	0.8069	1.0971	1.5648	4.6883	1.0309
8	1.0785	0.1000	4.0336	0.5398	1.0887	1.9934	12.159	1.9994
9	1.1000	2	0.1658	0.3304	1.0973	1.1745	4.5078	1.3023
10	0.8005	1.8529	7.0074	1.9348	1.1000	0.9380	3.0298	1.0773
11	0.724	1.5469	8.9783	1.2067	1.1000	1.3751	6.8277	1.2428
12	1.0921	1.999	0.1400	0.1021	1.1000	1.3834	10.409	1.1314
13	1.0978	1.8164	7.6800	1.1307	1.0999	1.8064	5.3205	1.0376
14	1.0995	0.8061	17.271	0.8055	1.1000	1.2789	3.6524	0.6800
15	1.100	0.49696	8.0730	0.9095	1.0999	1.7728	8.5405	1.4152
16	0.050	0.100	0.1400	1.9833	0.0501	0.1000	0.1404	1.5294
OF (s)	24.7896				21.0137			
Top,pr(s)	3.5440				1.8802			

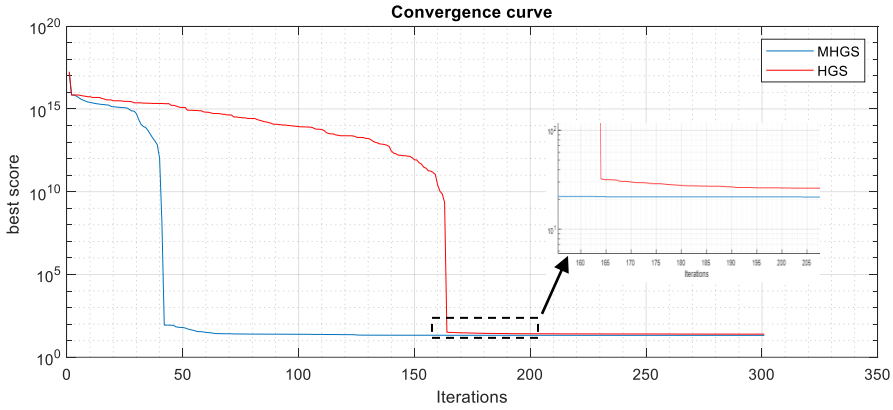

Figure 0-8**.** Convergence curve of the HGS vs MHGS optimization algorithms under the main configuration (C1).

Table 0-9: Optimized settings and operating times of DOCRs under scenario 2 (C2).

Relays	HGS				MHGS			
	TDS	PS	A	B	TDS	PS	A	B
1	1.0098	1.9964	1.1575	0.4435	0.8953	2	8.6508	1.37825
2	1.0983	1.4416	2.4449	0.9288	1.0972	1.8449	0.5251	0.72057
3	0.7923	0.1000	0.9096	0.1655	1.1000	1.6976	1.8559	0.70756
4	1.10000	1.9756	0.1400	0.1094	0.8307	0.8786	3.3177	0.77869
5	1.0773	1.3039	1.7569	0.5200	1.0999	0.8458	9.7753	1.13082
6	0.0500	0.1000	0.1400	0.1624	1.0487	0.1682	0.4338	2
7	1.1000	2	1.1927	0.8359	1.1000	1.0229	1.9475	1.16150
8	0.5520	1.6860	1.8973	0.8967	0.9037	1.9937	16.815	2
9	0.0500	1.3350	0.1400	0.0200	0.8279	0.7836	6.0788	1.45346
10	0.7580	1.0541	5.0164	0.9905	1.0988	1.5291	1.4813	1.05407
11	0.4049	2	1.1198	0.4850	1.1000	1.5416	2.1091	2
12	0.9978	0.1000	0.7545	0.1570	1.1000	0.7610	11.043	0.93809
13	0.3106	0.5576	0.7519	0.1462	0.7282	0.6366	2.5498	0.54624
14	0.8323	1.8092	0.9416	0.2077	0.8744	1.0262	3.3243	0.55739
15	0.4619	2	4.1810	0.5993	1.0771	1.3938	5.0193	1.09570
16	0.0500	0.1001	0.1405	0.7310	0.0767	0.1000	0.1975	2
OF (s)	22.7007				19.21927			
Top,pr(s)	5.08242				2.182842			

Table 0-10: Optimized settings and operating times of DOCRs under scenario 3 (C3).

Relays	HGS				MHGS			
	TDS	PS	A	B	TDS	PS	A	B
1	1.1000	1.5492	1.4905	1.9999	1.0973	1.5418	2.4572	1.0331
2	1.0567	1.9488	1.1403	1.9411	1.0990	1.3279	5.2177	1.3218
3	0.9714	1.9803	1.7323	0.6050	1.0996	1.1195	5.8940	1.1158
4	0.5409	1.9675	1.4905	1.9999	0.7228	1.7601	7.7922	1.4041
5	1.1000	1.1707	1.1403	1.9411	1.0996	1.0881	5.7047	1.3794
6	0.0500	0.1000	1.7323	0.6050	0.2447	0.5747	0.1488	1.9994
7	1.1000	1.2161	1.4905	1.9999	1.1000	1.9991	24.757	1.8294
8	1.0986	1.8070	1.1403	1.9411	1.1000	1.1460	2.3274	1.0473
9	1.1000	1.2908	1.7323	0.6050	1.0898	2	1.9910	1.3030
10	1.1000	1.6672	1.4905	1.9999	1.0978	1.6690	2.3511	1.7705
11	0.8907	1.9133	1.1403	1.9411	1.0999	1.5238	9.3223	1.4494
12	1.0998	1.9801	1.7323	0.6050	1.1000	1.3887	7.5982	1.0950
13	1.0720	0.1000	1.4905	1.9999	1.1000	1.2891	11.720	0.8269
14	0.6177	0.9747	1.1403	1.9411	1.1000	1.8138	5.0779	0.8743
15	1.0999	1.1264	1.7323	0.6050	1.1000	1.7889	7.2563	1.6314
16	0.0500	0.1000	1.4905	1.9999	0.0534	0.1420	0.6244	2.000
OF (s)	32.1151				27.1845			
Top,pr(s)	3.3332				2.0755			

Table 0-11: Optimized settings and operating times of DOCRs under scenario 4 (C4).

Relays	HGS				MHGS			
	TDS	PS	A	B	TDS	PS	A	B
1	1.0999	1.1768	2.4614	0.7714	0.6028	0.8168	6.9419	0.8977
2	1.0456	1.9999	1.0907	0.6763	0.2302	0.2635	6.4189	0.4063
3	1.0606	1.9982	0.1400	0.1542	0.8566	0.5656	76.969	1.6451
4	1.0997	1.7142	5.7151	1.1305	0.8330	0.1029	18.471	0.6721
5	1.0138	1.5996	3.6807	1.2117	0.3474	0.2426	26.326	0.9105
6	0.0500	0.1001	0.1400	0.1721	0.2855	0.2894	4.5787	1.9961
7	0.8088	1.8046	1.0292	0.3888	0.1899	0.4145	38.980	1.1396
8	1.0692	0.8765	1.8392	0.8260	0.2224	0.4216	6.7107	0.5381
9	1.0949	1.8332	1.4300	1.0887	0.2574	0.1415	79.999	1.2536
10	1.0702	0.5779	4.7293	0.9956	0.1267	1.0080	29.776	1.2296
11	1.0993	1.9991	1.0633	0.5489	0.3848	0.1498	15.224	0.8226
12	1.1000	0.1000	0.1400	0.0795	0.4011	0.2412	13.678	0.5593
13	1.1000	1.8312	0.1400	0.1887	0.2048	0.2744	12.535	0.5530
14	0.1704	1.6454	1.2923	0.1321	0.3794	0.6934	13.043	0.5881
15	0.5522	2	2.3984	0.6686	0.3777	0.8281	12.871	0.9061
16	0.0500	0.10088	0.1480	0.5819	0.1537	0.7272	0.1752	1.9979
OF (s)	58.6541				15.74555			
Top,pr(s)	3.4834				3.5461			

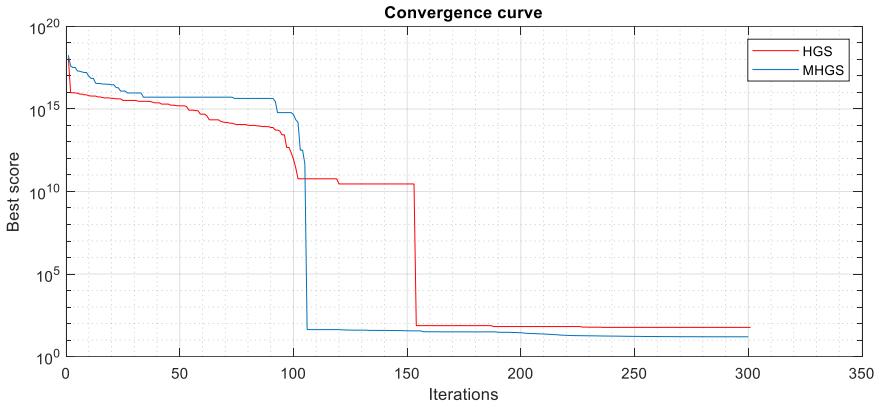

Figure 0-9. Convergence curve of the HGS vs MHGS optimization algorithms under an islanded system scenario (C4).

Table 0-12: Optimized settings and operating times of DOCRs under scenario 5 (C5).

Relays	HGS				MHGS			
	TDS	PS	A	B	TDS	PS	A	B
1	1.1000	0.1000	0.2627	0.0739	1.1000	1.9998	5.5766	1.3646
2	1.0950	1.7881	0.6798	0.5005	1.0999	2	7.5189	1.9803
3	0.3652	0.3318	16.892	0.6576	1.0263	2	43.828	1.8976
4	0.6220	1.9888	47.003	2	1.1000	1.6554	17.445	2
5	0.6305	1.9020	5.1402	0.8394	1.0999	1.9255	23.896	2
6	0.0502	0.1000	0.1400	0.6039	0.0640	0.1026	0.2389	2
7	1.0968	1.9988	39.005	2	1.0942	1.2531	79.999	2
8	1.0941	0.1000	76.867	1.1052	1.1000	1.9899	3.5940	1.4720
9	0.1516	0.1000	0.1400	0.0200	1.0999	2	3.5059	1.5570
10	0.7464	1.9864	0.1400	0.3073	0.7141	1.8782	4.5502	2
11	0.8365	2	10.190	1.5069	1.1000	1.2894	31.554	1.9999
12	0.4716	1.5653	0.1496	0.0436	1.1000	1.7904	12.799	1.3242
13	0.0500	0.1000	47.475	0.4124	1.0999	1.8649	13.590	1.3291
14	0.5381	1.6015	5.1488	0.6805	1.0999	1.8726	11.127	1.1828
15	1.0688	0.1000	0.8852	0.2233	0.9837	1.7190	21.373	2
16	0.0500	0.1000	0.1400	0.1732	0.0541	0.3876	0.1579	2
OF (s)	19.1346				15.6530			
Top,pr(s)	3.2674				1.18261			

Table 0-13: Optimized settings and operating times of DOCRs under scenario 6 (C6).

Relays	HGS				MHGS			
	TDS	PS	A	B	TDS	PS	A	B
1	1.1000	1.8819	0.9445	0.5198	0.5041	0.9936	41.823	1.4453
2	1.0613	1.9866	1.8775	0.9159	0.2749	0.2106	76.628	1.0146
3	0.3389	2	2.1501	0.5509	0.8907	1.2717	14.895	1.2158
4	1.0999	1.2074	0.2433	0.3469	0.2624	0.5989	28.280	1.4000
5	0.9171	0.9840	2.9718	0.6565	0.8263	0.3323	41.405	1.1468
6	0.0500	0.1000	0.1402	1.0133	0.2069	0.3281	24.811	1.7529
7	1.0141	1.9980	2.8325	0.8076	0.2231	0.4197	54.243	0.9139
8	1.0967	0.1000	2.9461	0.5070	0.7306	0.5791	24.396	1.3530
9	1.0999	1.9805	0.6105	0.7523	0.2776	1.4271	29.922	1.6065
10	1.0999	1.5677	1.6317	1.0396	0.1926	0.4551	12.469	0.7118
11	1.0992	1.9979	1.5504	0.7025	0.2293	1.0923	63.019	1.3789
12	1.0973	1.9937	2.0786	0.6071	0.5593	1.1362	51.002	1.3432
13	1.0988	0.1000	0.1400	0.1020	0.5786	0.7582	27.161	1.2244
14	0.9202	0.1000	1.9981	0.2630	0.7465	0.9775	20.889	0.9817
15	0.9972	1.6744	1.2620	0.4463	0.4640	0.5545	27.313	1.0062
16	0.1477	0.1000	0.1400	1.5273	0.4846	0.6359	30.621	1.9958
OF (s)	13.9261					11.4687		
Top,pr (s)	3.4652					1.9311		

Table 0-14: Optimized settings and operating times of DOCRs under scenario 7 (C7).

Relays	HGS				MHGS			
	TDS	PS	A	B	TDS	PS	A	B
1	1.1000	1.2112	0.1400	0.0982	0.6729	1.8978	24.0619	1.6643
2	0.7578	0.9487	4.8848	1.0651	0.5381	0.3914	70.3595	1.5772
3	0.5220	0.6645	73.920	1.2257	0.3550	1.5073	25.9067	1.1643
4	0.4574	2.0000	3.1647	0.6399	0.9335	0.9660	71.2231	1.9999
5	0.7784	1.8951	0.9856	0.4812	1.0703	0.1034	31.1883	0.9262
6	0.0500	0.1000	0.1400	0.0292	0.1530	0.7732	71.5749	1.9891
7	0.6175	1.4338	0.9632	0.3402	0.2553	0.5868	40.4475	0.9242
8	1.0910	1.9896	2.3955	1.2837	0.2306	1.8074	42.6986	1.9899
9	0.6252	0.2136	0.1400	0.1900	0.5235	0.6661	40.3844	1.4557
10	1.1000	0.3813	15.958	1.2442	1.0997	0.6038	51.3859	1.9999
11	1.0736	1.3980	33.129	1.6735	0.3037	1.8153	46.7777	1.5313
12	1.0965	1.9891	1.6910	0.2500	0.1661	1.8753	75.2916	1.4139
13	0.6620	0.1000	6.4067	0.4765	0.9762	0.7322	13.7202	1.0028
14	1.0209	1.8195	8.4315	0.8459	0.9106	0.7553	11.7248	0.8590
15	0.0500	1.9667	22.883	0.6077	0.2808	1.4903	70.5392	1.7217
16	0.0528	0.1000	0.1400	1.5751	0.2967	1.8808	19.8785	1.9999
OF (s)	26.5258				17.2151			
Top,pr (s)	4.46776				1.7928			

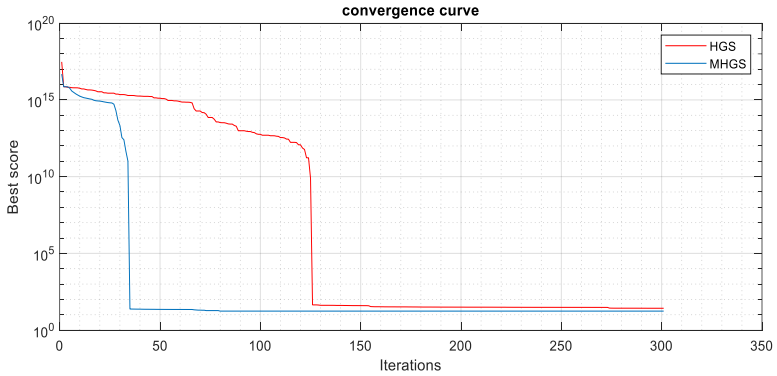

Figure 0-10**.** Convergence curve of the HGS vs MHGS optimization algorithms under a DG outage scenario (C 7).

Table 0-15: Optimized settings and operating times of DOCRs under scenario 8 (C8).

Relays	HGS				MHGS			
	TDS	PS	A	B	TDS	PS	A	B
1	1.1000	2	0.1717	0.0823	0.7497	1.5609	20.3470	0.9881
2	1.0527	1.9999	2.3879	0.7653	0.4027	0.2361	44.1764	0.9047
3	0.8203	0.3340	0.3974	0.4297	0.0697	0.8535	46.9420	0.5352
4	1.0965	0.3976	2.1928	0.3554	0.7212	1.4566	51.9273	1.5836
5	1.0027	0.2495	2.3148	0.3168	0.1126	0.6210	15.0329	0.4727
6	0.0507	0.1721	0.1423	0.0244	0.0512	1.4047	2.17075	0.6223
7	0.9489	1.9116	5.3849	0.8943	0.1154	1.0141	79.8020	1.0548
8	0.6570	0.1000	0.1439	0.0397	0.2900	0.7333	23.4390	0.9291
9	1.0430	0.1128	49.464	1.1274	1.0100	0.7197	20.7732	1.5112
10	0.8221	1.8883	1.9770	0.8427	0.6003	0.9672	21.9712	1.6563
11	1.0633	1.9897	0.9404	0.3632	0.9138	1.1326	7.68990	0.9991
12	0.5701	1.5022	14.922	1.0597	0.1468	1.7455	16.9138	0.5379
13	0.1971	0.1000	0.1400	0.0206	0.4546	0.5461	27.2857	0.8482
14	0.8798	1.6069	5.8023	0.5518	0.2929	0.4361	8.67718	0.4166
15	0.9047	1.7217	3.7464	0.8787	0.9666	0.5099	17.1313	1.1882
16	0.1045	0.1000	0.1400	2	0.0876	0.4589	50.3209	1.9987
OF (s)	109.4733				23.5476			
Top,pr (s)	4.6477				3.7193			

Table 0-16: Optimized settings and operating times of DOCRs under scenario 9 (C9).

Relays	HGS				MHGS			
	TDS	PS	A	B	TDS	PS	A	B
1	1.1000	0.1000	0.1400	0.0421	0.6094	1.6485	22.6099	1.5991
2	0.7393	0.5375	1.0289	0.3496	1.0663	1.0878	33.1190	1.9998
3	0.9735	0.6658	1.5732	0.5463	0.7742	0.9573	71.2193	1.9933
4	1.1000	0.5046	1.8421	0.5303	0.3614	0.4760	4.31274	0.7209
5	0.1915	1.9397	14.579	0.7848	1.0886	1.0979	74.0162	1.9912
6	0.0500	0.1000	0.1400	0.1241	0.6427	1.9958	8.85962	1.9999
7	1.0999	1.9362	3.2442	1.0726	0.9119	1.8968	55.4933	1.9999
8	1.0978	2	1.3487	0.9043	0.6748	1.8895	19.8957	1.9999
9	1.0999	0.1566	4.9494	0.7407	0.1933	1.7450	79.9953	1.9994
10	1.1000	0.4808	1.8740	0.5773	0.8375	0.5734	66.1021	1.9999
11	0.9104	1.8109	10.587	1.3629	1.0527	1.3901	39.5589	1.9999
12	0.0500	0.1054	1.1479	0.0200	0.7490	1.7250	65.2275	1.7405
13	0.1769	0.1000	1.5506	0.1397	1.0983	1.9627	65.3779	1.8627
14	0.3942	0.1000	0.1400	0.0200	1.0958	0.7984	11.4522	0.9893
15	0.2871	1.9837	53.760	1.6690	0.6138	1.7115	60.3636	1.9999
16	0.0524	0.1000	0.1400	1.8895	0.7067	0.6907	38.6609	1.9997
OF (s)	16.32573					13.84962		
Top,pr (s)	3.66815					1.37849		

Table 0-17: Optimized settings and operating times of DOCRs under scenario 10 (C10).

Relays	HGS				MHGS			
	TDS	PS	A	B	TDS	PS	A	B
1	1.0999	2	0.1704	0.1770	0.8924	1.7374	19.5486	1.7418
2	1.0435	1.3885	21.349	1.7622	0.7262	1.5385	30.1553	1.9999
3	0.5269	0.5204	10.293	0.7006	1.0958	1.3384	77.9691	1.7973
4	0.1798	1.9476	0.1470	0.0202	1.0997	1.1998	79.9732	1.8598
5	0.9538	1.7188	0.7326	0.2071	0.0799	1.1904	57.8642	0.6868
6	0.0500	0.1000	0.1590	1.1958	0.8626	0.7889	0.52581	1.9240
7	1.0997	1.4662	8.9801	1.0546	1.0085	0.6818	79.5599	1.5569
8	1.0938	2	3.4768	1.3587	0.8236	0.6506	71.1062	1.7528
9	1.0938	1.2223	3.4592	1.2024	0.8723	0.5390	76.4374	1.7404
10	0.6394	1.0958	1.1866	0.4648	0.4829	0.6480	78.8585	1.9794
11	1.0452	1.2921	1.7530	0.5552	0.5752	1.8489	79.7731	1.9999
12	1.1000	1.9999	8.5297	1.1808	1.0535	1.4549	68.8970	1.7462
13	0.5121	1.9957	1.4470	0.5206	0.6628	1.3201	69.2825	1.6021
14	1.0943	0.1000	6.0391	0.3846	1.0636	1.5674	3.62856	0.7131
15	0.9092	0.7394	13.855	1.0544	0.4073	1.4519	75.8994	1.9995
16	0.0515	0.1000	0.1437	1.8655	0.97507	1.7653	0.14207	1.0542
OF (s)	17.00213					15.2498		
Top,pr (s)	4.7013					1.5247		

Table 0-18: Optimized settings and operating times of DOCRs under scenario 11 (C11).

Relays	HGS				MHGS			
	TDS	PS	A	B	TDS	PS	A	B
1	1.0900	0.1000	0.1417	0.0595	0.2760	1.1048	56.0887	1.3574
2	1.1000	0.1000	26.725	0.9199	0.7331	0.1127	79.8292	1.0933
3	0.6095	1.3754	4.4048	0.7823	0.6835	1.8090	48.3522	1.9999
4	0.7426	0.1000	12.622	0.5647	0.6684	0.7550	43.4027	1.4753
5	1.0995	0.5405	68.178	1.4197	0.5069	0.4258	26.4729	0.9736
6	0.0500	0.1015	0.1400	0.0581	0.0801	1.2748	0.60660	1.0223
7	0.8567	1.2880	5.8545	0.8086	0.7221	0.6954	49.9649	1.2883
8	1.0806	1.7708	1.7427	0.9879	0.0686	1.2749	23.4956	0.8405
9	0.6600	0.6410	11.483	1.1785	0.5462	1.9591	15.6885	1.8810
10	1.0556	1.9468	2.8299	1.4426	0.3127	0.6429	77.9009	1.7028
11	1.0166	1.1539	0.6563	0.3308	0.1615	0.5830	68.1335	0.9982
12	1.0999	1.9999	5.4369	1.0148	0.8608	1.0786	79.9149	1.5578
13	0.0500	1.6227	0.4341	0.0211	1.0613	0.1463	11.6274	0.6399
14	0.1420	1.7817	6.2067	0.2937	0.3225	1.2732	50.9815	1.1706
15	0.9744	0.3738	22.762	0.9366	0.6697	1.3998	17.3855	1.4389
16	0.0511	0.1002	0.1400	0.4579	0.1766	0.5721	2.46219	1.0789
OF (s)	27.6113				13.2387			
Top,pr(s)	3.0417				1.78			

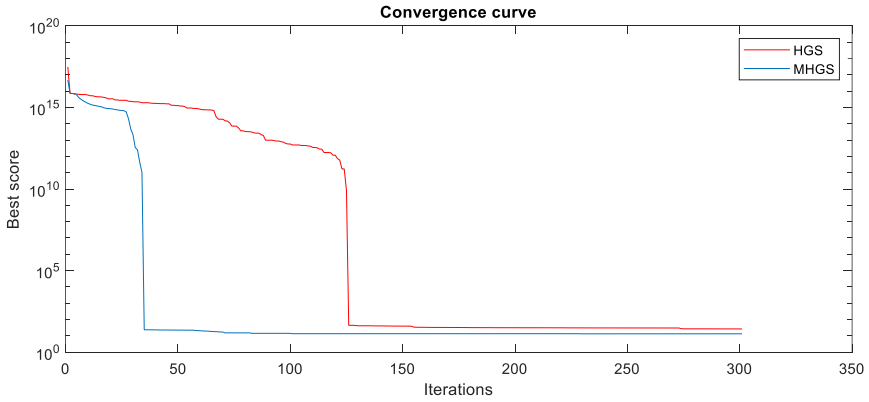

Figure 0-11**.** Convergence curve of the HGS vs MHGS optimization algorithms under a line outage scenario (C 11).

Table 0-19: Optimized settings and operating times of DOCRs under scenario 12 (C12).

Relays	HGS				MHGS			
	TDS	PS	A	B	TDS	PS	A	B
1	0.0500	0.2539	1.0794	0.0200	0.3894	1.0460	46.8701	1.3832
2	0.9291	1.9998	0.1400	0.0781	0.6088	0.8330	36.4808	1.5515
3	0.8300	0.1021	0.1400	0.0461	0.4951	0.8520	26.7608	1.0785
4	0.3233	0.1821	0.2008	0.0200	0.6887	0.9899	41.0566	1.6844
5	0.1755	1.9965	1.4489	0.1154	0.6344	0.6175	70.6576	1.4442
6	0.0500	0.1000	0.1400	0.1379	0.1158	0.1957	69.9655	1.6512
7	0.0500	0.1428	2.0366	0.0200	1.0455	1.2363	4.85768	0.9799
8	0.2292	2	0.1409	0.0200	0.4630	1.0316	28.6925	1.5280
9	1.1000	0.1040	0.2553	0.2119	0.7851	0.4953	16.5040	1.4201
10	0.4821	0.1000	0.2608	0.0214	0.5857	0.1000	31.3662	0.7579
11	0.9748	0.1870	4.4917	0.3767	0.5952	0.9997	57.8715	1.5425
12	1.1000	1.3133	0.1421	0.0891	0.4960	1.3472	75.4470	1.4950
13	0.0937	0.1000	0.3190	0.0216	0.6459	0.7559	53.2957	1.2234
14	0.0500	0.2857	1.7296	0.0200	0.6240	0.5756	31.0500	0.9307
15	0.3102	1.1379	0.1786	0.0200	0.2683	0.4683	56.4560	1.0938
16	0.0500	0.1000	0.2580	0.4656	0.7885	1.2325	47.3412	2
OF (s)	29.63782				24.6661			
Top,pr (s)	7.7534				2.3766			

Table 0-20: Optimized settings and operating times of DOCRs under scenario 13 (C13).

Relays	HGS				MHGS			
	TDS	PS	A	B	TDS	PS	A	B
1	1.1000	1.9999	25.6940	1.9174	1.0999	2	30.0842	2
2	1.0475	1.8208	12.4431	1.9999	1.1000	2	9.66750	1.9834
3	0.2470	1.9824	80	1.5743	1.0687	1.9967	6.91649	1.2258
4	1.0176	1.9920	3.5899	1.1948	0.5800	2	25.4795	2
5	0.7395	1.6561	53.856	1.9880	0.9780	2	28.7600	1.9997
6	0.0504	1.1661	0.1400	1.3220	0.0500	0.1222	0.27319	1.9995
7	1.0921	1.7112	33.553	2	1.0972	2	23.6532	1.9868
8	1.0988	1.9916	3.21513	1.1035	1.0592	1.9999	10.4268	1.5675
9	1.1000	1.8932	4.64163	1.6258	0.9068	1.9993	9.00205	1.9889
10	1.0999	1.9443	0.14000	0.1793	1.1000	1.6834	8.65665	2
11	1.0059	2	21.7653	1.9928	1.1000	1.9843	20.7105	2
12	0.8133	1.7707	80	1.6968	1.1000	2	80	1.8691
13	1.0999	1.9803	11.3024	0.4334	0.8411	2	11.3169	1.2619
14	1.0465	1.9564	56.6230	1.5333	1.0999	1.5623	80	1.6119
15	1.0877	1.9243	49.4122	2	1.1000	2	9.40132	1.4714
16	0.0500	0.1000	0.14000	1.7430	0.0676	0.6223	0.59691	1.9998
OF (s)	20.2509				18.9834			
Top,pr (s)	4.3558				1.4359			

Table 0-21: Optimized settings and operating times of DOCRs under scenario 14 (C14).

Relays	HGS				MHGS			
	TDS	PS	A	B	TDS	PS	A	B
1	0.0500	0.1357	1.0168	0.0200	1.0710	0.5730	41.2753	1.5308
2	0.7203	1.9999	0.4070	0.2294	0.0808	1.6027	74.5167	1.9999
3	0.0500	0.1413	1.5141	0.0200	0.2151	1.5004	68.9208	1.3176
4	0.8326	0.1043	0.1495	0.0339	1.0926	1.2304	69.7868	1.9999
5	0.1970	1.9999	0.1982	0.0200	0.6636	1.5519	15.8043	1.4541
6	0.0662	0.1000	0.1403	0.0200	0.9168	0.3143	58.7598	1.9999
7	1.1000	1.9998	0.2038	0.1033	0.6083	1.1535	61.1955	1.6486
8	0.2469	0.1000	0.1400	0.0200	0.4999	1.0903	62.2040	1.8744
9	0.0500	1.9999	0.5714	0.6305	0.7278	0.8239	54.5602	1.8688
10	0.4564	0.2696	0.1402	0.0200	0.2741	0.9854	26.9642	1.2864
11	0.0534	0.3332	2.0200	0.0338	0.6827	0.1013	17.1277	0.7660
12	1.0999	0.1073	1.8010	0.3321	1.0999	1.2571	26.2146	1.9430
13	0.1942	0.1086	1.1275	0.0882	0.4418	0.9856	25.8653	1.0714
14	1.0830	0.1446	0.1400	0.0200	0.8235	1.0444	15.2889	0.9411
15	0.9812	0.7826	1.0763	0.2369	0.8236	1.9999	36.3826	1.9582
16	0.0500	0.1000	0.1400	1.0721	0.8764	1.0901	22.7361	1.9999
OF (s)	26.7861				16.972			
Top,pr(s)	6.6205				1.42			

Table 0-22: Optimized settings and operating times of DOCRs under scenario 15 (C15).

Relays	HGS	MHGS						
	TDS	PS	A	B	TDS	PS	A	B
1	0.0500	0.1018	1.3562	0.0200	0.8770	1.9693	1.6549	0.6508
2	0.6185	1.9996	0.1400	0.0716	0.4434	1.1529	1.7457	0.4519
3	1.0385	0.1010	0.1400	0.0555	0.8569	1.8112	2.3074	0.7142
4	0.5010	0.1777	0.1400	0.0200	0.5020	1.9821	3.3527	0.7595
5	0.6158	1.7850	0.4765	0.1242	1.0361	1.0597	0.8595	0.3544
6	0.0500	0.1000	0.1400	0.1616	0.0507	0.3010	0.7204	2
7	0.9997	1.9968	0.9992	0.5612	0.5677	0.6737	1.1710	0.3078
8	1.1000	0.4319	0.1400	0.1201	0.5891	0.2974	0.6012	0.2874
9	0.0502	1.9999	2.4779	0.2793	1.0591	0.7129	0.5072	0.4718
10	1.0617	0.1000	0.1400	0.1810	0.7584	0.5884	0.6302	0.2246
11	0.0500	1.8169	0.9222	0.0200	1.0973	0.8238	1.4273	0.3847
12	1.0999	0.2493	0.3407	0.0200	0.3745	1.5162	6.5412	0.7135
13	0.2040	0.1000	0.1400	0.0202	1.0822	1.9119	1.2395	0.6641
14	1.0997	0.1000	0.1551	0.0297	0.7223	1.6001	0.7740	0.2455
15	0.0500	1.1451	0.1400	0.0766	1.1000	1.9957	0.7107	0.4086
16	0.0500	0.1000	0.1400	1.5526	0.0613	0.1998	0.1422	1.9997
OF (s)	44.80888				14.5476			
Top,pr(s)	9.0519				3.2248			

Table 0-23: results comparison of optimal operating times of primary relays for all possible configurations (N-1 contingency).

Configuration No.	Top,pr (s)					
	Method of [22]	Method of [27]	Method of [33]	Method of [23]	The proposed method using HGS algorithm	The Proposed method using MHGS algorithm
C1 (Grid-connected mode)	6.104	5.432	4.425	4.093	3.544	1.880
C2 (Islanded mode)	12.155	10.572	10.125	5.028	5.082	2.182
C3 (Outage of DG1)	7.742	6.465	5.964	4.509	3.333	2.075
C4 (Outage of DG2)	7.518	6.369	5.719	3.840	3.483	3.546
C5 (Outage of DG3)	7.968	6.826	6.587	4.642	3.267	1.182
C6 (Outage of L1-4)	5.378	4.645	4.185	2.956	3.465	1.931
C7 (Outage of L1-5)	5.375	4.453	4.331	2.714	4.467	1.792
C8 (Outage of L1-6)	6.197	5.394	4.622	2.881	4.647	3.719
C9 (Outage of L2-3)	3.723	3.015	2.197	2.887	3.668	1.378
C10 (Outage of L2-7)	4.392	3.273	2.834	1.882	4.701	1.524
C11 (Outage of L3-4)	3.948	3.024	2.594	2.491	3.041	1.78
C12 (Outage of L5-6)	5.572	4.743	4.495	4.066	7.753	2.376
C13 (Outage of L6-7)	4.428	3.342	2.788	1.625	4.355	1.435
C14 (Outage of EX1)	6.890	5.843	5.081	2.767	6.620	1.42
C15 (Outage of EX2)	9.934	9.114	8.083	4.825	9.051	3.224
Total operating times of relays in all configurations (s)	**97.324**	**82.508**	**74.03**	**51.206**	**70.477**	**30.831**

B. Discussion

Table 4.8 shows the optimal time dial settings, pickup current and curve settings for DOCRs in Scenario 1. As previously stated, Scenario 1 considers only the main setup (grid-connected scenario, no line outages and all DGs are connected). As can be observed, according to the objective function, the total operating time of main relays, backup relays and CTI for all fault sites has been reduced. Under Scenario 1, the total running time of the main relays is 1.8802s, which is 47% faster than the original HGS approach, and the operation was completed with less iterations, as evidenced by the convergence curve in Fig.4.8.

Table 4.9 and table 4.10 show the optimal current, time and curve parameters of DOCRs in Scenarios 2 and 3 respectively, where EG1 and EG2 are disconnected. The advantages of optimizing four user-defined settings for DOCRs are demonstrated by comparing the obtained test results under the original HGS and the modified one. Using the MHGS technique, in the second case, the overall operating time of DOCRs utilizing the prior objective function was decreased from 22.7007 sec to 19.21927 sec, and in the third situation, it was lowered from 32.1151s to 27.1845s. In addition, the total working time of the primary relays in the event of near end failures only has been reduced by 58% and 48%, respectively. This validates the advantages of the revised method.

Table 4.11 shows the ideal DOCR setting for Scenario 4. As previously described, the system is totally islanded, one group of settings are configured to all DOCRs to insure the distribution system protection in islanded mode of operation. Comparing the sum of operating times using MHGS with the HGS technique, the best score obtained using the objective function by the original algorithm was 58.6541. Furthermore, the developed method reduced both the primary operating time, backup operating time, and coordination time interval to get 15.74555 s as the best score obtained with the fewest iterations, as shown in the convergence curve in Fig.4.9.

Tables 4.12-4.14 provide the best DOCR parameters, such as current settings, time settings, and user-defined curve parameters. Depending on the condition of DGs and upstream networks, different groups of settings are applied to DOCRs in the suggested protection strategy for various network topologies that include a DG outage. The benefits of the proposed technique are illustrated. For example, in Scenario 7, the minimum score of the objective function was reduced from 26.5258sec to 17.2151sec utilizing the MHGS methodology. Furthermore, the overall working time of the primary relays in the case of near end failures was calculated and found to

be reduced by more than 60%, from 4.4677s with HGS to 1.7928s using MHGS. The convergence curve in Fig.4.10 clearly shows how the MHGS converges quickly while ensuring the search for the best feasible objective function outcome.

Tables 4.15-4.22 show the optimum DOCR parameters, current settings, time settings and user defined curve settings in Scenarios 8-15 where each one of them represent a different topology with a single line outage. In the suggested protective method, DOCRs are subjected to a variety of situations. Using scenario 11 as an example, table 4.18 shows the four user-defined parameters, the best objective function value produced thus far, which is decreased by 52% using the MHGS method when compared to the original. Besides, in the case of a near end short circuit, the sum of all the primary relay working periods with the HGS technique was 3.0417s, but with the MHGS, the total operating time was 1.78s, representing a 41% decrease compared to the original one. Fig.4.11 depicts how the MHGS converges rapidly and produces superior outcomes.

In order to compare the operation timeframes of DOCRs obtained using an adaptive protection scheme with a modified optimization algorithm (MHGS), the original algorithm and with different techniques presented in [22, 23, 27, 33], all studies are summarized in Table 4.23. It should be emphasized that only the operating times of the main relays with faults occurred at near-end locations were evaluated. The results of the tests show that the suggested technique improves the operation times for the relays in all network topologies owing to the N-1 contingency over the other strategies. In the case of all topologies and operation modes owing to N-1 contingency, the overall operating times of the primary relays has clearly been reduced compared to the proposed technique using HGS algorithm and the protection methods of [22, 23, 27, 33] . After comparing test results under the N-1 contingency, different group of settings are applied to DOCRs in the proposed adaptive protection strategy, depending on different types of outages that may occur in the system. The advantages of the adaptive protection strategy were emphasized. It should be noticed that using the MHGS approach, the progress of the protection scheme is faster than the original one. Indeed, better solutions may be discovered in the adaptive scheme since adding more parameters may expand the possible region of the optimization challenge.

4.4Conclusion

The purpose of this research work was to address the problem of coordinating dual-settings relays for near-end and far-end line failures in power distribution systems comprising DGs. The goal was to improve the coordination of Directional Overcurrent Relays (DOCRs) using an adaptive protective coordination scheme. To this, a new version of the Hunger Game Search Algorithm (HGS) is proposed. The latter consists is an update of the original algorithm named MHGS where two significant modifications are carried out; 1) the computation of the hungry weights and 2) new approach to update the search agent's position. The suggested technique used a user-defined dual-setting numerical DOCRs model, which was applied to the all N-1 contingency-based topologies of the IEEE 14 bus system's distribution part. The findings demonstrated that the proposed Algorithm effectively accomplished coordination without breaking any constraints. The protection system's speed was determined to be appropriate for various sorts of network operation. The MHGS algorithm's development enabled fast searching within viable regions, the discovery of global optima, and a decreased number of iterations. Furthermore, as compared to the original HGS algorithm and all current well-known optimization approaches described in the literature, the suggested method greatly reduced the overall working time of the relay and proved the MHGS algorithm's higher performance. Further research and implementation of this method can contribute to improving relay coordination in practical MGs as well as complicated power systems with heavily penetrated DGs.

CHAPTER 5 General conclusion and future work

The objective of this study was to solve the issue of relay coordination in electrical networks. The fundamental concept of protective systems presented in Chapter 2 served as a critical framework for our investigation. The second chapter acted as a guidepost, providing a broad review of protective systems as well as an informative understanding of the optimal coordination design process. Building upon this knowledge, chapter 3 of this work delved into the critical aspect of coordinating Directional Overcurrent Relays (DOCRs). By treating DOCRs' coordination as an optimization problem, the research aimed to minimize the response of the protective system, considering factors such as Plug setting (PS), Time dial setting (TDS) and using an updated version of the marine predators optimization technique titled EMPA. The proposed algorithm was tested on deferent power systems (3-bus, 8-bus, 9-bus, and 15- bus test systems). The results are compared with most recently published optimization algorithms (SA, DE, MILP, HS, IHSA-NLP, MEFO, HWOA, MWCA and MRFO) and the findings demonstrate that the suggested EMPA technique is an effective and dependable tool for coordinating directional overcurrent relays. Moving forward to Chapter 4, the research extended its focus to the coordination of dual-settings relays for near-end and far-end line failures in power distribution systems incorporating Distributed Generators (DGs). This critical aspect was addressed through an adaptive protective coordination scheme, introducing an updated version of the Hunger Game Search Algorithm (HGS). The suggested technique used a user-defined dual-setting numerical DOCRs model, which was applied to the all N-1 contingency-based topologies of the IEEE 14 bus system's distribution part. This modified algorithm, termed MHGS, demonstrated superior performance in terms of fast searching within viable regions, discovering global optima, and reducing the overall relay working time compared to existing optimization approaches. Furthermore, as compared to the original HGS algorithm and all current well-known optimization approaches described in the literature, the suggested method greatly reduced the overall working time of the relay and proved the MHGS algorithm's higher performance. By tackling the coordination issues in modern power systems, our research has made major contributions to the discipline. The desire to reconcile rising power consumption with environmental concerns prompted a thorough investigation of microgrid protection techniques.

An adaptive method has been successfully developed by integrating a modified metaheuristic algorithms. the comparison with the state of the art techniques highlight the importance in the field of electrical networks protection.

Looking ahead, this study sets the framework for future efforts that will enhance the field of relays coordination in power systems. As we continue ahead, the following pathways provide intriguing exploration opportunities:

- Incorporating advanced technologies, like as artificial intelligence and machine learning, into protective coordinating systems might improve flexibility and response to dynamic grid situations.
- Extending the proposed approaches to bigger power networks would be useful in evaluating the scalability and efficacy of the coordinating mechanisms in more complex and linked systems.
- Real-Time Adaptive Coordination schemes with Large Networks Simulation: Exploring real-time adaptive coordination schemes, specifically by utilizing real-time simulators to simulate large networks, presents an avenue for comprehensive testing and validation of the proposed strategies. This approach allows for the emulation of complex network dynamics and the assessment of adaptive coordination performance in realistic, dynamic scenarios.
- Implementation and Field Testing: Putting theoretical advances into practice by performing field tests and applying the proposed coordination mechanisms in real-world microgrid settings would give useful insights and evaluate the approaches' effectiveness.

In essence, future research in this domain can investigate the intersection of modern technology against emerging threats and practical scalability, ensuring that relay coordination systems remain at the leading edge of ensuring the stability and reliability of electrical networks in the coming years.

References

1. Belmadani, H., et al., *A twofold hunting trip African vultures algorithm for the optimal extraction of photovoltaic generator model parameters.* Energy Sources, Part A: Recovery, Utilization, and Environmental Effects, 2022. **44**(3): p. 7001-7030.
2. Mahari, A. and H. Seyedi, *An analytic approach for optimal coordination of overcurrent relays.* IET Generation, Transmission & Distribution, 2013. **7**(7): p. 674-680.
3. Zeineldin, H., E. El-Saadany, and M. Salama, *Optimal coordination of overcurrent relays using a modified particle swarm optimization.* Electric Power Systems Research, 2006. **76**(11): p. 988-995.
4. Alkaran, D.S., et al., *Optimal overcurrent relay coordination in interconnected networks by using fuzzy-based GA method.* IEEE Transactions on Smart Grid 2016. **9**(4): p. 3091-3101.
5. Korashy, A., et al., *Hybrid whale optimization algorithm and grey wolf optimizer algorithm for optimal coordination of direction overcurrent relays.* Electric Power Components and Systems 2019. **47**(6-7): p. 644-658.
6. Swathika, O. and S. Hemamalini, *Graph theory and optimization algorithms aided adaptive protection in reconfigurable microgrid.* Journal of Electrical Engineering & Technology 2020. **15**(1): p. 421-431.
7. Bedekar, P.P. and S.R. Bhide, *Optimum coordination of directional overcurrent relays using the hybrid GA-NLP approach.* IEEE Transactions on Power Delivery, 2010. **26**(1): p. 109-119.
8. Sarwagya, K., P.K. Nayak, and S.J.E.P.S.R. Ranjan, *Optimal coordination of directional overcurrent relays in complex distribution networks using sine cosine algorithm.* Electric Power Systems Research, 2020. **187**: p. 106435.
9. Elsadd, M.A., et al., *Adaptive optimum coordination of overcurrent relays for deregulated distribution system considering parallel feeders.* Electrical Engineering, 2021. **103**(3): p. 1849-1867.
10. Kudkelwar, S. and D. Sarkar, *Online implementation of time augmentation of over current relay coordination using water cycle algorithm.* SN Applied Sciences, 2019. **1**(12): p. 1-15.
11. Rajput, V.N. and K.S. Pandya, *Coordination of directional overcurrent relays in the interconnected power systems using effective tuning of harmony search algorithm.* Sustainable Computing: Informatics Systems, 2017. **15**: p. 1-15.
12. Khurshaid, T., et al., *Modified particle swarm optimizer as optimization of time dial settings for coordination of directional overcurrent relay.* Journal of Electrical Engineering & Technology, 2019. **14**(1): p. 55-68.
13. Shih, M.Y., C.A. Castillo Salazar, and A. Conde Enríquez, *Adaptive directional overcurrent relay coordination using ant colony optimisation.* IET Generation, Transmission & Distribution, 2015. **9**(14): p. 2040-2049.
14. Shih, M.Y., A. Conde, and C. Ángeles-Camacho, *Enhanced self-adaptive differential evolution multi-Objective algorithm for coordination of directional overcurrent relays contemplating maximum and minimum fault points.* IET Generation, Transmission & Distribution, 2019. **13**(21): p. 4842-4852.
15. Gokhale, S. and V. Kale, *An application of a tent map initiated Chaotic Firefly algorithm for optimal overcurrent relay coordination.* International Journal of Electrical Power & Energy Systems, 2016. **78**: p. 336-342.

16. Khurshaid, T., et al., *Improved firefly algorithm for the optimal coordination of directional overcurrent relays.* IEEE Access, 2019. **7**: p. 78503-78514.
17. Khurshaid, T., et al., *An improved optimal solution for the directional overcurrent relays coordination using hybridized whale optimization algorithm in complex power systems.* IEEE Access, 2019. **7**: p. 90418-90435.
18. Khurshaid, T., et al., *Improved firefly algorithm for the optimal coordination of directional overcurrent relays.* IEEE Access, 2019. **7**: p. 78503-78514.
19. Korashy, A., et al., *Optimal coordination of standard and non-standard direction overcurrent relays using an improved moth-flame optimization.* IEEE Access, 2020. **8**: p. 87378-87392.
20. Korashy, A., et al., *Optimal coordination of distance relays and non-standard characteristics for directional overcurrent relays using a modified African vultures optimization algorithm.* IET Generation, Transmission & Distribution, 2023.
21. Tripathi, J.M. and S.K.J.E.P.S.R. Mallik, *An adaptive protection coordination strategy utilizing user-defined characteristics of DOCRs in a microgrid.* Electric Power Systems Research, 2023. **214**: p. 108900.
22. Entekhabi-Nooshabadi, A.M., H. Hashemi-Dezaki, and S.A.J.A.S.C. Taher, *Optimal microgrid's protection coordination considering N-1 contingency and optimum relay characteristics.* Applied Soft Computing, 2021. **98**: p. 106741.
23. Ataee-Kachoee, A., H. Hashemi-Dezaki, and A.J.E.P.S.R. Ketabi, *Optimized adaptive protection coordination of microgrids by dual-setting directional overcurrent relays considering different topologies based on limited independent relays' setting groups.* Electric Power Systems Research, 2023. **214**: p. 108879.
24. Sorrentino, E. and J.V.J.E.P.S.R. Rodríguez, *A novel and simpler way to include transient configurations in optimal coordination of directional overcurrent protections.* Electric Power Systems Research, 2020. **180**: p. 106127.
25. Samadi, A., R.M.J.I.J.o.E.P. Chabanloo, and E. Systems, *Adaptive coordination of overcurrent relays in active distribution networks based on independent change of relays' setting groups.* International Journal of Electrical Power & Energy Systems, 2020. **120**: p. 106026.
26. Asl, S.A.F., M. Gandomkar, and J.J.E.P.S.R. Nikoukar, *Optimal protection coordination in the micro-grid including inverter-based distributed generations and energy storage system with considering grid-connected and islanded modes.* Electric Power Systems Research, 2020. **184**: p. 106317.
27. Beder, H., et al., *A new communication-free dual setting protection coordination of microgrid.* IEEE Transactions on Power Delivery, 2020. **36**(4): p. 2446-2458.
28. Gashteroodkhani, O., et al., *A protection scheme for microgrids using time-time matrix z-score vector.* International Journal of Electrical Power & Energy Systems, 2019. **110**: p. 400-410.
29. Torshizi, N.H., et al., *An adaptive characteristic for overcurrent relays considering uncertainty in presence of distributed generation.* International Journal of Electrical Power & Energy Systems, 2021. **128**: p. 106688.
30. Chaitanya, B., et al., *An improved differential protection scheme for micro-grid using time-frequency transform.* International Journal of Electrical Power & Energy Systems, 2019. **111**: p. 132-143.
31. Khanbabapour, S. and M.H.J.I.T.o.P.D. Golshan, *Synchronous DG planning for simultaneous improvement of technical, overcurrent, and timely anti-islanding protection indices of the network to preserve protection coordination.* IEEE Transactions on Power Delivery, 2016. **32**(1): p. 474-483.
32. Fani, B., et al., *Protection coordination scheme for distribution networks with high penetration of photovoltaic generators.* IET Generation, Transmission & Distribution, 2018. **12**(8): p. 1802-1814.

33. Sadeghi, S., H. Hashemi-Dezaki, and A.M.J.E.P.S.R. Entekhabi-Nooshabadi, *Optimized protection coordination of smart grids considering N-1 contingency based on reliability-oriented probability of various topologies.* Electric Power Systems Research, 2022. **213**: p. 108737.
34. Bedekar, P.P., S.R. Bhide, and V.S. Kale. *Optimum coordination of overcurrent relays in distribution system using dual simplex method*. in *2009 Second International Conference on Emerging Trends in Engineering & Technology*. 2009. IEEE.
35. Chattopadhyay, B., M. Sachdev, and T. Sidhu, *An on-line relay coordination algorithm for adaptive protection using linear programming technique.* IEEE Transactions on Power Delivery, 1996. **11**(1): p. 165-173.
36. Asadi, M., et al. *Optimal overcurrent relays coordination using genetic algorithm*. in *2008 11th International Conference on Optimization of Electrical and Electronic Equipment*. 2008. IEEE.
37. Rajput, V.N. and K.S. Pandya, *A hybrid improved harmony search algorithm-nonlinear programming approach for optimal coordination of directional overcurrent relays including characteristic selection.* International Journal of Power and Energy Conversion, 2018. **9**(3): p. 228-253.
38. IEC, S., *Measuring relays and protection equipment-Part 151: Functional requirements of over/under current protection.* IEC 60255-151, 2009.
39. Mansour, M.M., S.F. Mekhamer, and N. El-Kharbawe, *A modified particle swarm optimizer for the coordination of directional overcurrent relays.* IEEE transactions on power delivery, 2007. **22**(3): p. 1400-1410.
40. Thangaraj, R., M. Pant, and K. Deep, *Optimal coordination of over-current relays using modified differential evolution algorithms.* Engineering Applications of Artificial Intelligence, 2010. **23**(5): p. 820-829.
41. Faramarzi, A., et al., *Marine Predators Algorithm: A nature-inspired metaheuristic.* Expert systems with applications, 2020. **152**: p. 113377.
42. Abdel-Basset, M., et al., *Parameter estimation of photovoltaic models using an improved marine predators algorithm.* Energy Conversion and Management, 2021. **227**: p. 113491.
43. Houssein, E.H., et al., *An improved marine predators algorithm for the optimal design of hybrid renewable energy systems.* Engineering Applications of Artificial Intelligence, 2022. **110**: p. 104722.
44. Shaheen, A.M., et al., *A novel improved marine predators algorithm for combined heat and power economic dispatch problem.* Alexandria Engineering Journal, 2022. **61**(3): p. 1834-1851.
45. Khan, N.H., et al., *Adopting Scenario-Based approach to solve optimal reactive power Dispatch problem with integration of wind and solar energy using improved Marine predator algorithm.* Ain Shams Engineering Journal, 2022. **13**(5): p. 101726.
46. He, Q., et al., *Improved Marine Predator Algorithm for Wireless Sensor Network Coverage Optimization Problem.* Sustainability, 2022. **14**(16): p. 9944.
47. Abd Elaziz, M., et al., *An improved Marine Predators algorithm with fuzzy entropy for multi-level thresholding: Real world example of COVID-19 CT image segmentation.* Ieee Access, 2020. **8**: p. 125306-125330.
48. Abdel-Basset, M., et al., *A hybrid COVID-19 detection model using an improved marine predators algorithm and a ranking-based diversity reduction strategy.* IEEE access, 2020. **8**: p. 79521-79540.
49. Dinh, P.-H., *An improved medical image synthesis approach based on marine predators algorithm and maximum gabor energy.* Neural Computing Applications, 2022. **34**(6): p. 4367-4385.
50. Abdel-Basset, M., et al., *New binary marine predators optimization algorithms for 0–1 knapsack problems.* Computers & Industrial Engineering, 2021. **151**: p. 106949.

51. Hu, G., et al., *An improved marine predators algorithm for shape optimization of developable Ball surfaces.* Engineering Applications of Artificial Intelligence, 2021. **105**: p. 104417.
52. Houssein, E.H., et al., *An automatic arrhythmia classification model based on improved marine predators algorithm and convolutions neural networks.* Expert Systems with Applications, 2022. **187**: p. 115936.
53. Sampaio, F.C., et al., *Adaptive fuzzy directional bat algorithm for the optimal coordination of protection systems based on directional overcurrent relays.* Electric Power Systems Research, 2022. **211**: p. 108619.
54. Amraee, T., *Coordination of directional overcurrent relays using seeker algorithm.* IEEE Transactions on Power Delivery, 2012. **27**(3): p. 1415-1422.
55. Singh, M., B. Panigrahi, and A. Abhyankar, *Optimal coordination of directional over-current relays using Teaching Learning-Based Optimization (TLBO) algorithm.* International Journal of Electrical Power & Energy Systems

2013. **50**: p. 33-41.
56. Mansour, M.M., S.F. Mekhamer, and N. El-Kharbawe, *A modified particle swarm optimizer for the coordination of directional overcurrent relays.* IEEE transactions on power delivery, 2007. **22**(3): p. 1400-1410.
57. Albasri, F.A., A.R. Alroomi, and J.H. Talaq, *Optimal coordination of directional overcurrent relays using biogeography-based optimization algorithms.* IEEE Transactions on Power Delivery, 2015. **30**(4): p. 1810-1820.
58. Khurshaid, T., et al., *An improved optimal solution for the directional overcurrent relays coordination using hybridized whale optimization algorithm in complex power systems.* IEEE Access, 2019. **7**: p. 90418-90435.
59. Noghabi, A.S., J. Sadeh, and H.R.J.I.T.o.P.D. Mashhadi, *Considering different network topologies in optimal overcurrent relay coordination using a hybrid GA.* IEEE Transactions on Power Delivery, 2009. **24**(4): p. 1857-1863.
60. Sulaiman, M., S. Muhammad, and A. Khan, *Improved solutions for the optimal coordination of docrs using firefly algorithm.* Complexity, 2018. **2018**.
61. Ezzeddine, M., R. Kaczmarek, and M. Iftikhar, *Coordination of directional overcurrent relays using a novel method to select their settings.* IET generation, transmission & distribution, 2011. **5**(7): p. 743-750.
62. Korashy, A., et al., *Modified water cycle algorithm for optimal direction overcurrent relays coordination.* Applied Soft Computing, 2019. **74**: p. 10-25.
63. Bouchekara, H., M. Zellagui, and M.A. Abido, *Optimal coordination of directional overcurrent relays using a modified electromagnetic field optimization algorithm.* Applied Soft Computing, 2017. **54**: p. 267-283.
64. Bouchekara, H., et al., *A variable neighborhood search algorithm for optimal protection coordination of power systems.* Soft Computing, 2021. **25**(16): p. 10863-10883.
65. Damchi, Y., et al., *MILP approach for optimal coordination of directional overcurrent relays in interconnected power systems.* Electric Power Systems Research, 2018. **158**: p. 267-274.
66. Rajput, V.N. and K.S. Pandya, *A hybrid improved harmony search algorithm-nonlinear programming approach for optimal coordination of directional overcurrent relays including characteristic selection.* International Journal of Power and Energy Conversion, 2018. **9**(3): p. 228-253.
67. Alam, M.N., B. Das, and V. Pant, *A comparative study of metaheuristic optimization approaches for directional overcurrent relays coordination.* Electric Power Systems Research, 2015. **128**: p. 39-52.

68. Akdag, O. and C.J.E.P.S.R. Yeroglu, *Optimal directional overcurrent relay coordination using MRFO algorithm: A case study of adaptive protection of the distribution network of the Hatay province of Turkey.* Electric Power Systems Research, 2021. **192**: p. 106998.
69. Kalage, A.A. and N.D. Ghawghawe, *Optimum coordination of directional overcurrent relays using modified adaptive teaching learning based optimization algorithm.* intelligent industrial systems, 2016. **2**(1): p. 55-71.
70. Srinivas, S. and K.S. Swarup, *A new mixed integer linear programming formulation for protection relay coordination using disjunctive inequalities.* IEEE Power and Energy Technology Systems Journal, 2019. **6**(2): p. 104-112.
71. Merabet, O., et al., *Optimal coordination of directional overcurrent relays in complex networks using the Elite marine predators algorithm.* Electric Power Systems Research, 2023. **221**: p. 109446.
72. Draz, A., et al., *Slime mould algorithm constrained by the relay operating time for optimal coordination of directional overcurrent relays using multiple standardized tripping curves.* Neural Computing and Applications, 2021. **33**: p. 11875-11887.
73. Yang, Y., et al., *Hunger games search: Visions, conception, implementation, deep analysis, perspectives, and towards performance shifts.* Expert Systems with Applications, 2021. **177**: p. 114864.
74. Saleh, K.A., H.H. Zeineldin, and E.F.J.I.T.o.I.I. El-Saadany, *Optimal protection coordination for microgrids considering N $-$1 contingency.* IEEE Transactions on Industrial Informatics, 2017. **13**(5): p. 2270-2278.
75. Azari, M., K. Mazlumi, and M.J.E.E. Ojaghi, *Efficient non-standard tripping characteristic-based coordination method for overcurrent relays in meshed power networks.* Electrical Engineering, 2022: p. 1-18.

List of Publications

Journal papers:

1. Merabet, O., Bouchahdane, M., Belmadani, H., Kheldoun, A., & Eltom, A. (2023). Optimal coordination of directional overcurrent relays in complex networks using the Elite marine predators algorithm. *Electric Power Systems Research*, *221*, 109446.

Conference papers:

2. Oussama, M., Mohamed, B., Hamza, B., Aissa, K., Ahmed, E., & Rafik, B. (2023, March). An optimal coordination of directional overcurrent relays using a Gorilla troops optimizer. In 2023 International Conference on Advances in Electronics, Control and Communication Systems (ICAECCS) (pp. 1-5). IEEE.

3. Oussama Merabet, Mohamed Bouchahdane, Hamza Belmadani, Aissa Kheldoun and Ahmed Eltom. A honey badger algorithm applied to the optimal coordination of directional overcurrent relays. The First International Conference on Advanced Renewable Energy Systems ICARES'22

4. Oussama Merabet, Hamza Belmadani, Aissa Kheldoun, Mohammed Bouchahdane, Intissar Hattabi, Louiza Ait mouloud. Optimal coordination of directional overcurrent relays using Evaporation rate water cycle optimization algorithm. The 1st National Conference on Electronics, Electrical Engineering, Telecommunications, and Computer Vision C3ETCV'23, November 06, 2023, Boumerdes, Algeria.

5. Oussama Merabet , Belmadani Hamza, Kheldoun Aissa, Bouchahdane Mohamed, Ait Mouloud Louiza, Hattabi IntissarAn. Adaptive microgrid protection scheme based on dual settings DOCRs.
   The 1st National Conference on Green Energy (NCGE' 2023) November 14-15, 2023, Boumerdes, Algeria.